Max-Planck-Institut für Biochemie
Abteilung für Membran- und Neurophysik

Study of structure and function of GroESL chaperonin system using small angle scattering

Elena Manakova

Vollständiger Abdruck der von der Fakultät für Chemie der Technischen Universität München zur Erlangung des akademischen Grades eines

Doktors der Naturwissenschaften

genehmigten Dissertation.

Vorsitzender:		Univ.-Prof. Dr. A. Gierl
Prüfer der Dissertation:	1.	Univ.-Prof. Dr. J. Buchner
	2.	Priv.-Doz. Dr. H. Heumann
		Ludwig-Maximilians-Universität München

Die Dissertation wurde am 2.11.2001 bei der Technischen Universität München eingereicht und durch die Fakultät für Chemie am 15.11.2001 angenommen.

Acknowledgements

I am very grateful to Dr. Hermann Heumann for the possibility to carry out this work at the Max-Planck-Institute of Biochemistry, for his attention, encouragement and financial support. In our small group a very friendly atmosphere was present during all my stay in Martinsried. I thank all the members of H.Heumann group for help and collaboration.

I thank very much Dr. Manfred Roessle and Jörg Holzinger for carrying out the "physical part" of small angle scattering experiments, for very interesting discussions and for the great help at all stages of our work.

I want to thank Dr. Roland May for his very kind attention to our project and critical reading of the manuscript.

I am grateful to Dr. K.Vanatalu, who has grown all the deuterated cells used in this work.

I would like to thank Prof. Dr. J.Buchner and Dr. M.Beissinger for providing of the strain producing mutant maltose binding protein and giving me the opportunity to purify deuterated protein.

I thank also Prof. Dr. F.-U.Hartl and Dr. F.Weber for providing of the strain overproducing SR1 GroEL mutant and protocol for GroEL purification.

I thank Dr. Renata Stegmann and Dr. Sabine Nieba-Axmann, who started the project and gave me an introduction into protein purification and principles of neutron small angle scattering.

Big thanks to Dr. Saulius Gražulis for giving me insight into the great field of protein crystallography and invaluable help with computational work.

I am grateful to Dr. Irina Gutsche and Oana Mihalache for EM pictures of symmetric complexes. Dr. I.Gutsche I want to thank also for very interesting discussions and numerous creative ideas.

Contents

1 Introduction

1.1 The problem of protein folding.

The problem of protein folding, i.e. conversion of the information encoded in a linear chain of amino acids into three-dimensional protein structure has gained a huge interest in the last decade. There is a solid experimental evidence that the primary sequence contains all the information needed for proper folding of an active enzyme [3]. In practice, an unfolded protein chain can reach its active, native conformation upon infinite dilution, at low temperature and in the presence of some stabilising agents. Many small proteins could be denatured and refolded quantitatively into the native state, but for larger proteins it is usually not the case. Larger proteins have a higher probability to be captured in a "trap" conformation. As a trap one can consider a local minimum in the energy landscape, where protein molecules could be accumulated in a conformation which is energetically stable, but not a native one. To escape of such traps the folding intermediate has to be annealed or unfolded to some degree, to get enough free energy to leave the local minimum. Another problem are intermolecular interactions in solution. *In vitro* refolding experiments usually start by rapid dilution of an unfolded polypeptide from denaturant into a refolding solution. Unfolded proteins normally have hydrophobic patches exposed outside the globule, and therefore have a strong tendency to aggregate. Usually *in vitro* refolding is successful when the concentration of the protein is kept as low as possible, thus avoiding contact between sticky folding intermediates.

On the other hand, conditions for protein folding in a living cell are far from infinite dilution and low temperature. The concentration of proteins in cytosol is estimated to be around 300-400 mg/ml [149]. Any misfolded species is immediately transferred to proteases of the protein degradation system. At this concentration of biopolymers in cytosol the probability of aggregation for partially unfolded polypeptides is extremely high. Therefore *de novo* folding in the cell differs significantly from the refolding of chemically or thermally denatured polypeptides studied *in vitro*.

The folding of separate domains of a polypeptide chain in the cell starts as soon as the corresponding part of polypeptide leaves a ribosome. Domain folding is fast enough to be completed during the synthesis of the next portion of the chain comprising the next domain. Further, secondary structure elements have to interact with each other to form a protein globule, where hydrophobic patches are buried inside, thus stabilising the tertiary structure and enabling an interdomain interaction. At this point partially folded polypeptide chains are aggregation prone. Nevertheless, the majority of protein chains synthesised in the living cell successfully reaches their active conformation, much more effectively than

in vitro. The reason for this is that intracellular protein folding is an assisted process. Living cells have developed a special set of proteins called chaperones which play an active role in protein folding.

1.2 Molecular chaperones

Molecular chaperones are proteins which assist the folding of substrate protein to the native state. The main difference of molecular chaperones from other folding catalysts (for example, peptidyl prolyl isomerases or protein disulfide isomerases) is that they form stoichiometric complexes with their substrates during the folding process. Chaperones do not act catalytically in this process, they rather bind the substrate protein in an unfolded state stoichiometrically thus shifting the equilibrium between various folding intermediate species towards a productive refolding. Not only in stress conditions some proteins need to be refolded – certain chaperones act also on such normal processes as folding of polypeptides leaving a ribosome, transport of newly synthesised protein chains into the periplasma or intracellular organellae and assembly of oligomeric proteins.

Chaperones do not participate in any enzymatic activity of their substrates. They form more or less tight complex with them [1, 31]. Several chaperone systems are active in *E.coli*. Most of them are known as heat shock proteins. The best studied chaperone system is the GroEL (Hsp60) and GroES (Hsp10), also called chaperonin and co-chaperonin, respectively.

There are two main hypotheses proposed to explain chaperone function. Both of them have an experimental support. The first model implies that chaperones prevent possible aggregation just by isolation of aggregation prone species from each other. The substrate protein folds in this case while bound to the chaperone or when it is released in solution. Therefore, the yield of refolding is increased by suppressing the irreversible aggregation, but refolding rate in this case remains unchanged comparing with spontaneous reaction.

There are also experimental evidences that chaperones can actively unfold misfolded species to give them another chance to reach a native state. This mode of chaperoning is described as an "iterative annealing" [28, 113, 124, 126, 133]. Chaperone possess in this case an "unfoldase" activity, lowering the rate of refolding compared with refolding in solution. Binding and release of non-native species is demonstrated for relatively small substrate polypeptides, such as cyclophilin and barnase [99, 147]. Some proteins, however, are in a native-like state while bound to GroEL (DHFR [46], β-lactamase [44])

1.3 Chaperonin family in *E.coli*

1.3.1 Structure of the GroE operon and expression

The chaperonin system of *E.coli* comprises two proteins belonging to one gene family groE: GroEL ("large") and GroES ("small"). The name comes from the phage lambda major coat gene E, whose mutations are complemented with the host groE gene [41]. In genome groEL and groES are organised in a single operon under the control of two promoters: heat shock promoter, recognised by σ^{32}-RNA polymerase, and constitutive promoter, active at normal growth temperature. GroE belongs to the conserved family of heat shock proteins which are expressed in a cell in response to different environmental stress conditions such as suddenly increased temperature or chemicals [31, 101]. The appearance of damaged or aggregated proteins is an inductor. GroEL along with its co-chaperonin GroES is expressed to the relatively high level constitutively (1-2% of total protein in *E.coli*). Expression of the chaperonins is strongly induced by temperature, their content reaches 10-15% [31, 98] of the total cell protein.

1.3.2 Function of GroE system *in vivo*

Chaperonins are essential for the survival of bacterial cell, deletion of their genes is lethal [36]. All known groE mutants are leaky or they are condition-mutants (temperature sensitive, for example). This fact also supports the view that these genes are absolutely required for survival.

GroE proteins are involved in morphogenesis of several bacteriophages [60, 62]. T4 carries even its own analogue of GroES (gp31), which replaces GroES from bacterial host to assist refolding of phage proteins [129].

Eukaryotic analogues of bacterial chaperonins are found in the matrix compartment of mitochondria and in the stromal compartment of chloroplasts. Chloroplast analogue of GroEL (RuBisCo subunit binding protein) is present at the high concentration about 13 μM, due to the high abundance of its natural substrate, namely the large subunit of ribulose bisphosphate carboxylase (RuBisCo). This protein is also one of the most studied substrate proteins for bacterial GroEL, it was the first refolding chaperonin system reconstituted *in vitro* [48].

Chaperonins of the eukaryotic cytoplasm and archaebacteria, although closely related to bacterial counterpart, are structurally and functionally different and are considered as Group II chaperonins (rev. [54]). There is no GroES analogue found at present for eukaryotic chaperonins.

Taking into account that subunits of GroEL and GroES are synthesised in equal amount (the transcription of both genes starts from the one promoter) and

ATP	5-10 mM
ADP	1-2 mM
Mg^{2+}	20-40 mM
K^{+}	150-300 mM
GroES:GroEL	2:1
GroEL	2,6 μM (oligomer)
total protein	300-400 mg/ml

Table 1: GroEL,GroES, salts and nucleotides in *E.coli* [31, 82, 89]

oligomeric structure of both proteins (chaperonin as a tetradecamer and co-chaperonin as a heptamer), the proposed *in vivo* stoichiometric ratio GroES:GroEL could be 2:1 (Table 1).

Table 1 gives an overview of intracellular conditions existing in bacterial cell. Concentrations of salts and nucleotides are more or less similar to the concentrations normally used *in vitro*. The main difference between *in vitro* refolding studies and the situation in the living cell are "molecular crowding" effects (rev. [1]). These effects may have a big influence on the rates of diffusion and effective concentrations of components of all intracellular reactions.

The flux of proteins synthesised in *E.coli* through GroE system was estimated to be 10-15% of total protein chains [33]. Some of the *in vivo* substrates of GroEL were identified and found to represent a variety of unrelated enzymes responsible for different metabolic pathways. The only common feature of GroEL substrates seems to be the size of protein. GroEL can bind polypeptides not exceeding 50-60 kDa [33, 63, 131], although interaction of GroEL with protein as large as 100-200 kDa was also reported. Earlier estimations based on calculation of the amount of protein chains synthesised in *E.coli* cell gave a more modest value about 2-4% of the total [89].

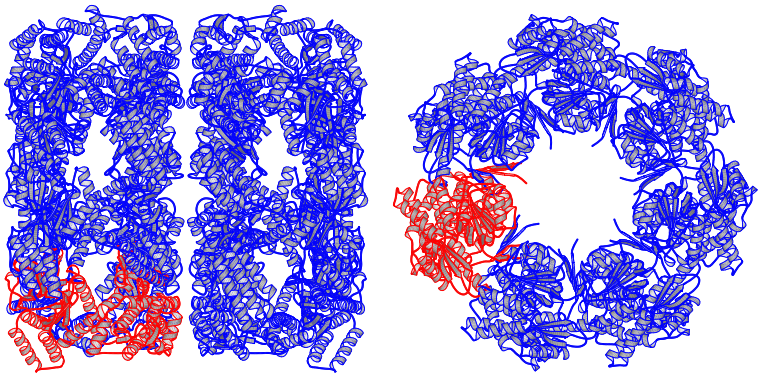

(a) (b)

Figure 1: (a) Side view of GroEL oligomer, one subunit is highlighted in red. (b) Top view of one GroEL ring, one subunit is highlighted in red. The amino acid residues closing each ring from the inner side are not resolved in the crystal, therefore GroEL looks like a hollow cylinder. Images are generated using atomic coordinates of the mutant GroEL [15, 16].

2 Structural features of the GroE chaperonin system

GroEL is an oligomeric protein, namely tetradecamer. Its 14 subunits are organised in two seven-membered rings, stacked to each other (Fig.1a). Each ring has a cavity, which is closed from the inner side. This fact is not obvious from the crystallographic data. The C- and N-terminal parts of GroEL subunits forming the inner part of equatorial domains are disordered. Therefore, these parts of GroEL molecule are not resolved in the x-ray structure. Combination of small angle neutron scattering measurements and model calculations based on the crystallographic results allows to put the invisible amino acids in the middle of GroEL cylinder, thus separating the cavity of both GroEL rings from each other [121, 122]. The double ring of GroEL is opened from both ends. GroEL is a big protein, its molecular weight is (14×57 kDa) 800 kDa.

A subunit of GroEL consists of three parts: equatorial domain, apical domain and intermediate domain (Fig.2b). Equatorial domain makes most of the contacts between subunits in each ring and between both rings. Apical domain is relatively rich in hydrophobic residues, which form a substrate binding site [34, 37]. Intermediate domain connects the first two parts of the monomer. There are two very

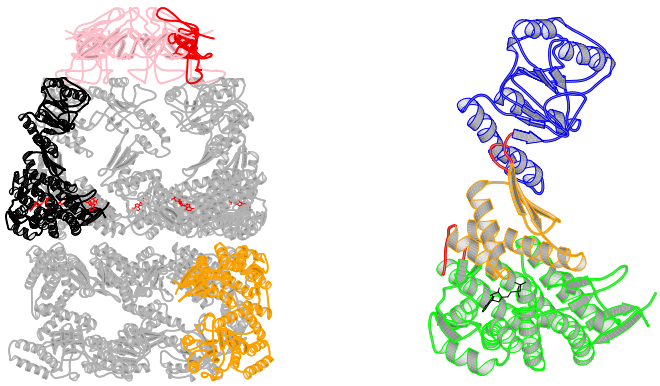

(a) (b)

Figure 2: (a) GroEL (light grey) in complex with GroES (pink). In order to demonstrate an organisation of a multimer one subunit of both rings of GroEL and GroES is highlighted. ADP bound in the upper ring of GroEL is shown in red. (b) Structural organisation of GroEL monomer. Domains are shown in different colours: equatorial domain in green, apical domain in blue, intermediate domain in yellow. Hinge regions are shown in red. This subunit is taken from the upper GroEL of the GroEL-GroES complex in (a). Bound ADP is shown in black. Images are generated from atomic coordinates of GroEL-GroES complex formed in the presence of ADP [137].

flexible hinges between apical and intermediate domains and between equatorial and intermediate domains.

GroEL is an ATPase, hydrolysing ATP rather slowly compared to other enzymes. An ATP binding pocket is located on the top of the equatorial domain. The sequence of ATP binding pocket is conserved and can be found in the most of other ATPases (residues 87-94).

Co-chaperonin GroES is also an oligomeric protein. Its seven subunits are organised in a one dome-like ring [65]. The molecular weight of an oligomer is (7×10 kDa) 70 kDa. The function of GroES is to bind to an open ring of GroEL thus closing its cavity (Fig.2a). Substrate protein allocated in the GroEL cylinder is captured under GroES and thus isolated from bulk solution. Polypeptide is prevented in this way from undesirable intermolecular interactions. ATPase activity of GroEL becomes more co-operative in the presence of GroES.

Unfolded polypeptides are bound initially at the opening of GroEL ring. In the most cases it is an interaction between hydrophobic residues of apical domains of GroEL and hydrophobic residues displayed by unfolded protein. After binding of GroES substrate is replaced into the cavity of GroEL ring.

3 The chaperonin system: interaction of components

3.1 Members of the system: GroEL, GroES, ATP, ADP, substrate protein

GroE system is a very complicated machinery, self-regulating by the interplay of several components. Adenine nucleotides are main allosteric regulators of the chaperone activity of GroEL. GroEL is switched from one mode or state to another, each state having completely different affinities to both its substrates (polypeptide to be folded and ATP, as a substrate for ATPase) after binding of ATP. Binding of ATP or ADP changes the affinity of GroEL with respect to the substrate protein [120] and GroES [7, 51]. Binding of ATP by GroEL ring is a highly co-operative process, as demonstrated in numerous time resolved fluorescence measurements. GroEL does not contain tryptophane residues in the primary sequence. It can be labelled either chemically with fluorescent dye or genetically by inserting tryptophane. When one subunit of GroEL binds ATP, the affinity of the residual subunits of the ring with respect to ATP increases. In other words transitions of the subunits in one ring is a co-operative process.

Binding of ATP occurs in two steps [70]. The first stage is a weak complex between GroEL and ATP, with a K_d of about 4 mM. This complex isomerises very quickly into the tight complex, having dissociation constant of 5-10 μM. The transition from a first, weak complex to the second, tight one occurs with an apparent rate constant of 180/sec. In the presence of GroES these transitions occur in a more concerted fashion, resulting in a higher co-operativity of ATP hydrolysis [53, 78]. ATP bound at GroEL becomes captured in the nucleotide binding sites. Upon binding of nucleotide, as well as GroES and a substrate protein, initially identical rings of the GroEL become asymmetrical. Conformational differences between liganded and unliganded rings are clearly seen in the crystal structure of the GroEL-GroES complex (see Fig.2a). There is a negative co-operativity between two rings of GroEL [140]. Due to this negative co-operativity an affinity of the second ring with respect to the GroES or nucleotides is decreased remarkably.

3.2 Nucleotides

As it has been already mentioned GroEL possesses an ATP binding site in each subunit. A tetradecamer can bind 14 molecules of ATP and hydrolyses them producing ADP. The rate of hydrolysis is rather slow compared with other known ATPases. The summary of the steady state rate constants extracted from different publications is presented in Table 2. The ATPase activity depends on K^+

ions [123, 125, 130]. GroEL binds nucleotides as a complex with Mg^{2+}, as all other known ATPases.

The bisigmoidal dependence (Fig.37) of the initial rates of ATP hydrolysis by GroEL on the concentration of ATP is described by a "nested model" for the co-operativity proposed by Yifrach and Horovitz [141]. This model combines two theoretical descriptions of allosteric behaviour of multisubunit enzymes: the classical approach of Monod-Wyman-Changeuax and the Koshland-Nemethy-Filmer model for sequential transitions. The first model is applied to the transition of the GroEL subunits in the one seven-membered ring between two states. The first state is the unliganded GroEL having low affinity to ATP and high affinity to unfolded protein substrate and the second state is the ATP bound state of GroEL with the opposite features.

The second theory describes the negative co-operativity between two rings of GroEL, each ring comprising an unit of the concerted hydrolysis where all seven subunits act simultaneously. The negative co-operativity reflects the fact that after binding of nucleotide (it is true also for GroES binding) by one ring another ring can bind it only at the higher concentration of nucleotide.

There is a positive co-operativity between the seven subunits of one GroEL ring with respect to ATP hydrolysis [13, 53]. In other words all seven subunits act in a concerted fashion. A positive co-operativity was demonstrated also for the binding of ATP by the fluorescently labelled GroEL [70, 73], Trp-inserted mutant of GroEL [26, 143] and by calorimetry [68].

Recently it was found out that the binding of nucleotides other than ATP occurs in a non co-operative fashion. It was demonstrated for the binding of ADP using pyrene-labelled GroEL by Inobe et al. [68], and Cliff et al. [26]. Recent isothermal titration calorimetry [68] experiments gave also a strong experimental support for this observation. These findings contradict with previous results [70, 13]. From a comparison of the Hill coefficients one can see that binding of nucleotides other than ATP proceeds in a much less co-operative way.

As long as the fluorescence reflects the conformational transitions upon nucleotide binding, the changes in the signal caused by binding of ADP are far smaller than ATP induced (for pyrene-labelled GroEL). A contact with γ-phosphate may be a key element, switching the randomised binding activity of seven equal sites to the highly co-operative behaviour of the GroEL ring as a single "unit" in the reaction cycle.

The allosteric behaviour of the GroEL-GroES system as well as GroEL without co-chaperonin upon the binding of the nucleotides is in principle the same as measured in the ATPase assay. Possible explanation could be that the co-operative behaviour of the system is determined by the nucleotide binding, whereas the cleavage of the phosphate bond itself does not have co-operative properties.

3.3 GroES

3.3.1 Interaction with GroEL in the presence of adenine nucleotides

Both proteins bind to each other in the presence of adenine nucleotides (ATP, ADP, non-hydrolysable analogues of ATP) [23]. GroES binds to the GroEL ring loaded with seven nucleotides (designated here and further on as a "*cis*-ring" with respect to GroES). In the absence of nucleotides there is no significant interaction, K_d for this case was estimated by the sedimentation equilibrium centrifugation [7] to be in the millimolar range (Table 4).

Binding of GroES (Table 4) occurs faster than the transition of GroEL from the state with low affinity for ATP to the high affinity state, whose rate is approximately 180/sec [70].

3.3.2 The main effects of the GroES binding

The main consequences of GroES binding on the functional properties of GroEL are summarised as follows:

1) Nucleotides bound in the *cis*-ring of GroEL become captured under GroES. ATP or ADP can not escape from the nucleotide binding site (as discussed in great detail by Xu et al. [137]) until GroES dissociates.

2) The substrate protein bound at first at the hydrophobic patches of the apical domains of GroEL is displaced upon binding of co-chaperonin into the cavity and thus isolated from a bulk solution. GroES acts as a lid which prevents escape of unfolded protein out of GroEL cylinder.

3) The inner walls of the GroEL cavity as demonstrated by Roseman et al. [107] and x-ray crystallography [137] expose polar amino acids upon GroES binding. One can speculate that already the binding of ATP must cause this effect. GroES only fixes this conformation or makes this transition more co-operative.

GroEL conc. μM (monomer)	GroES	inhibition %	original value	k_{cat} μM ATP hydrolysed/ min·μM (monomer)	refs.
-	-	-	26,6/min·oligomer	1,9	132
3,5	-	-	3/min	3	49
0,017	-	-	1,125μM P_i/16 min·17,5 nM (monomer)	4	42
-	-	-	0,065/sec	3,9	143
4,2	-	-	800 μM P_i/30 min	7,5 (37°C)	69
4,2	+	50	-	-	69
-	-	-	0,15/sec·"active site"	4,5	73
-	-	-	3,8μM ATP/mg·15 min	4,4	86
-	-	-	0,1/sec·monomer	6	130
0,35	-	-	V_{max}=1,42 μM/min	4,06	67
0,35	+	44	32/min	2,3	67
0,188 (mutant)	+	-	0,03/sec	1,8	109
1-10	-	-	5/min	5	123
1-10	+	50	2,5/min	2,5	123
-	-	-	0,04/sec	2,4	70
-	+	55	0,018/sec	1,08	70
-	-	-	0,12/sec·"active site"	3,6	22
-	+	65	0,042/sec·"active site"	1,26	22
0,35	-	-	0,058/sec	3,5	141
0,53	-	-	78 nmol ATP/min·mg	4,5 (25°C)	88
0,53	+	54	36 nmol ATP/min·mg	2,07 (25°C)	88
0,53	-	-	232 nmol ATP/min·mg	13,2 (37°C)	88
0,53	+	54	108 nmol ATP/min·mg	7,1 (37°C)	88
0,53	-	-	368 nmol ATP/min·mg	21 (45°C)	88
0,53	+	30	258 nmol ATP/min·mg	14,7 (45°C)	88

Table 2: Rates of hydrolysis of ATP by GroEL with or without GroES.

nucleotide	first ring K_d or $K_{1/2}$ μM	second ring K_d or $K_{1/2}$ μM	GroES	method used	refs.
ATP	5	-	-	-	144
ATP	$K_{1/2}$ 16	160	-	steady-state ATPase activity	141
ATP	K_M 7	-	-	ATPase activity	130
ATP	$K_{1/2}$ 10	-	-	fluorescence	22
ATP	$K_{1/2}$ 10	-	-	fluorescence	70
ATP	$K_{1/2}$ 4000	-	-	fast kinetics, fluorescence	70
ATP	$K_{1/2}$ 5	-	+	fluorescence	70
ATP	apparent K_d 23	-	+	-	5
ADP, after cleavage	$K_{1/2}$ 10	-	-	fluorescence	22
ADP	apparent K_d 5	-	-	fluorescence	22
ADP	$K_{1/2}$ 62,5 (strong binding)	$K_{1/2}$ 790 (weak binding)	-	fluorescence	68
ADP	-	$K_{1/2}$ 140	-	isotherm.titration calorimetry	68
ADP	$K_{1/2}$ 200	-	-	refolding activity	57
ADP	-	$K_{1/2}$ 2300	-	fluorescence	70
ADP	$K_{1/2}$ 20	-	+	refolding activity	57
ADP	$K_{1/2} < 0{,}07$	-	+	fluorescence	70
ATPγS	$K_{1/2}$ 40	-	-	refolding activity	57
ATPγS	$K_{1/2}$ 33 (strong binding)	$K_{1/2}$ 500 (weak binding)	-	fluorescence	68
ATPγS (26°C)	-	$K_{1/2}$ 26,7	-	isotherm.titration calorimetry	68
ATPγS (5°C)	$K_{1/2}$ 20,3	-	-	isotherm.titration calorimetry	68
ATPγS	$K_{1/2}$ 5	-	+	refolding activity	57
AMP-PNP	$K_{1/2}$ 800 (strong binding)	$K_{1/2}$ 2500 (weak binding)	-	fluorescence	68
AMP-PNP	$K_{1/2}$ 290	-	-	fluorescence	70
AMP-PNP	$K_{1/2}$ 100	-	+	fluorescence	70

Table 3: Dissociation constants for adenine nucleotides.

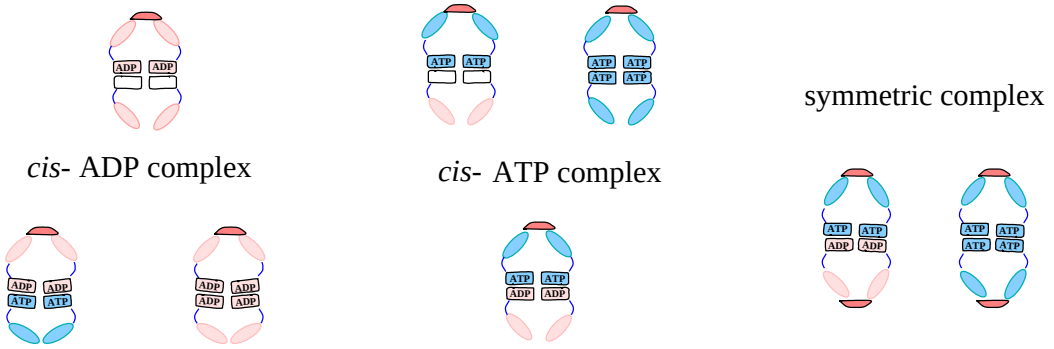

Figure 3: Schematic picture of the possible complexes between GroEL and GroES

4) GroES regulates the ATPase activity of GroEL increasing the degree of the co-operativity of the nucleotide binding (and hydrolysis) [53].

5) The steady state ATPase reaction is inhibited in the presence of GroES to the 30-50% level [23]. As shown in [109], this effect is caused by an additional reaction step which becomes limiting an ATPase rate, namely, the conversion of the *cis*-ADP conformation of the GroEL-GroES complex into the *cis*-ADP* conformation. This transition is slower than the cleavage of a phosphate. In the presence of an unfolded substrate this step becomes faster, depending, probably, on the protein and denaturant used. The presence of GroES slows down the transition to this "activated" ADP-state.

GroES seems to stabilise or to fix certain conformations of the GroEL. These conformations depend on the nucleotides (ADP or ATP) bound to GroEL. GroES is a strong regulator of the GroEL activity with respect to the adenine nucleotide binding and hydrolysis.

There are three possible GroEL-GroES complexes to consider (Fig.3): the *cis*-ADP complex, the *cis*-ATP complex and the symmetric complex with two GroES molecules bound to one GroEL. *Cis*-complexes may contain also nucleotide in their *trans*-ring, thus one can take into account also *cis*-ADP/*trans*-ATP GroEL-GroES complex, *cis*-ADP/*trans*-ADP GroEL-GroES complex, *cis*-ATP/*trans*-ADP GroEL-GroES complex and *cis*-ATP/*trans*-ATP GroEL-GroES complex.

3.3.3 *cis*-ADP GroEL-GroES complex

The 1:1 (asymmetric) complex formed in the presence of ADP is a most stable complex *in vitro*. Its half-life time (in the absence of ATP) is in the range of hours [58, 123, 124]. However, the relevance of this complex for the situation *in vivo* is rather questionable, since ATP is present in the cell at high concentration (Table 1). In the presence of ATP GroES is exchanged after each round of ATP

hydrolysis [22, 124]. As soon as *trans*-ring of the *cis*-ADP complex binds seven molecules of ATP, the *cis*-ring becomes committed to the discharge of bound GroES and ADP.

There are huge conformational differences between the *cis*- and *trans*-rings of the GroEL complexed with GroES as shows the crystal structure ([137], Fig.2a). The main consequences of ADP and GroES binding with respect to the conformation of GroEL subunits are as follows:

1) The *cis*-cavity increases its volume two-fold compared with the *trans*-cavity;

2) Mainly hydrophobic amino acid residues of the GroEL substrate binding site are involved in the new contacts between subunits and GroES. As a result, the inner surface becomes essentially polar.

3.3.4 GroEL-GroES complexes formed in the presence of ATP

The question about the conformational changes in GroEL upon binding of ATP was addressed first in the crystal structure of a mutant GroEL with and without ATPγS [14, 15]. Comparison of these structures does not show large differences between them. The conformation of the chaperonin complexed with ATPγS is similar to the unliganded GroEL. Possible reason for that might be the distorted interring communication in this particular mutant [2] and not a best choice of an ATP analogue.

Electron microscopy studies have demonstrated the rotation of the apical domains, which turns the substrate-binding sites away from the channel in the direction of the intersubunit contacts of GroEL upon ADP and ATP binding [107]. This EM study was carried out with wild type chaperonin [107]. GroEL and GroEL-GroES complexes formed in ATP, ADP and AMP-PNP were compared to each other with 30 Å resolution. Reorientation of the equatorial domains caused by nucleotide binding could be transmitted to the lower ring or to the apical domains of the same ring of GroEL. According to the suggested model binding of ATP caused twisting of apical domains outwards the GroEL cavity. In the case of ADP binding this rotation of the apical domains is less pronounced. AMP-PNP, an unhydrolysable analogue of ATP, caused an intermediate effect. Later these conclusions were confirmed by analysis of the crystal structure of *cis*-ADP complex.

Some structural features of chaperonin system in the presence of ATP could be deduced from investigation of chaperonins in the presence of unhydrolysable analogues of ATP, such as ATPγS or AMP-PNP. To some degree these nucleotides can simulate an ATP bound conformation of GroEL, which is otherwise difficult to stabilise due to hydrolysis.

GroES bound with GroEL	nucleotide	conc. mM	GroEL conc. nM	on-rate 1/M·sec	off-rate 1/sec	K_d nM	method used	ref.
1	ADP	-	-	-	-	0,3-0,5	fluorescence	57
1	ADP	0,2	var.	4×10^5	$0{,}5\times10^{-4}$	0,1-0,2	SPR	58
1	ADP	-	var.	-	$t_{1/2}$ 4 hrs	-	-	58
1	ADP	-	-	1×10^5	-	0,5-3	fluorescence	70
1	ADP	2	var.	$1{,}3\times10^4$	$1{,}1\times10^{-4}$	8,3	SPR	75
1	ADP	2	6250	-	-	5	nat.PAGE	121
1	ADP	-	-	-	$t_{1/2} > 5$ hrs	-	gel filtration	124, 125
1	ADP	no free	-	-	0,004	-	fluorescence	22
1	ADP	var.	135	-	-	20	fluorescence	51
2	ADP	var.	135	-	-	555	fluorescence	51
1	ADP	-	-	-	-	26	EM, XL	123
1	ADP	1	6140	$5{,}6\times10^5$	-	-	SAXS	page 50
1	AMP-PNP	2,5	var.	5×10^5	3×10^{-4}	0,6	SPR	58
2	AMP-PNP	1	135	-	-	20% of symm.	fluorescence	51
2	AMP-PNP	30	12500	-	-	500	SANS	39
1	ATP	2	var.	11-12$\times10^5$	195×10^{-4}	17	SPR	58
1	ATP	2	var.	$1{,}7\times10^5$	$2{,}8\times10^{-3}$	16,4	SPR	75
1	ATP	-	-	$> 4\times10^7$	-	-	fluorescence	22
2	ATP	1	135	-	-	20% of symm.	fluorescence	51
1	ATP	0,05	6140	$1{,}14\times10^6$	-	-	SAXS	page 52

Table 4: Dissociation constants of GroEL-GroES complexes.

3.3.5 Symmetric complex

Each GroEL oligomer possesses two initially equivalent GroES binding sites. Theoretically, both of them are able to bind GroES, but after binding of the first GroES rings of GroEL are not equivalent any more and the second GroES can be bound only with a very low affinity and only in the presence of ATP or ATP analogues. ADP seems to be a strong inhibitor of the symmetric complex formation [83, 111]. But there is one report about a very weak binding of the second GroES in the presence of ADP [51]. Due to steric reasons formation of symmetrical particles from two *cis*-ADP rings as present in asymmetric complex is unlikely [114, 137].

On the other hand, formation of the symmetric complexes is stimulated by a mixture of ADP and AMP-PNP, as demonstrated by Gorovits et al. in [51] (in this study ADP and AMP-PNP were used). From that point of view a symmetric complex is a pseudo-symmetric complex. Thus, domain shifts in the ATP bound ring could somehow compensate rearrangements in the ADP bound ring.

Symmetric complex was initially found in EM images [57, 83, 111]. EM studies (Fig.4) have proved the appearance of the symmetric complex in the presence of high concentration of AMP-PNP and molar excess of GroES.

The functional significance of the symmetric complex is still not clear. On one hand, the abundance of this complex is shown to correlate with the conditions of the most effective protein folding by the chaperonin system [5, 6, 27, 84, 85, 119, 127]. Taking into account known intracellular ATP concentrations and the natural stoichiometry of chaperonins (Table 1) symmetric GroEL-GroES complex seems to be favoured *in vivo*. From the other hand, the functional significance of this state of chaperonin system is a matter of debate. In some cases the optimal refolding conditions are found at 1:1 stoichiometry of GroEL-GroES complex [32, 58, 80, 100, 135].

There is also a very attractive model of GroEL-GroES system acting as a two-stroke engine [139], which is still a hypothesis. In this model the symmetric complex is proposed to be a transient state in the reaction cycle of chaperonin.

Symmetric complex could be considered as an intermediate unstable form, because of a very low affinity of the second molecule of GroES to the asymmetric GroEL-GroES complex.

In the presence of ATP or its unhydrolysable analogues GroEL can bind two molecules of GroES forming symmetrical particles. Such complex is difficult to detect because the second GroES is bound weakly and dissociates readily during gel shift analysis or gel filtration. Quantification of symmetric complexes based on EM data is not accurate because one can take into account only the side views. Cross-linking used in the earlier studies of the symmetric complex formation can

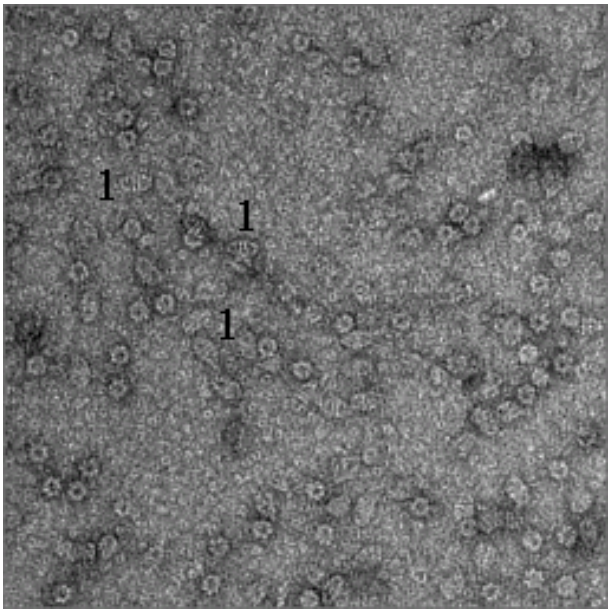

Figure 4: EM image representing symmetric complexes of GroEL and GroES formed in the presence of 30 mM AMP-PNP. GroES:GroEL 5:1 (oligomeric concentration). Some symmetrical particles are marked with "I".

influence the equilibrium in the solution, because particles once fixed with the cross-linking reagent can not dissociate any more. Small angle neutron scattering does not have these disadvantages and can be applied effectively for the estimation of dissociation constant of the second GroES bound to GroEL. In this work K_d of the formation of symmetric complex between GroEL and GroES was estimated using small angle neutron scattering (page 31). This method allows a quantitative estimation of symmetric particles existing in solution at equilibrium.

3.4 Substrate polypeptide

The role of chaperonin system GroE in protein folding was demonstrated for a vast amount of different substrate proteins. There are both, bacterial proteins [33, 63], as well as the products of eukaryotic and viral genes expressed in *E.coli* [50, 66, 72, 76, 91, 92, 93] whose folding is assisted by GroE chaperonins.

Substrate protein	Spontaneous refolding	Stoichiometry of binding to GroEL	Refolding by GroEL	Refolding with GroEL-GroES	Influence on the ATPase	Refs.
Ribulose bisphosphate carboxylase, natural substrate of Hsp60 in chloroplasts, 52 kDa	quantitative spont. refolding at 10°C	correlation with symm. particles	tight complex with GroEL, no release with nucleotides	with ATP refolding is faster than spont.		48
Maltose binding protein, 40 kDa	two-step refolding, no aggregation	1:2 (fluoresc. titration) and EM (in symm. complex)	retardation of refolding, nucl. increase K_d, most effectively ATP			57, 118
Maltose binding protein Y283D folding mutant, 40 kDa	two-step refolding, no aggregation	1:2 (fluoresc. titration)	arrest of refolding, nucl. increase K_d, most effectively ATP			118, 119
Malate dehydrogenase (mitochondrial)	aggregation as a side reaction (reversible at the beginning), yield 10%		aggregation prevented, release with ATP, yield 25%	with ATP yield of native state 80%	3-2 × stimulation	5, 102, 108, 109, 127

Table 5: Some proteins used as substrates for chaperonin mediated protein folding.

Of course, each protein has its own refolding behaviour, which is also dependent on the denaturation and renaturation conditions. Some proteins, especially of a smaller size, do not require a chaperonin at all (barnase, for example), binding to GroEL can even retard their refolding [99, 147].

All known substrates of GroEL fall in two groups. Proteins from the first group require the complete chaperonin system (GroEL, GroES and ATP hydrolysis) for refolding. They are called the stringent substrates [48, 108, 115].

In the second group there are proteins which could reach a native state after only one round of binding to GroEL. They do not need ATP hydrolysis [19, 56, 59, 96]. ATP in this case can be replaced by a non-hydrolysable ATP analogues and ADP. The proteins of the second group usually refold themselves spontaneously in the solution with high efficiency. GroEL in the absence of its cofactors forms a tight complex with these substrate proteins. Addition of a nucleotide results in the release of the substrate by lowering the affinity of GroEL to the unfolded protein. GroEL usually increases a yield of refolding remarkably, especially in the presence of cofactors (GroES and ATP). Substrate protein bound to GroEL is isolated from the undesirable interactions in solution, that could lead to unspecific aggregation. Therefore, GroEL in this case simply simulates conditions of an infinite dilution for the substrates which are effectively refolded spontaneously.

The ATP costs of refolding are estimated for some substrates [5, 95]. For instance, renaturation of one molecule of RuBisCo requires about 10 turnovers of the ATP hydrolysis by GroEL and about 100 molecules of ATP [5]. It is interesting to note that energetic costs of *de novo* protein synthesis are approximately 10 times larger than that of refolding process (1 ATP and 3 molecules of GTP are consumed to synthesise one peptide bond [134]) [21].

3.4.1 Size of the substrate protein and the cavity of GroEL

The size of the GroEL cavity was estimated by EM image analysis and crystallographic data. The *cis*-cavity of GroEL-GroES allows to accommodate proteins up to 70 kDa in the partially unfolded state. The volume of the *cis*-cavity of the ring sealed with GroES is nearly twice as large as compared to the *trans*-cavity [137]. The *trans*-ring therefore can accumulate an unfolded protein about 30 kDa.

The binding of much bigger proteins is also reported [25, 64, 71, 136, 148]. *In vivo* such big substrates comprise a minority among the proteins found to co-precipitate with GroEL [63]. It is hard to imagine which role GroES plays in the refolding of such a big protein. If the substrate is bound to one ring, binding of GroES to the other ring may stop the ATPase cycle. One can speculate that it can happen in the following way: one GroEL ring binds an unfolded protein

Substrate protein	Spontaneous refolding	Stoichiometry of binding to GroEL	Refolding by GroEL	Refolding with GroEL-GroES	Influence on the ATPase	Refs.
Rhodanese, 33 kDa	aggregation as a side reaction, yield 10%	1:2(EM)	tight complex with GroEL, release with any nukl.	release and refolding with any nucl.		8, 17, 59, 116, 135
Citrate synthase, natural substrate of Hsp60, 50kDa	no spont. refolding due to aggregation	1:2	tight complex with GroEL, release only with ATP	release and refolding with ATP, yield 30%		20, 52
β-Lactamase		1:1	binds to GroEL in a native-like state at 48°C, release only with ATP			43, 44, 146
Lactate dehydrogenase	yield 12%		no nucl. K_d 7 nM, ADP K_d 30 nM, AMP-PNP K_d 70 nM, ATP K_d 120 nM (release)	ATP effective refolding (50%), K_d 440 nM, ADP K_d 34 nM, AMP-PNP K_d 150 nM	20 × stimulation	38, 70, 120
α-Lactalbumin, 14,2 kDa	quantitative spont. refolding		GroEL retards spont. reaction, release only with ATP		3 × stimulation	74, 94, 142, 128

Table 6: Some proteins used as substrates for chaperonin mediated protein folding.

tightly, as it has exposed hydrophobic residues, then the opposite ring binds ATP, catches GroES, performs hydrolysis and waits for a signal to release the ligands. This signal is normally coming from the *trans*-ring of GroEL with ATP bound in it. What could happen if the *trans*-cavity is occupied with the some sticky protein? Or is it the hydrolysis in the *cis*-ring that already provides some rearrangements in the *trans*-ring, triggering ejection of the substrate protein?

3.4.2 Affinity of the chaperonin to a substrate is regulated by nucleotides

The affinities of GroEL to unfolded polypeptide chain depends on the adenine nucleotide bound to GroEL (for example, dissociation constants for lactate dehydrogenase binding to the GroEL in the presence of different nucleotides are presented in [120]). GroEL loaded with ATP has a lowest affinity to the substrate, the highest affinity has a GroEL ring containing no nucleotides, and an ADP loaded GroEL is in the middle.

The state with the highest affinity to a substrate protein is an empty unliganded GroEL or GroEL ring. In the suggested reaction cycle (Fig.5) such states are 1, 2, 3, 4, 5, 8, 9. These states are considered to be the acceptor states for unfolded protein. Binding of ATP enhances dissociation of substrate protein. The possible structural reason for this is the twisting of apical domain outwards the GroEL channel. In principle, at this stage the protein is free to dissociate into the solution, but since GroES forms a complex with GroEL much faster, than the switching in the affinity of GroEL for unfolded polypeptide occurs, the substrate protein is displaced into the cavity with higher probability. In fact the substrate protein and GroES are competing for the same binding site (as shown by mutational analysis – [37]). Upon binding of ATP GroEL enters a refolding state. Substrate releasing state could be located after the dissociation of GroES, which takes place between the two subsequent turnovers of hydrolysis (states 14, 15, 16, 17 in Fig.5).

3.5 Interaction between GroEL and GroES during ATPase cycle

Initial points to this schema:

1. There is a functional asymmetry between both rings, which is kept from the moment when first ring binds ATP (or ADP);

2. There is no hydrolysis in *trans*-ring when *cis*-ring binds ADP. It is a non-competitive inhibition [73];

3. Hydrolysis can not occur simultaneously in both rings, because ATP bound under GroES is committed for hydrolysis [26, 73];

4. Dissociation of nucleotides is possible only from that ring which is not closed with GroES [123, 137];

5. Symmetric complex is an unstable transition state when *cis*-ADP/*trans*-ATP chaperonin complex decays by an associative mechanism. Gorovits et al. [51] have demonstrated the appearance of these particles when GroEL is loaded with the mixed nucleotides. So far there is no AMP-PNP usually in the cell, the only possible variant is ADP and ATP;

6. Extremely long life-time of *cis*-ADP GroEL-GroES complex allows to exclude its spontaneous conversion into GroEL(ADP) and further on to an empty GroEL;

7. What happens first: hydrolysis of *cis*-ATP or binding of ATP in *trans*-ring? According to Rye et al. [109] hydrolysis precedes a binding of GroES and substrate protein to a *trans*-ring of GroEL;

8. The binding of ATP in *trans*-ring triggers dissociation of *cis*-ADP complex, formed after hydrolysis of *cis*-ATP [108].

An empty GroEL (state 1 in Fig.5) can bind seven molecules of ATP in one ring (states 2 or 3). From this moment the rings are not equal any more due to the negative cooperativity between them. At this point there would be suggested two possible ways: 1) ATP could be hydrolysed or the second ring can bind another portion of ATP, thus GroEL enters a hydrolytic cycle; 2) due to its big affinity to GroEL in the presence of ATP GroES can be bound to the ATP loaded ring of GroEL forming *cis*-ATP complex (states 4 or 5). Following steps depend on the concentration of ATP. It is not quite clear whether the *trans*-ring binds next seven molecules of ATP, producing states 6 and 7 or whether hydrolysis in a *cis*-ring occurs faster, resulting in states 8 and 9. It is also not clear whether the *cis*-ATP or the *cis*-ADP complex could bind ATP in the *trans*-ring with a higher affinity. From the answering this question depends which pathway is a most probable one: $4 \rightarrow 8 \rightarrow 10$ ($5 \rightarrow 9 \rightarrow 11$) or $4 \rightarrow 6 \rightarrow 10$ ($5 \rightarrow 7 \rightarrow 11$). Anyway, one round of hydrolysis is finished at this stage. It is known that this reaction proceeds in quantised manner [124] (also time resolved ATPase activity on the page 55), GroEL cleaves seven molecules of ATP in one turnover and results in asymmetrical with respect to the nucleotides *cis*-ADP/*trans*-ATP complex (states 10 or 11). States 8 and 9 both are in fact the most stable *in vitro* *cis*-ADP complexes, whose crystal structure was successfully solved [137]. While decay of these complexes is extremely slow, it is possible to neglect it until ATP will be bound by a *trans*-ring. That means, that the most probable state after the hydrolysis is finished, is the asymmetric state 10 or 11. After one turnover the system has to be reloaded, ADP in the *cis*-ring should be released. Dissociation of the ADP is possible only after the dissociation of the GroES [137]. As it is

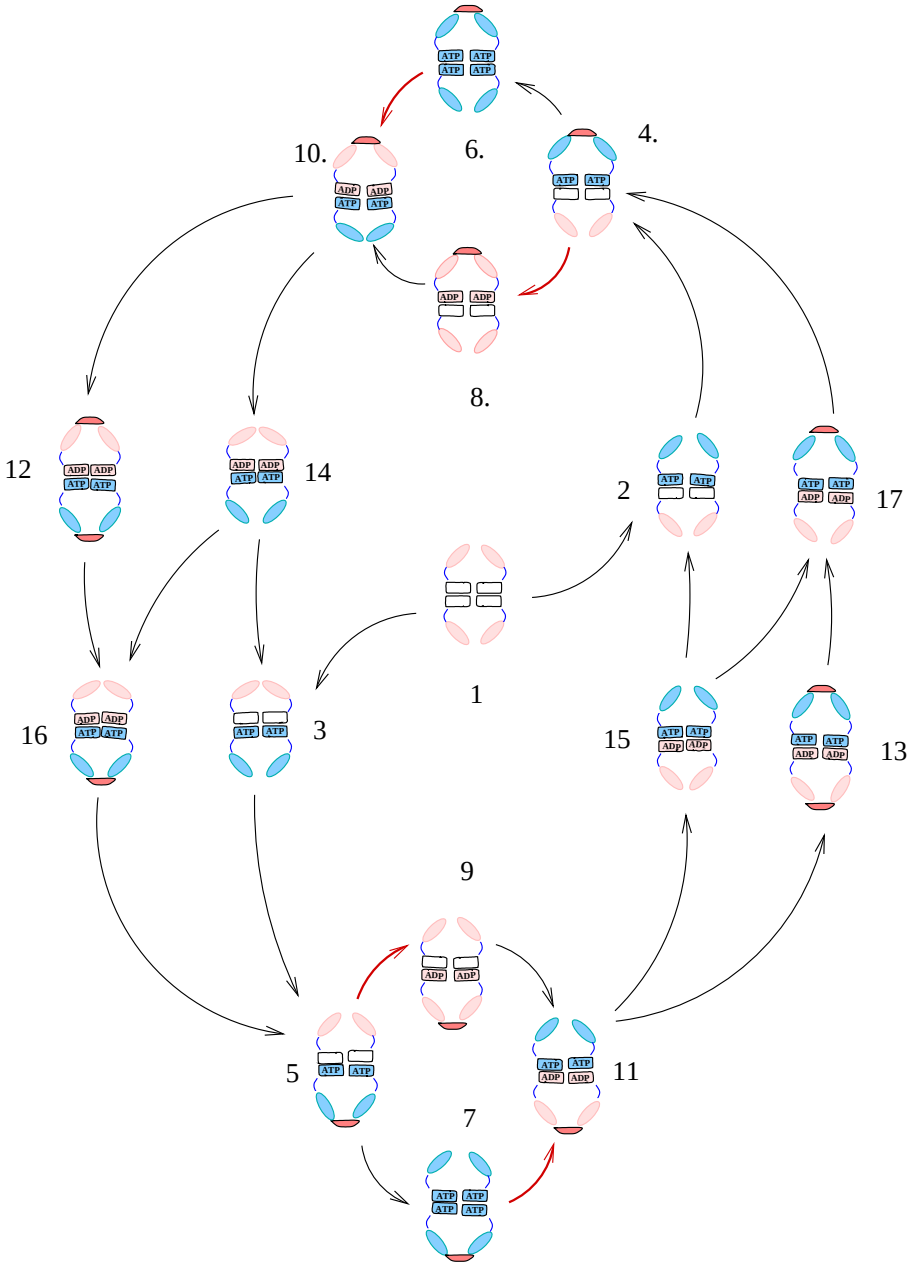

Figure 5: Proposed reaction cycle of GroEL-GroES chaperonin system.

discussed in [139] and shown in [108] it is a binding of the ATP in the *trans*-ring, but not a hydrolysis which triggers the release of the GroES from the *cis*-ring. This could proceed in two ways: 1) by the associative mechanism ($10 \rightarrow 12 \rightarrow 16$ or $11 \rightarrow 13 \rightarrow 17$), assuming the formation of the symmetric complex, which is nevertheless asymmetric with respect to the nucleotides; 2) by the dissociative mechanism with the free GroEL as an intermediate state ($10 \rightarrow 14 \rightarrow 3 \rightarrow 5$ or $11 \rightarrow 15 \rightarrow 2 \rightarrow 4$). In this case it is also not quite clear whether the ADP dissociates first (giving states 2 or 3) or GroES binds to the former *trans*-ring, now loaded with ATP, faster. In the latter case the pathway could be $10 \rightarrow 14 \rightarrow 16 \rightarrow 5$ or $11 \rightarrow 15 \rightarrow 17 \rightarrow 4$. States 4 and 5 are the starting points for the next turnover.

4 Role of γ-P_i contacts in allosteric regulation of GroEL

Although there is a great progress made recently in the investigation of the chaperonin function, some aspects are still unclear. One of these aspects concerns the role of a γ-phosphate of ATP bound to GroEL [139]. The conformational changes upon nucleotide binding are demonstrated by electron microscopy [107] and fluorescence studies [22, 26, 70]. There are significant differences between the ATP and ADP bound states of GroEL or chaperonin complexed with GroES. The contacts of GroEL nucleotide binding sites with the γ-phosphates of ATP cause also significant changes in the affinity of GroEL to GroES and substrate protein.

EM and x-ray crystallography show that rotation of apical domains is responsible for the altering of a substrate binding behaviour of GroEL. In an ADP bound GroEL hydrophobic amino acids of the substrate binding site on the apical domains are mostly exposed outside. This orientation favours the binding of the unfolded protein whose hydrophobic patches normally hidden in globule are exposed. In the ATP bound state of chaperonin, however, apical domains are rotated outwards of the cavity and entrance of the GroEL cage is formed mostly with the charged residues. This can explain the reduced affinity of ATP loaded GroEL to the unfolded protein.

EM shows that no significant movements of equatorial domains occur upon binding of nucleotides. From the other hand, in the crystallised *cis*-ADP complex the bottom of the *cis*-ring made of equatorial domains is tilted upwards. The *trans*-ring compensates the stress caused by this conformation by the opposite movement.

Thus, fluorescence studies and known x-ray structures of chaperonin demonstrate that the ATP and ADP bound states of GroEL differ distinctly from each other as well as from the unliganded GroEL. Numerous data about GroEL and GroEL-GroES refolding activity, EM and ATPase activity also suggest that the domain movements caused by ADP or ATP binding are not the same. These two conformations are principally different. This could be outlined also from different amplitudes of the fluorescence or fluorescence anysothropy changes [26, 68, 70, 73]. Contacts of the γ-phosphates obviously play a very important role.

ATP bound state due to hydrolysis exists only transiently. The structural information about these and following conformation during the ATPase cycle of GroEL could be obtained in two ways.

One can fix transition states of the reaction cycle by inhibition of reaction at certain step. This could be achieved by using different analogues of nucleotides

(for example, unhydrolysable analogues of ATP such as AMP-PNP and complexes of ADP with aluminium or beryllium fluoride described in the section 4.2).

Another possibility to investigate these conformations is to follow the structural changes of chaperonin during the reaction cycle using time resolved techniques. X-ray small angle scattering in combination with the stopped flow device provides sufficient temporal resolution (described in the next section). This method was used in this work.

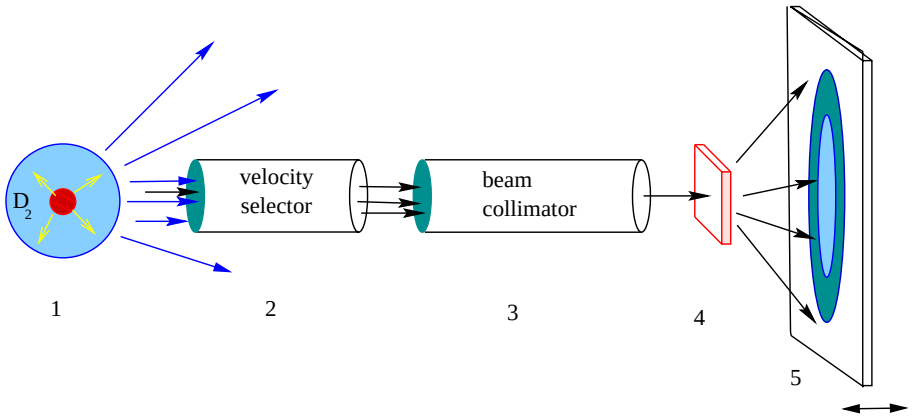

Figure 6: Scheme of the small angle neutron scattering instrument. 1 – neutron source (reactor); 2 – mechanical velocity selector; 3 – collimator; 4 – sample holder; 5 – movable detector in the evacuated tube.

4.1 Small angle scattering methods applied for the GroEL-GroES system of *E.coli*

Small angle scattering of biological macromolecules in solution is one of the modern biophysical methods. Structural information is obtained by scattering of x-rays or neutrons on the randomly distributed molecules in solution. Usually small angle solution scattering methods deal with elastic scattering, where neutrons (or x-ray radiation) interact with atomic nuclei (or the electron density of the molecule) coherently and without a change of energy.

4.1.1 Experimental set-up for SANS and SAXS experiments

The SANS instrument typically consists of four main parts: selector, collimator, sample holder and a two-dimensional detector in the evacuated tube. Neutrons produced by nuclear reaction have a high energy and have to be cooled down in a "cold source", a tank filled with liquid D_2. Cold neutrons coming out of the "cold source" are guided into the mechanical velocity selector. Only particles with a certain wavelength can pass the selector and the selected wavelength depends on the rotational speed of the selector. The distribution of the selected wave length is not very narrow (10% of nominal value of wavelength at half-maximal height). Then the neutron beam is guided into "optical" part of the instrument – the collimator, where it passes a system of neutron guides and apertures of different size. After the collimator the neutrons hit a scattering sample.

The detector uses the nuclear reaction with BF_3 or ^3He to produce charged particles that can be detected in the classical way. In the case of BF_3 ^{10}B nucleus

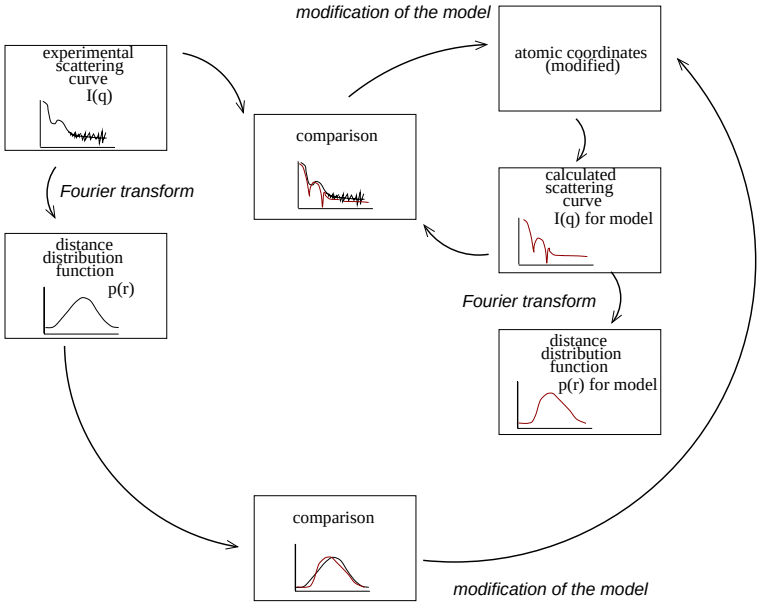

Figure 7: Strategy of interpretation of small angle scattering data.

disintegrates giving ^{7}Li and α-particles, which are finally counted. Similarly, ^{3}He after collision with neutron produces an ^{3}H and H^+. To prevent interaction of a sensitive detector with primary beam, whose intensity by far exceeds the scattered one, a beam stop is put in front of the detector. Detector is placed in vacuum in order to avoid scattering of neutrons by air. For resolving small scattered angles (this range corresponds to the largest distances in the molecule of interest, about 100-200 Å, even up to 2000 Å for some devices), the detector has to be moved further away from the sample. In order to get information about smaller distances and larger scattering angles the detector has to be moved closer to the sample.

The instruments using x-ray radiation are made in similar way. Scattered photons are detected by CCD device.

The primary data typically obtained in a small angle scattering experiment is a two-dimensional picture on the detector, which looks like a set of concentric rings of scattered intensities. This picture will be azimuthally averaged to result in a one-dimensional scattering curve (Fig.8). Fourier transformation of this curve results in a distance distribution function $p(r)$, which can be interpreted as a distribution of probabilities to find a certain distance between any two scattering centres in the biopolymer. The form and dimensions of these functions allow one to make conclusions about the overall shape of the molecule, its oligomeric state and so on. Due to the spatial and temporal averaging of the small angle scattering data it is not possible to calculate atomic coordinates of the molecule. If the crystallographic data are already available, one can calculate the distance distribution

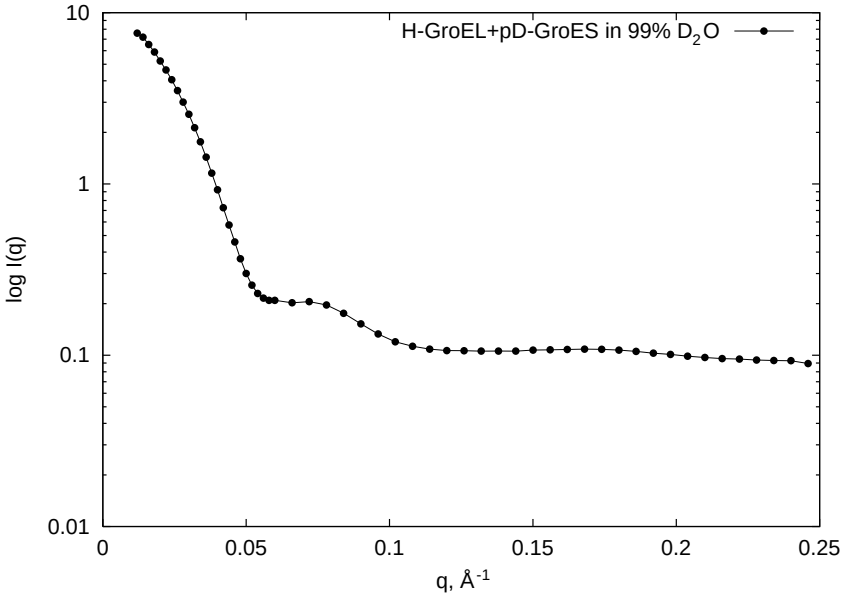

Figure 8: An example of the scattering curve of H-GroEL in 99% D_2O.

function also from the atomic coordinates in order to compare the conformation of the protein in the crystal and in the solution. Comparison of distance distribution functions obtained experimentally and calculated from crystallographic data provides information about the conformational state of the protein in solution, as shown schematically in Fig.7.

The resolution of small angle scattering methods (10-20 Å) is not much lower than that of electron microscopy, but due to a random orientation of molecules in the solution information is partially lost. Despite this fact small angle scattering methods provide complementary information to x-ray crystallography and EM. These methods often use very special buffer conditions which are usually sensitive to even modest variations. In fact, buffers used for crystallisation are normally far from physiological conditions. There are high salt concentration, precipitants, extreme pH values, because in the process of crystallisation the normally soluble protein is forced to form an insoluble phase in a controlled way. EM is sensitive to the presence of salt in the sample.

Although protein crystallography remains the most powerful method of structural analysis, there are some advantages of small angle scattering. A very useful feature of both small angle scattering techniques is the very flexible choice of solution conditions and temperature of the sample. X-ray small angle scattering has an advantage of extremely short exposure times, which allows one to follow the conformational changes during protein the protein reaction cycle with 300 msec resolution [105, 106]. Due to the high intensity of synchrotron radiation sources, a satisfactory statistics require relatively short exposure time.

nucleus	scattering length
H	-0.3742
D	0.6671
C	0.6651
N	0.94
O	0.5804
Mg	0.53
P	0.51
S	0.2847
K	0.37

Table 7: Scattering lengths for the atoms, most frequent in biopolymers. Note the very different values for H and D.

The resolution of the larger distances in the molecule in neutron small angle scattering is better than for x-ray scattering. Even a very long exposure to the neutrons does not damage significantly a protein sample. But the most exiting feature of SANS when it is applied for investigation of oligomeric protein complexes is the possibility to make one of the reacting proteins invisible. This experimental technique is called a "contrast variation" and is described in the next section.

4.1.2 Method of contrast variation

Neutrons are scattered by atomic nuclei. Scattering lengths (amplitudes) of biologically relevant nuclei are listed in Table 7. Scattering lengths of protons and deuterons are dramatically different and have an opposite sign. The sum of the scattering amplitudes per unit volume is the scattering density of the substance. The difference between the scattering densities of the macromolecule (due to the fact that biopolymers consist mostly of C, N, P, O and H atoms) and the buffer, which is mostly water, creates the contrast between the molecule of interest and solution. This contrast could be varied by changing of D_2O content of the buffer. Another way to change a contrast is the using of proteins where protons are replaced with deuterons.

Exchanging protons by deuterons does not change significantly chemical behaviour of the protein. In fact, protons readily exchangeable in solution are widely exploited by NMR. Unexchangeable protons can be replaced with deuterons by cultivation of bacteria (also yeast or algae) using medium made of heavy wa-

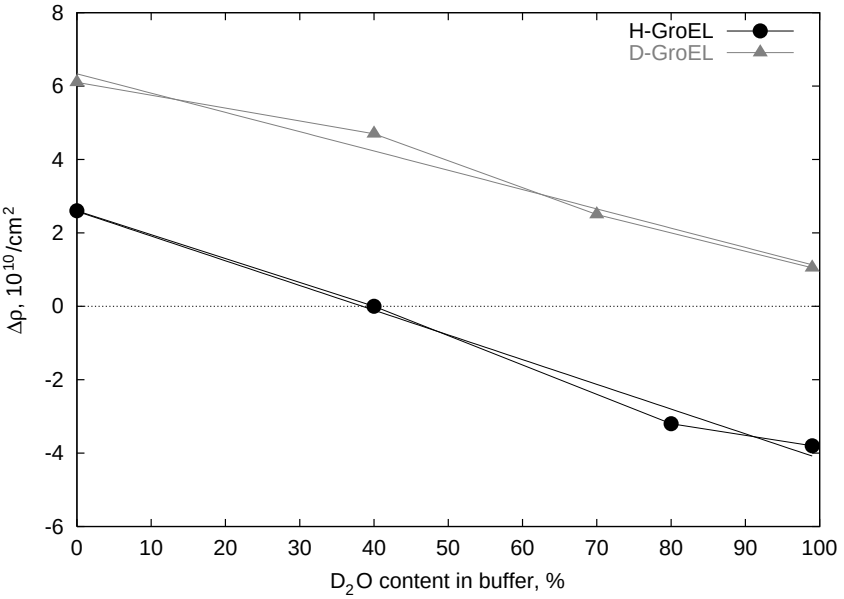

Figure 9: Contrast of protonated and deuterated protein (H-GroEL and D-GroEL) in a buffers with varied D_2O content. Note that at 99% D_2O, the contrast of the H-protein is negative, whereas the D-protein has still a positive contribution.

ter. The contrast dependence of D- and H-proteins (deuterated and protonated proteins, respectively) on the D_2O content of buffer is presented in Fig.9. The practical approach using the change in the contrast of polymers by varying content of D_2O is called "contrast variation method", a technique used widely in SANS.

The method of contrast variation can be illustrated by a comparison of two $p(r)$ functions obtained from the equivalent protein samples, whose distance distribution functions are presented on Fig.10. It is a complex between H-GroEL and its substrate protein D-MBP Y283D [118]. The right curve corresponds to the sample in 93% of D_2O, where protonated GroEL has a high contrast with respect to the buffer. Due to the rather big differences in molecular weight between GroEL and maltose binding protein the contribution of the latter to the scattering curve is too small to be detected reliably. Therefore the shape of the chaperonin-substrate complex looks roughly like that of GroEL. In buffer made of 40% D_2O (the left curve in Fig.10) H-GroEL scatters at low angles exactly as buffer, i.e. it is practically invisible in a such solution, whereas its deuterated substrate protein still has a very good contrast. There are two maxima to be seen: one at approximately 30 Å and another one at 125 Å. The first maximum corresponds to the main dimension of the maltose binding protein. It is not possible to distinguish a free protein in solution from the one bound to GroEL in this case. The second peak with a smaller height reflects pair distances between

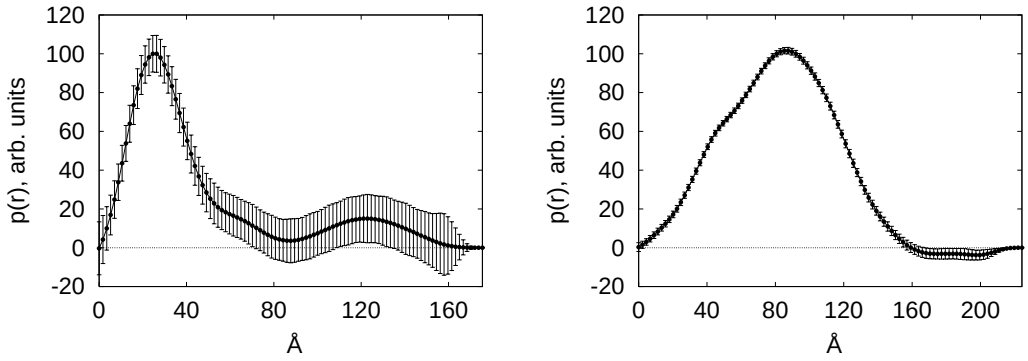

Figure 10: Comparison of the distance distribution functions of H-GroEL complexed with a deuterated substrate protein MBP Y283D measured at the different contrast to the buffer. The left curve was obtained in buffer containing 40% D_2O, this $p(r)$ corresponds to deuterated substrate protein MBP Y283D. The right curve was obtained for the complex of GroEL and MBP Y283D in solution with 93% D_2O, where both components are visible, but the contribution of MBP is negligible compared to GroEL.

two molecules of the substrate protein bound to the same molecule of GroEL. It is in agreement with fluorescence and EM studies of the interaction between GroEL and MBP Y283D [118, 119].

4.1.3 Design of the stopped flow apparatus used for SAXS experiments

This approach and experimental set-up were developed and adjusted for use at the ESRF beam line ID2 (Grenoble, France) by Dr. M.Rößle [105, 106]. High flux synchrotron radiation source of ESRF was used successfully for this study. The experiments were performed on ESRF ID2 beam line equipped with detector based on CCD elements. High flux of photons allows to minimise time slices to 300 msec, which is a good time scale to perform a time resolved kinetic measurements. On the other hand time resolution is limited by acceleration rate of stepping motors used for these experiments. This parameter also puts limits for the minimal volume of the samples. Stepping motors should move certain amount of steps to reach a constant speed.

The stopped flow machine based on the device purchased by "Applied Photophysics" (UK) was used for these experiments. Fig.11 presents a scheme of experimental set-up used at ESRF. The device consists of two stepping motors, the first motor drives syringes containing separated components of the reaction. After mixing the reaction solution fills a tubing, which ends up with a capillary, exposed to the radiation. A syringe driven by the second stepping motor replaces mixed sample with the buffer, thus pushing the reaction mixture through the cap-

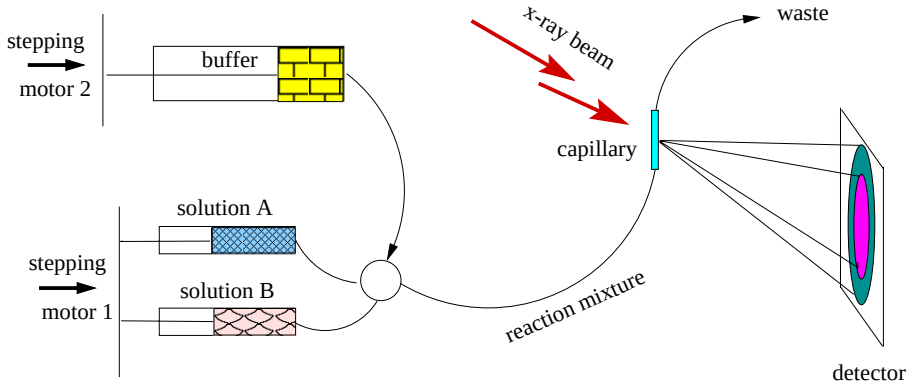

Figure 11: Scheme of the stopped flow device used for the time resolved x-ray scattering experiments at ESRF (Grenoble).

illary. This syringe was introduced in order to reduce the radiation damage of the protein. This effect becomes visible after approximately 10 sec of exposure to the beam. The speed of solution flow through device was adjusted to replace every single portion of solution, which is at the moment in the capillary with a new not irradiated portion, thus preventing an overexposure of a probe. This modification allows to increase the time of exposition of the sample to the beam in order to get scattering data with better statistics.

For the time resolved ATPase assay (page 55) was used a combination of described stopped flow machine with a quenched flow device. The schematic view is presented in a Fig.32.

4.2 X-ray crystallography of transition states of GroEL hydrolytic cycle

4.2.1 AlF_x/BeF_x as a powerful tool for ATP/GTPases

Fluoroaluminate and fluoroberyllate compounds in combination with nucleoside diphosphates are effective inhibitors of hydrolysis of β-γ phosphate bond cleavage by known ATPases and GTPases. Variety of complex compounds formed by Al^{3+} and Be^{2+} with F^- depends on concentration of F^- ions. At 10 mM concentration of NaF predominant species are AlF_3 or AlF_4^- and BeF_3^- [18, 47]. Such complexes closely resemble phosphate, having very similar central ion size and bond lengths [10, 11]. This suggestion was confirmed in numerous x-ray structures of ATP and GTP hydrolysing enzymes complexed with ADP/GDP and fluorides of aluminium and beryllium.

BeF_3^- in phosphate kinase [138] and myosin motor domain [40] was found to

have a tetrahedral shape. It is assumed that this complex simulates an ATP or ADP$*$P$_i$ bound state of the corresponding proteins, that means a conformation "before" and "after" reaction of hydrolysis of ATP.

At 10 mM F^- fluoroaluminates are present in solution as two main species: AlF_4^- and neutral AlF_3. AlF_3*ADP complex found in crystal structures of archaebacterial chaperonin thermosome [30] and phosphate kinase [138] has a geometry of a trigonal bipyramid, with F^--ions forming a plane. Axial ligands of aluminium are water or catalytic histidine in a catalytic centre of enzyme and oxygen of β-phosphate of ADP. AlF_4^- is present in many other crystals is an octahedral complex, where F^--ions are also organised in an equatorial plane and the axial positions are occupied with catalytic water and bridge oxygen [9, 40, 103, 104, 117]. Fluoroaluminates therefore mimic a pentacoordinated P$_i$ in a transition state of hydrolysis. AlF_3 in this case fits better the geometry of a phosphate than AlF_4^-.

These analogues turn out to be very useful for protein crystallography of nucleoside triphosphate hydrolysing enzymes. They dissociate usually very slowly and have a high affinity to enzymes, thus allowing more insight in structural aspects of reaction, which are otherwise inaccessible due the problem to prevent hydrolysis of bound substrate (ATP or GTP).

In order to visualise the conformation of the transient state of ATP hydrolysis when the bond between β- and γ-phosphate of ATP is ready to be cleaved was made an attempt to crystallise GroEL and GroEL-GroES complex with ADP in the presence of aluminium fluoride.

5 Results

5.1 SANS experiments

5.1.1 Complete matching of partially deuterated proteins

D-proteins produced by *E.coli* grown on 99% D_2O with deuterated glucose as a carbon source would be matched fully at approximately 120% D_2O in buffer (Fig.9). This matching is impossible, but one can lower the content of D_2O in the growth medium, thus lowering the degree of deuteration. This approach was used in order to get partially deuterated protein which has no contrast in 99% D_2O. For that purpose an *E.coli* strain producing GroEL and GroES was grown in minimal medium containing 82% D_2O with protonated glucose as a carbon source [81]. Such partially deuterated bacteria were successfully cultivated by Dr. Kalju Vanatalu (Institute of Physics and Biophysics, Tallinn, Estonia). Partially deuterated (designated here as pD-proteins) chaperonins purified from these cultures are matched subsequently at 99% and 97% D_2O. Proteins purified from these bacteria were analysed by mass spectrometry and compared with H-GroEL (Fig.12). The distribution of molecular weight of the pD-GroEL is broader than of its unlabelled counterpart. pD-GroEL is obviously not as homogeneous as H-GroEL. The possible reason for this may be not equivalent growth conditions during cultivation (bacteria might use the rests of H_2O in medium much more effectively than by D_2O).

The exact matching point for pD-GroEL was found by contrast variation method described earlier. D_2O content of the buffer containing pD-GroEL and H-GroES in the presence of ADP was varied. The variation was started from buffer having 99% D_2O. Then small portions of buffer made of H_2O were added to the sample, thus lowering the D_2O content by 2%. The scattering density of the buffer becomes equal to that of pD-GroEL at 97% D_2O. Result of such an experiment is shown in Fig.13.

pD-GroEL matching is proven if the $p(r)$ of H-GroES was obtained from the scattering curve of the complex. pD-GroEL in this case is practically invisible at 97% D_2O in buffer.

5.1.2 Titration of the second GroES binding site of GroEL

In order to estimate K_d of the GroES bound to GroEL the titration of H-GroEL with pD-GroES was performed in the conditions of contrast matching of GroEL. This is possible in buffer, containing 40% D_2O, where the scattering lengths densities for H-GroEL and buffer are the same and GroEL contribution in the

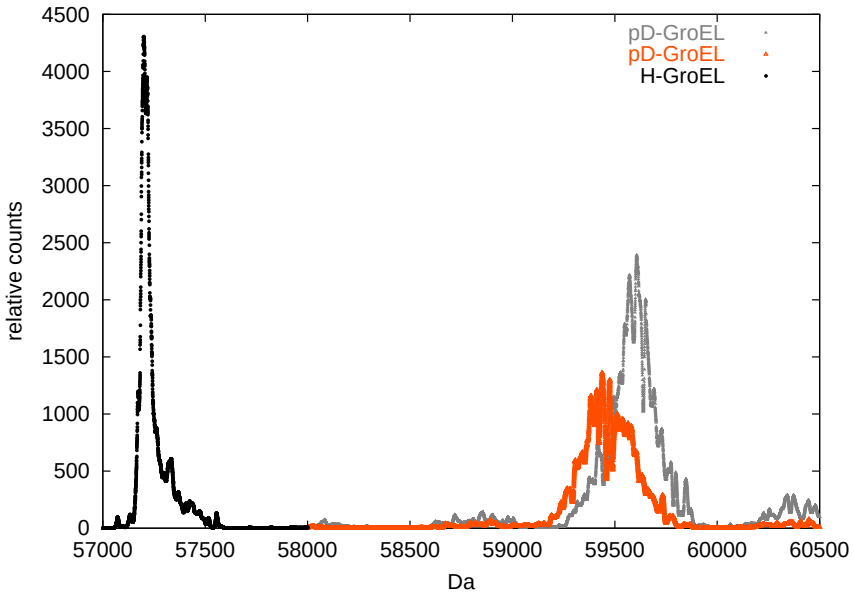

Figure 12: Comparison of mass spectra of partially deuterated GroEL (pD-GroEL) and wild type GroEL (H-GroEL).

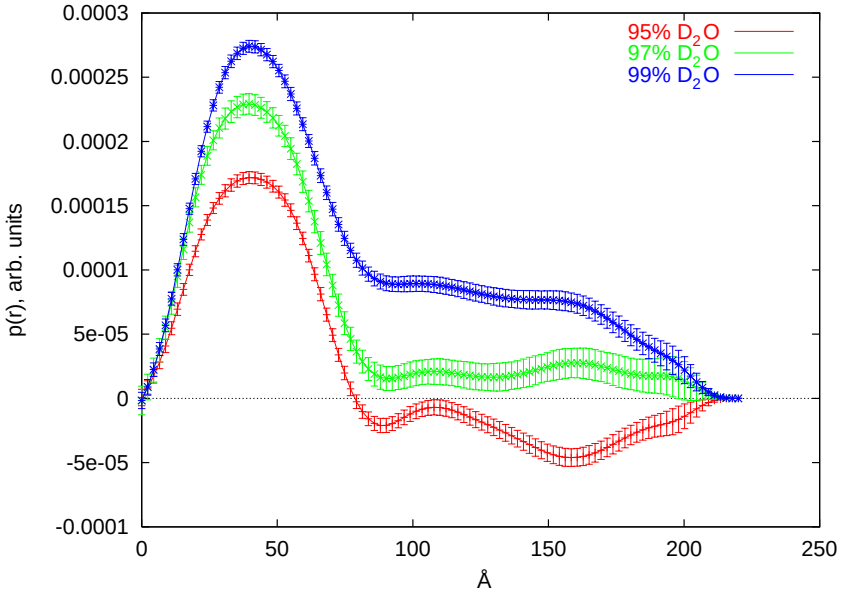

Figure 13: Distance distribution functions of the complexes between pD-GroEL and H-GroES in buffers with varied D_2O content.

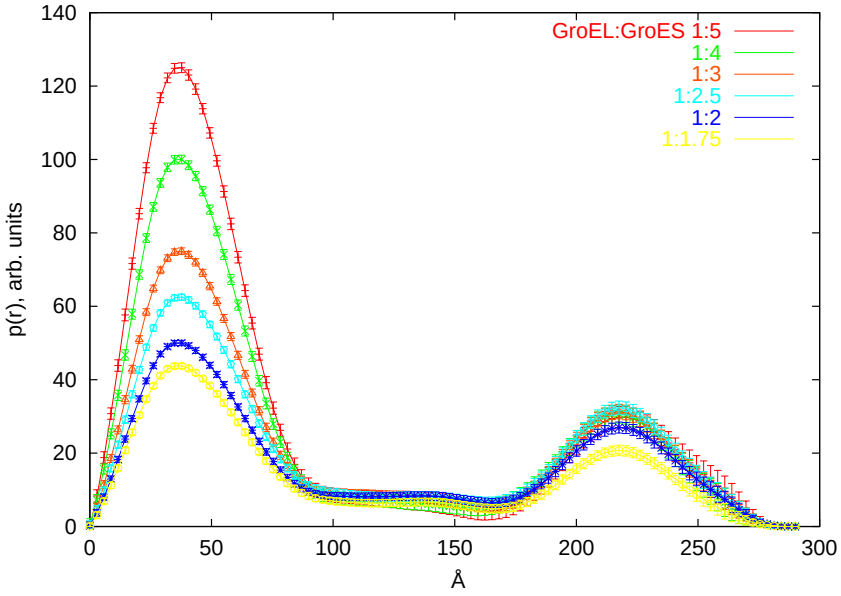

Figure 14: Titration of the second binding site of H-GroEL with pD-GroES in 40% D_2O, so that H-GroEL in practically invisible.

scattering curve is minimised. 30 mM AMP-PNP was present in the solution to enable formation of the symmetric complex between GroEL and GroES.

The titration was started from the stoichiometric ratio GroES:GroEL 5:1 (calculated for the concentration of oligomers). When the measurement of the sample was completed it was diluted with the solution containing the same concentration of GroEL and no GroES in order to lower the GroES:GroEL molar ratio. This reaction scheme was chosen in order to keep concentration of GroEL constant, and each point of the titration series has a lower concentration of GroES than the previous one and has to be measured longer. There would be another possibility to carry out the titration, namely to keep GroES concentration constant and add GroEL containing solution to each sample. In that case the difference between GroEL concentration at the beginning of titration and at the end would be too big. From these reasons the first scheme was preferred.

Scattering curves obtained for each point were Fourier transformed to result in distance distribution functions $p(r)$. $p(r)$ is the probability to find a certain distance r in the molecule. When symmetric particles are present in the solution one can see two peaks in the corresponding $p(r)$ function (Fig.14). One peak at lower distances reflects the interactions of the scattering centres inside one molecule of GroES, whereas the second peak corresponds to the intermolecular interference between two GroES bound to one GroEL. Saturation was achieved at a GroES:GroEL molar ratio 2,5:1. All curves are normalised to the amount of GroES in each sample (proportional to the area of the first peak). The distance

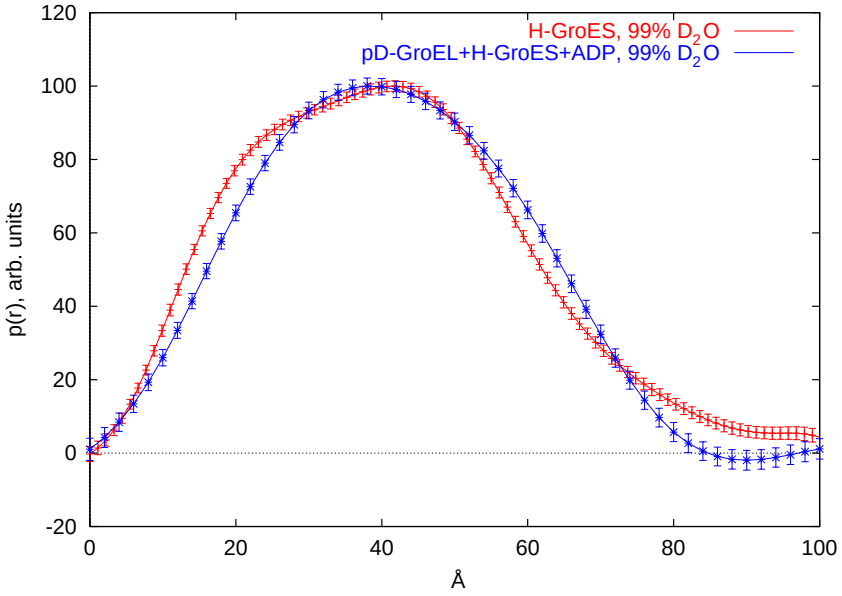

Figure 15: Comparison of distance distribution functions of the H-GroES complexed with pD-GroEL (in this case pD-GroEL is fully matched) in the presence of ADP and H-GroES in the absence of GroEL in 99% D_2O.

between the centres of gravity of two GroES molecules in symmetric complex is 220 Å, as seen from the distance distribution function. Maximal distance found in this complex is 270 Å.

5.1.3 GroES free and bound to GroEL

The aim of this experiment was to compare conformation of GroES free and in complex with GroEL. Two $p(r)$ functions were obtained in conditions of complete matching of GroEL (Fig.15). As seen from the shape of the distance distribution functions, the conformation of the GroES bound to GroEL differs significantly from the free GroES in solution. The shoulder clearly seen in the $p(r)$ of the free GroES at the distances 20-30 Å disappears upon binding to the chaperonin. The maximal distance in the molecule does not change significantly.

5.1.4 SANS fails to see changes in GroEL binding of cofactors

Comparison of the $p(r)$ functions obtained for GroEL in solution containing any adenine nucleotides and unliganded chaperonin did not reveal any significant differences between these two conformational states (data not shown). The distance distribution functions shown in Fig.16 correspond to the unliganded D-GroEL in 99% D_2O and D-GroEL in complex with GroES and AMP-PNP measured in 40%

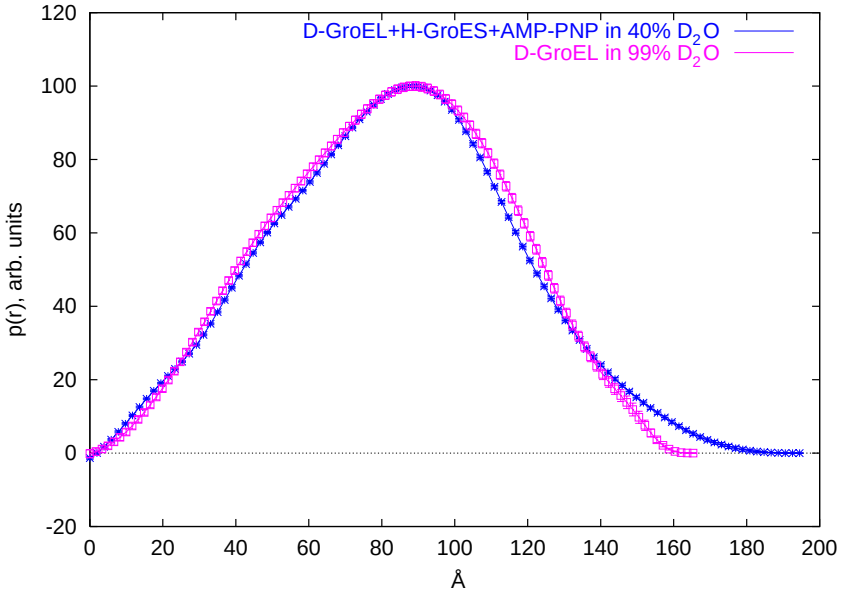

Figure 16: Comparison of the distance distribution functions of the D-GroEL complexed with GroES (H-GroES is fully matched in 40% D_2O) in the presence of AMP-PNP and unliganded D-GroEL in 99% D_2O.

D_2O. Despite the different contrast both curves have similar shape. The small differences seen at 120 Å distance are insignificantly above the error range. In fact, SANS is sensitive to changes in the overall shape of the molecule. This is probably not the case for the rotation of apical domains which is demonstrated by EM to be the main rearrangement in GroEL upon binding of the nucleotides. The large shifts of GroEL domains upon its interaction with cofactors, does not lead to any observable changes in the distribution of intramolecular distances.

In contrast to GroEL, the thermosome, the archaebacterial chaperonin homologue shows conformational states, that are very well resolved by SANS when mixed with different nucleotides [55].

5.2 Crystallisation of the pseudo-ATP bound states of GroEL and GroEL-GroES complex

In order to get more insight into the ATP bound state of the chaperonin system attempts to crystallise the intermediate states of hydrolytic cycle of GroEL were undertaken.

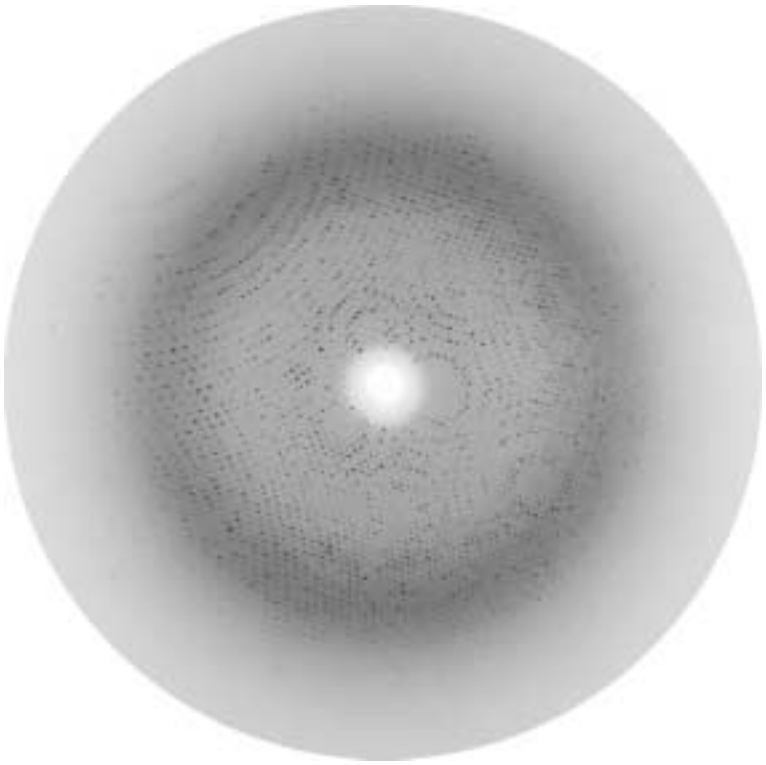

Figure 17: The diffraction pattern of GroEL co-crystallised with AlF_x (GroEL/AlF_x+ADP in the Table 8) obtained at the synchrotron "Elettra" hard x-ray beam line (Trieste)

crystal	a, Å	b, Å	c, Å	α	β	γ	space group
GroEL AMP-PNP (1)	135.6	262.4	238.2	90.00	90.00	90.00	P222
GroEL+CS (2)	135.572	262.382	283.204	90.00	90.00	90.00	P222
GroEL AlF_x+ADP (3)	135.820	166.414	364.117	81.640	91.796	66.998	P1
1aon.pdb GroEL+GroES	255.260	265.250	184.400	90.00	90.00	90.00	$P2_12_12$
1der.pdb ATPγS	135.571	260.112	150.200	90.00	101.14	90.00	$P12_11$
1oel.pdb	178.380	204.980	280.980	90.00	90.00	90.00	$C222_1$

Table 8: Cell parameters for several crystals of GroEL (first three entries) in comparison with known crystal structures.

Crystallisation was performed in several directions:

1) GroEL ($\pm$GroES) in the presence of the low concentration of AMP-PNP (1 mM) in order to mimic a conformation resembling GroEL with ATP bound in one ring. Crystals grown in these conditions have a good diffraction (3,5-4 Å), but data are not yet collected.

2) Complex of GroEL with citrate synthase (CS) G276A mutant. This folding mutant is known to form a tight complex with GroEL, which could be isolated by gel filtration [145]. The cell parameters of one of the tested crystals are more or less the same as for crystal of GroEL in the presence of low concentration of AMP-PNP. The data collected from this crystal are processed using molecular replacement method. The atomic coordinates of GroEL mutant (1oel.pdb) were used as a model. No differences were found between these two conformations of chaperonin. There are two possible explanations of this fact: 1) there is no substrate protein bound to GroEL in the crystal; 2) conformation of GroEL does not change upon binding of this particular substrate, though it is rather big protein having a size of 50 kDa.

3) GroEL ($\pm$GroES) complexed with ADP$*AlF_x$ modelling a transition state during cleavage of the bond between β- and γ-phosphates of ATP, as described on page 37. Aluminium fluoride complexed with ADP simulates a pentacoordinated transition state of the phosphate ion, as demonstrated by x-ray crystallography. The data set was collected at the synchrotron "Elettra" (Trieste, Italy) (Fig.17), but not yet processed fully. The cell parameters are completely different from the crystals obtained for mutant GroEL complexed with ATPγS and GroEL

crystallised in *cis*-ADP complex [65, 137] (Table 8). There are three chaperonin oligomers found in the cell unit.

4) GroEL (±GroES) in the presence of high concentration of AMP-PNP (30 mM). These conditions favour formation of the symmetric complexes. All attempts to get measurable crystals in these conditions have failed.

5.3 Single turnover of GroEL ATPase as seen by the time resolved SAXS

5.3.1 Conformational changes of GroEL during its ATPase cycle are reflected by the time resolved changes in R_g of the molecule.

The question of the structural changes of GroEL during its reaction cycle was addressed mostly by indirect structural studies using fluorescence or fluorescence anisotropy changes of labelled chaperonins after mixing with nucleotides. Time resolved SAXS offers a possibility to follow structural changes during the time course of ATPase cycle of unlabelled GroEL in a real time scale, due to a rather slow rate of hydrolysis of ATP by GroEL. This study is an attempt to visualise the changes in conformation of GroEL or GroEL-GroES complex during a single cycle of ATPase reaction. These experiments were performed using device described on page 36.

Three series of the small angle scattering experiments were performed:

1. GroEL (solution A) was mixed with ATP (solution B);

2. GroEL (solution A) was mixed with GroES and ATP (solution B);

3. Preformed GroEL-GroES complex made with ADP (solution A) was challenged with ATP (solution B).

Some additional measurements were carried out as references: GroEL mixed with buffer, GroEL mixed with ADP, GroEL mixed with GroES and ADP. In this work radius of gyration was used as a structural parameter. It is a radius of a sphere, which has the same rotational moment as a molecule of biopolymer. R_g reflects an overall shape of the molecule. The R_g values were calculated for each set of data. Each experimental curve represents an average of four experiments.

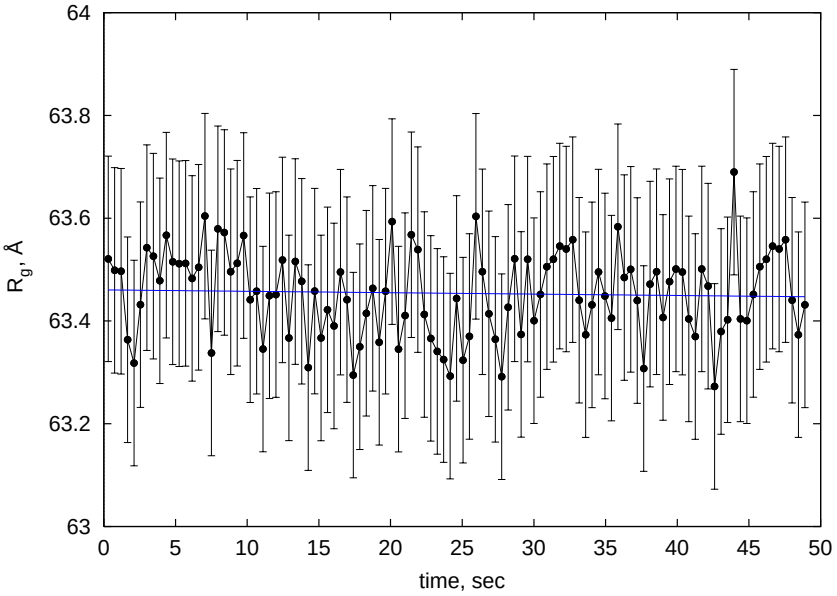

Figure 18: Time dependence of R_g of GroEL after mixing with buffer (reference measurement). Concentration of GroEL monomers 88 μM. Solid line is a linear fir of the data.

5.4 Time resolved structural changes of the unliganded GroEL

5.4.1 GroEL mixed with buffer (reference)

This measurement is a reference for the first set of experiments. It was performed in order to verify that GroEL does not change itself when mixed with buffer in the stopped flow machine. Solution containing GroEL was in one syringe (solution A in Fig.11), solution of ADP in another (solution B in Fig.11). From the time dependent scattering curves R_g values for every time slice were calculated and averaged for four experiments. R_g does not change during the time of experiment and its mean value is 63,4±0,2 Å. This value is slightly smaller than measured in SANS experiments probably due to a slightly different contrast between protein and buffer in both cases (Fig.18).

5.4.2 GroEL mixed with ADP (reference)

The aim of this measurement was to find out whether the addition of ADP changes an R_g. Experiment was carried out in the same way as a previous one, only the buffer was replaced with ADP solution. Concentration of ADP after mixing with GroEL was 1 mM. Linear fit of the data shown in Fig.19 gives a mean

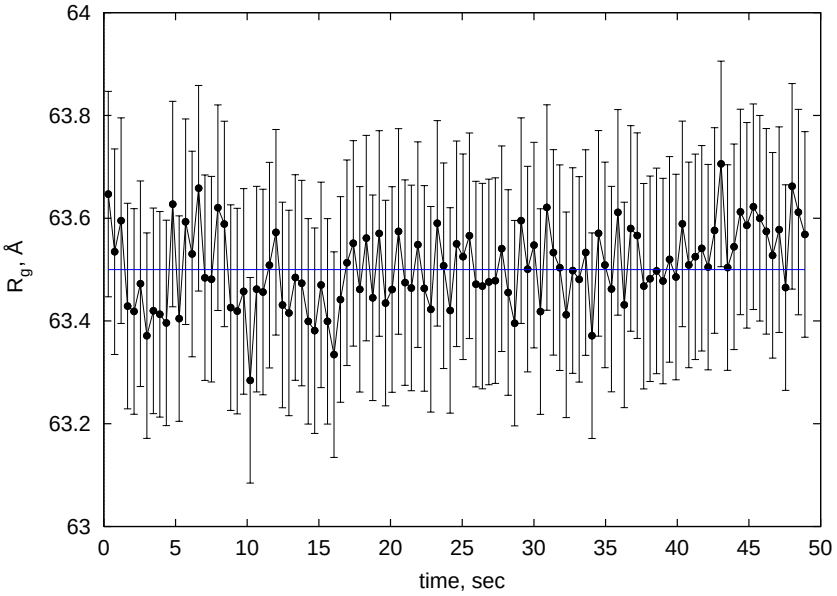

Figure 19: Time dependence of R_g of GroEL (88 μM monomers) mixed with 1 mM ADP. Solid line is a linear fit of the data.

R_g value for GroEL with seven bound molecules of ADP, which is 63,5±0,3 Å. This value is similar to the R_g of unliganded GroEL.

5.4.3 GroEL mixed with ATP, single turnover conditions

Conformational changes of GroEL during first round of hydrolysis are reflected by changes in R_g of chaperonin, as seen from the data shown in Fig.20. During one turnover of ATPase reaction GroEL hydrolyses seven molecules of ATP bound in one of its rings. In order to get one round of reaction ATP was added to GroEL in a concentration which is two times lower than the concentration of GroEL monomers. In this case it was 50 μM of ATP to 88 μM of GroEL monomers, corresponding to 5 mg/ml of GroEL.

Two phases of the reaction can be differentiated. During the first 8 seconds R_g remains stable at the value corresponding to the unliganded GroEL 63,3 Å (linear fit of the data for the first 8 sec is shown in Fig.21, left panel). After that time R_g raises until saturation at 63,8 Å. This part of the curve can be fitted with a single exponential function (conformational changing one can consider as a monomolecular reaction) giving a rate constant 0,04/sec (Fig.21, right panel).

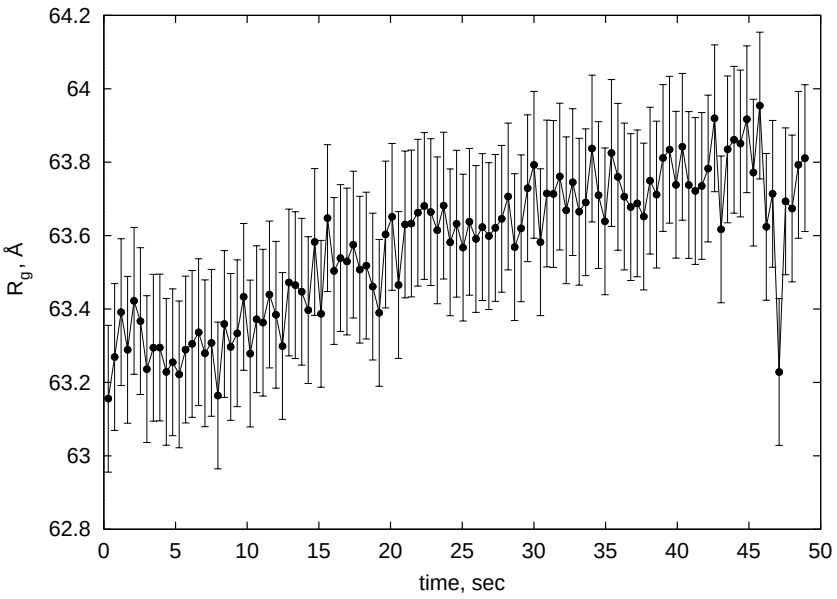

Figure 20: Time dependence of R_g of GroEL (88 μM of GroEL monomers) after mixing with 50 μM ATP.

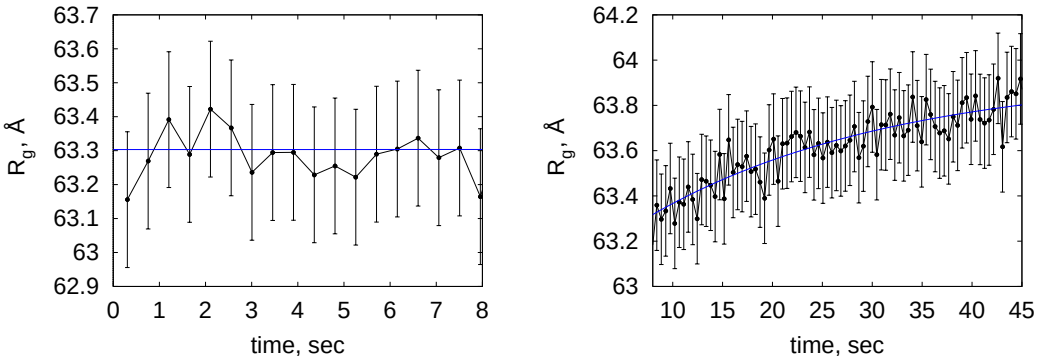

Figure 21: Time dependence of R_g of GroEL (88 μM of GroEL monomers) after mixing with 50 μM ATP. Solid line represents a fit of the data shown in Fig.20. Left panel: first part of the curve (0 - 8 sec) is a linear fit. Right panel: the second part of the curve (8 - 50 sec) is fitted with a single exponential.

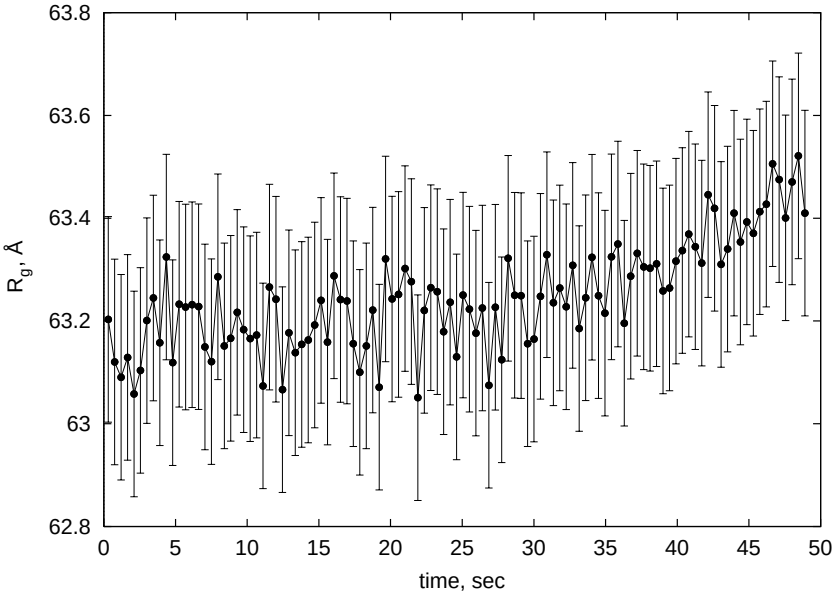

Figure 22: Time dependence of R_g of GroEL (88 μM monomers) after mixing with 500 μM ATP.

5.4.4 GroEL mixed with ATP, multiple rounds of hydrolysis

The measurement was carried out in order to model conditions of the steady state reaction. In this experiment GroEL was rapidly mixed with 10 times larger concentration of a substrate (500 μM), which is enough for 10 rounds of reaction. Time course of R_g (Fig.22) shows similar biphasic behaviour as in the previous case, but duration of the first phase with the stable R_g (63,3 Å) value is 3-4 times longer. The reaction was not followed till saturation, since the experiment was designed only for the first round of hydrolysis. R_g reached a value 63,5 Å. Linear fit of the experimental results is presented in Fig.23.

5.5 Formation of GroEL-GroES complex

5.5.1 GroEL mixed with ADP and GroES

This measurement (Fig.24) is a reference giving R_g value of *cis*-ADP chaperonin complex for subsequent SAXS experiments. The time dependence of R_g value allows to estimate apparent rate constant for the association of GroEL and GroES in the presence of ADP. Formation of *cis*-ADP is finished in the first 8 sec after the mixing of components. The initial value at the time 0 sec assumed to be 63,5 Å for GroEL alone. Association of GroEL and GroES is a reaction of second order, but the data could be fitted to the single exponential with the assumption

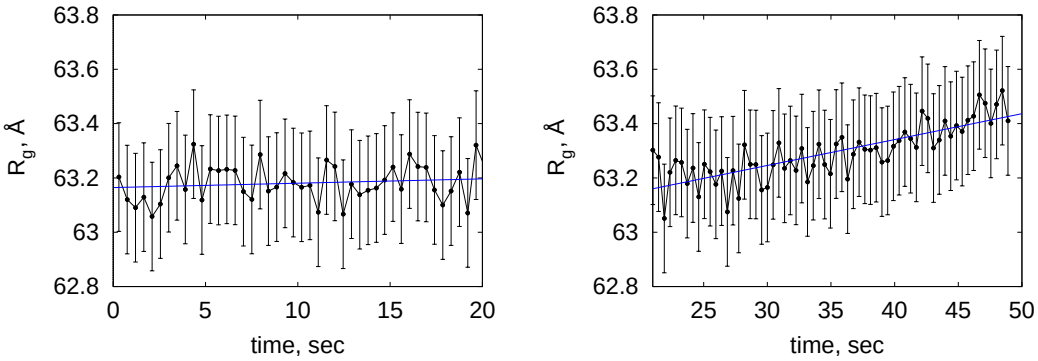

Figure 23: Time dependence of R_g of GroEL (88 μM monomers) after mixing with 500 μM ATP (Fig.22). Left panel: linear fit of the data for the first 20 sec. Right panel: linear fit of the data from 25 sec to 50 sec. Linear fit is shown with solid line.

that the contribution of unbound GroES to the R_g of the complex is negligible. Obtained rate constant has a value of 5,6×10 ^{5}/M·sec, it is in line with data presented in Table 4. R_g reaches a saturation at 66,1 Å in 8 sec. This state corresponds to the stable *cis*-ADP complex.

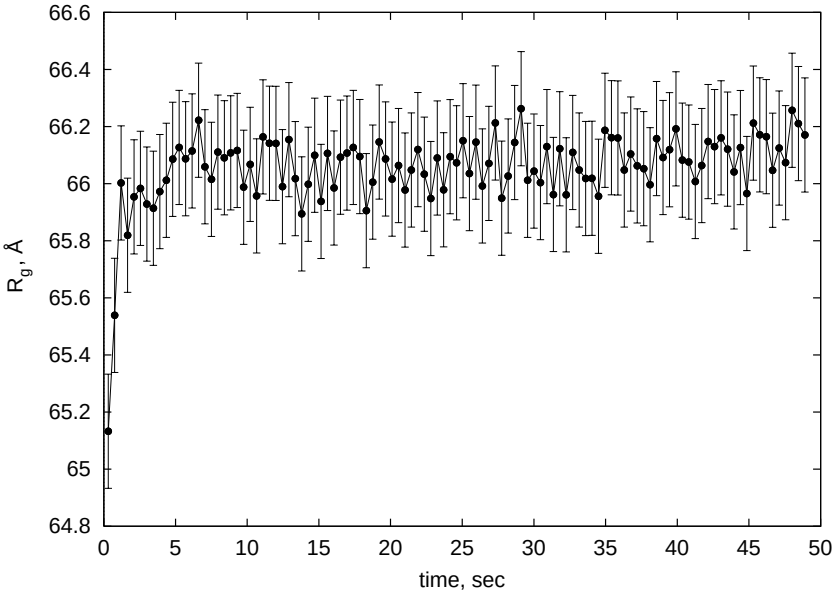

Figure 24: Time dependence of R_g during formation of GroEL-GroES complex in the presence of 1 mM ADP (reference measurement). Protein concentrations (monomers): GroEL 88 μM, GroES 44 μM.

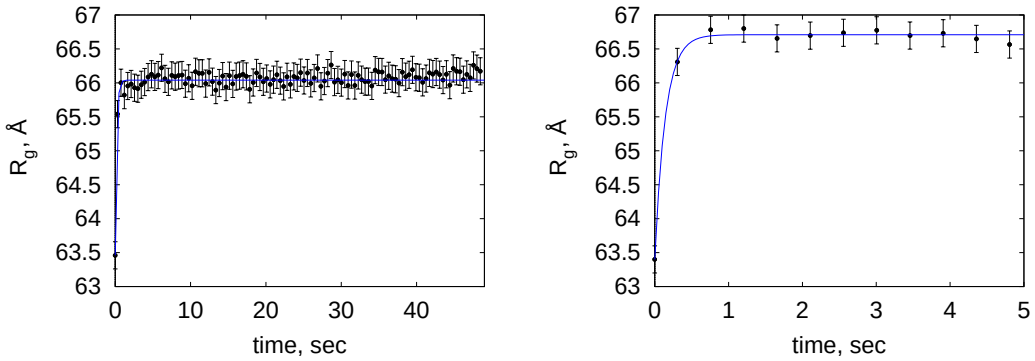

Figure 25: Estimation of the rate constant of the association of GroES with GroEL in the presence of 1 mM ADP (left panel) and 50 μM ATP. Solid line represents a fit of the initial parts of the data shown in Fig.24 and Fig.26 (0 - 5 sec).

5.5.2 Binding of GroES to GroEL in the presence of ATP

The aim of this experiment was to follow changes of R_g during formation of hydrolytically active *cis*-ATP GroEL-GroES complex. The concentration of ATP allows only one round of hydrolysis. GroES oligomer was present in equimolar concentration with respect to GroEL.

After introduction of GroES behaviour of R_g during the reaction becomes more complex, as Fig.26 shows. There are three phases observed. During a first phase radius of gyration increases rapidly from the level of unliganded GroEL (63,4 Å) to 66,7 Å indicating the formation of the complex between GroEL and GroES. Using the same assumption as in the previous experiment one can estimate the rate constant of GroEL-GroES complex formation (the fit is shown in Fig.25, right panel). This procedure gives a value $1{,}14\times10^6$/M·sec, which is in line with known results (Table 4). Association reaction is completed in 5 sec after mixing.

Chaperonin complex proceeds then linearly to the next conformation with lower R_g reaching 66,1 Å in 15 sec. It is the second phase observed in this experiment. During next 10 sec R_g remains constant at the level 66,2 Å. The third phase is again an increase in R_g to the rather high level 66,8 Å. This increase does not reach a saturation in the observed time scale.

5.5.3 Binding of GroES to GroEL in the presence of ATP (steady state hydrolysis)

This measurement was performed in order to obtain time dependence of radius of gyration in a conditions of steady state hydrolysis. GroEL was mixed with the solution containing equimolar amount of GroES and ATP in concentration which

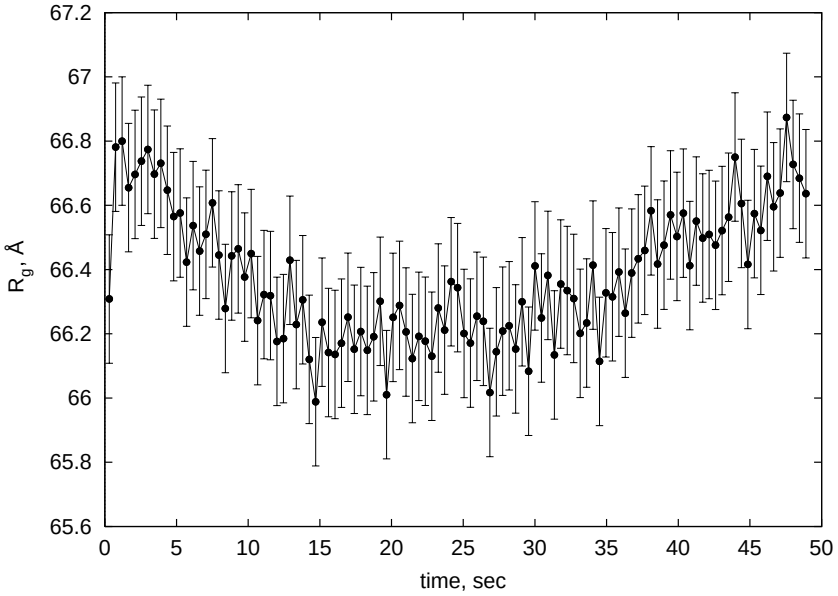

Figure 26: Time dependence of R_g during formation of GroEL-GroES complex in the presence of 50 μM ATP. Protein concentrations (monomers): GroEL 88 μM, GroES 44 μM.

is enough for 10 rounds of hydrolysis. In contrast to the previous experiment (Fig.26) the R_g value during steady state hydrolysis presented in Fig.27 does not show any time dependent changes. Remarkably, R_g remains on the constant level which looks like an averaged value as compared to the single turnover reaction.

5.5.4 GroEL-GroES complex during a single turnover of the GroEL ATPase

Preformed *cis*-ADP GroEL-GroES complex was challenged with ATP in this experiment. The aim was to observe the dissociation of GroES which is known to occur in each round of ATPase cycle of GroEL.

Only two phases were observed during the same time scale of reaction (Fig.28). First phase is an increase of R_g value from initial *cis*-ADP complex with R_g 66,0-66,1 Å to an active "hydrolysing" state with higher R_g (66,5 Å).

Then system is converted into a state with lower R_g (66,1 Å), which is close to the value for the *cis*-ADP complex. The rate constant for this transition obtained by a single exponential fit as shown in Fig.29 is 0,13/sec. In the last 10 sec there is a slight increase in R_g. Therefore a longer measurement is required in this case.

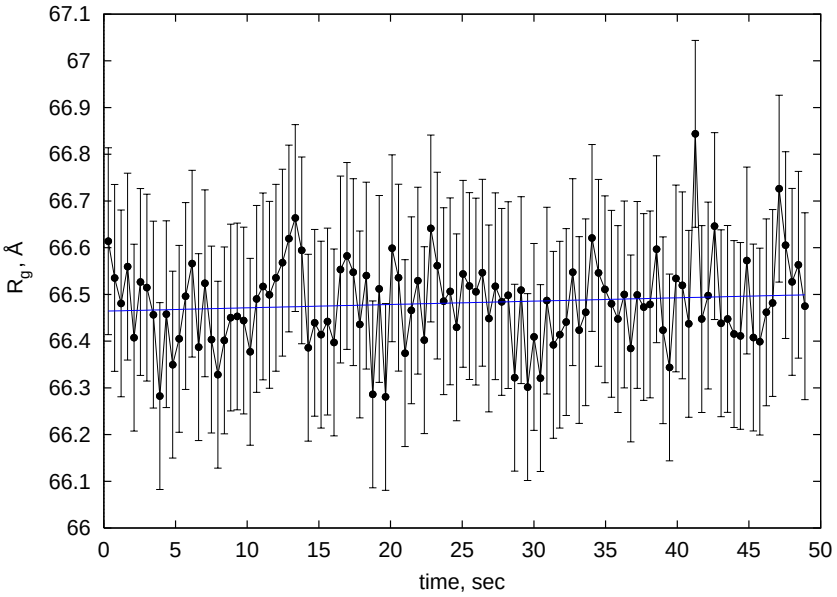

Figure 27: Time dependence of R_g during formation of GroEL-GroES complex in the presence of 500 μM ATP. Protein concentrations (monomers): GroEL 88 μM, GroES 44 μM. Linear fit of the data is shown by solid line.

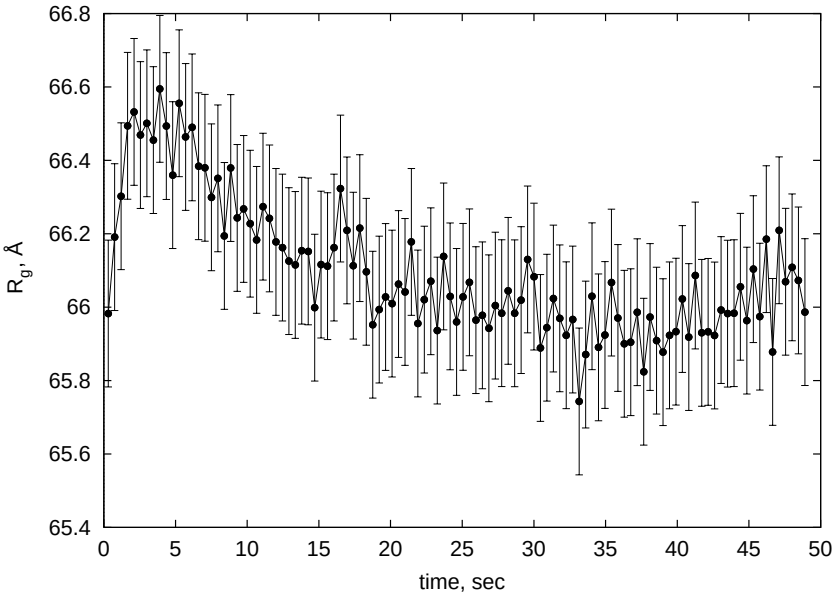

Figure 28: R_g of the asymmetric GroEL-GroES complex formed with ADP (100 μM) after mixing with 50 μM ATP. Protein concentrations (monomers): GroEL 88 μM, GroES 44 μM.

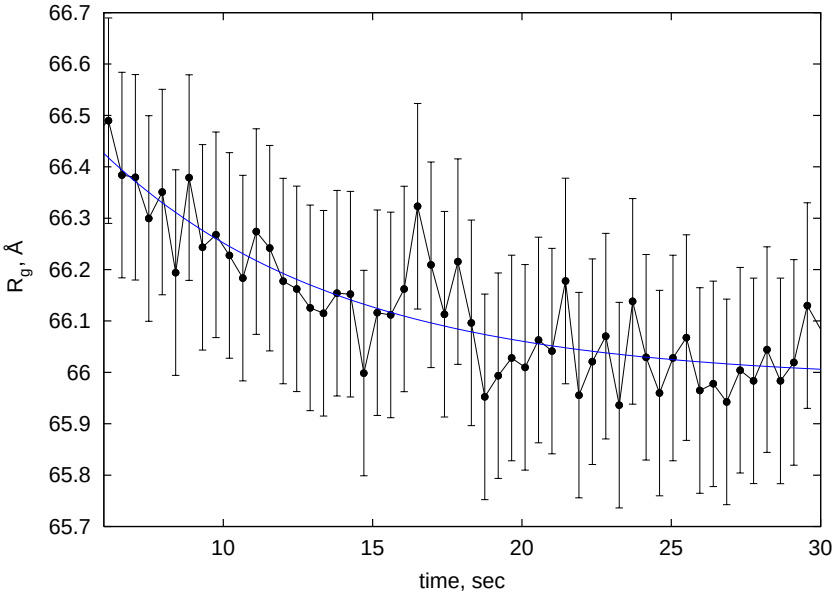

Figure 29: Single exponential fit of the data shown in Fig.28 (5 - 30 sec).

5.5.5 GroEL-GroES complex during multiple rounds of hydrolysis

Fig.30 shows a time course of R_g for the preformed *cis*-ADP GroEL-GroES complex in the conditions of a steady state hydrolysis. Directly after mixing of the reaction components R_g increased from the "ground" level for *cis*-ADP complex to the "hydrolysing" state whose R_g is approximately 66,5 Å. Then follows the linear decrease of R_g back to the ADP bound state.

5.6 Time resolved measurements of the ATPase activity of GroEL

This set of experiments was performed in order to supplement the time resolved SAXS measurements described in the previous sections. The similar equipment was used. The aim of ATPase activity studies was to find out in which way the enzymatic activity correlates with the structural changes measured by SAXS. For the detection of the phosphate a spectrophotometric assay based on the reaction of malachite green dye with the phosphomolybdate was applied. The schematic drawing of the quenched flow machine is shown in the Fig.32.

The experimental device is based on the alternating movement of two stepping motors. The first motor pushes two syringes containing the separated components of the reaction (for example, solution A is GroEL solution, solution B is an ATP solution) into the storage tubing, where the reaction mixture stays for the

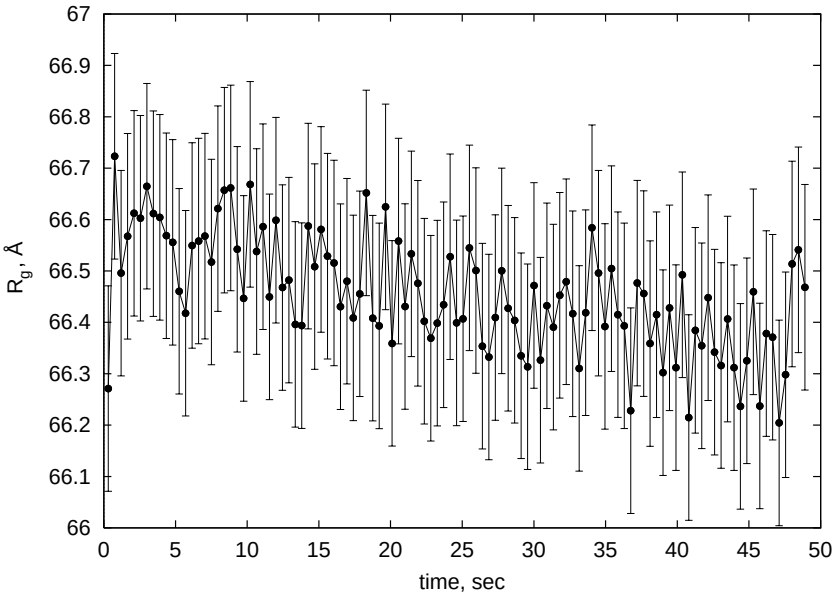

Figure 30: R_g of asymmetric GroEL-GroES complex formed with ADP (100 μM) after mixing with 500 μM ATP. Concentration of proteins (monomers) GroEL 88 μM, GroES 44 μM.

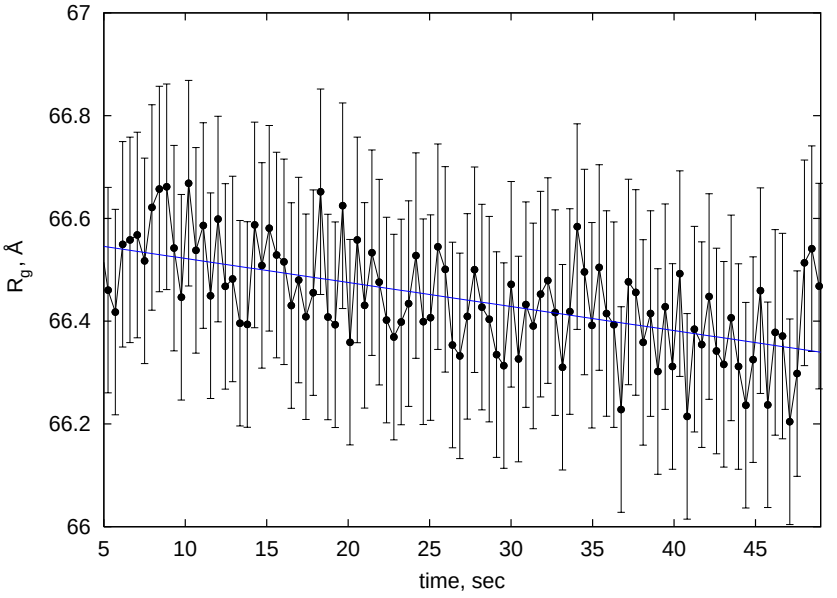

Figure 31: Linear fit of the data shown in Fig.30 (5 - 50 sec).

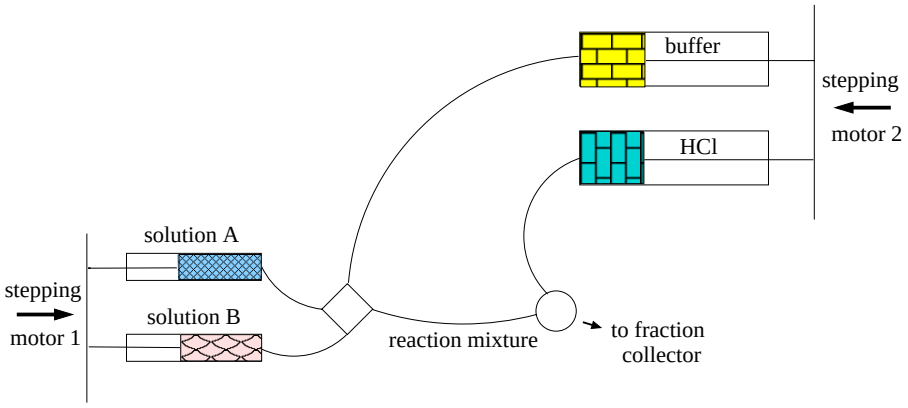

Figure 32: Scheme of the quenched flow device used for the ATPase activity assay.

certain period of time. After incubation is finished, the second stepping motor drives other two syringes. The first one is filled with the buffer, which displaces the reaction mixture from the storage tubing. The second syringe contains a diluted HCl solution to stop the reaction. The reaction mixture displaced from the storage tubing with the buffer coming from the first syringe is simultaneously mixed with HCl. The buffer remaining in the storage tubing is replaced by the new portion of the reaction mixture when the cycle is repeated.

The main results are shown in Fig.33. There are results of three experiments:

1) GroEL (solution A) mixed with ATP (solution B);

2) GroEL (solution A) mixed with GroES and ATP (solution B);

3) Preformed complex between GroEL and GroES made with ADP (solution A) mixed with ATP (solution B).

Concentration of GroEL in all cases was 86 μM (monomers), GroES was 88 μM, both when added separately and in the preformed complex, ATP always had a concentration 500 μM.

5.7 ATPase activity of GroEL (steady state)

These set of experiments was performed in order to check the quality of the protein preparations used in the small angle scattering experiments and crystallisation. Results obtained are in line with the published data. Steady state rate of ATP hydrolysis by GroEL in these preparations was always in the range of 3,5/min per monomer of GroEL. Actually, errors in such measurements come mostly from errors in estimation of the concentration of the protein. The inhibition of ATPase activity of GroEL by aluminium and beryllium fluorides was demonstrated for the first time.

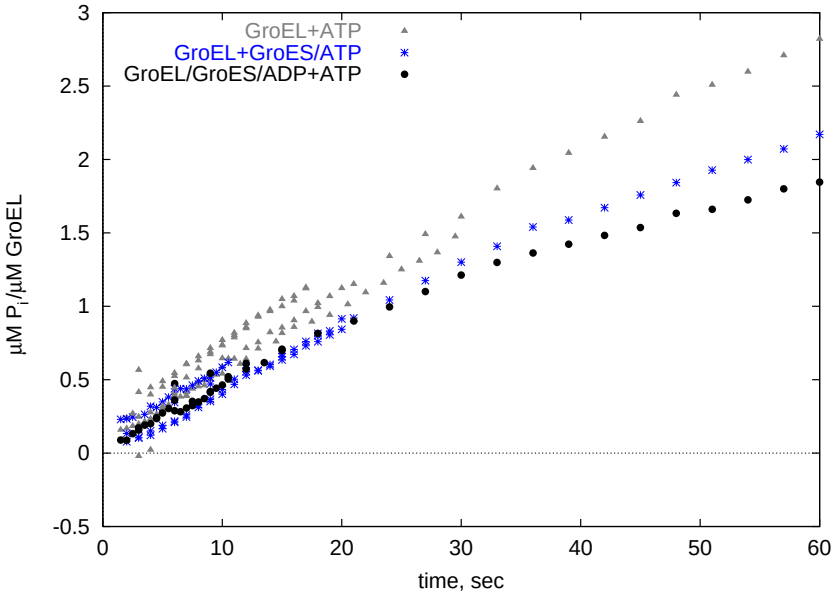

Figure 33: Fast kinetics of the hydrolysis of ATP by GroEL with or without GroES. Concentrations: GroEL (monomers) 86 μM, GroES (monomers) 88 μM, ATP 500 μM.

5.7.1 Choice of P_i estimation method

The steady state ATPase activity of GroEL was measured with the help of colour assay based on the reaction of malachite green dye with phosphomolybdate [61]. This reaction allows to measure the concentrations of phosphate in a broad range (5 to 100 μM) (typical calibration curve is shown in Fig.34).

For higher protein concentrations used in the time resolved experiments the assay was modified as described in [77]. The malachite green assay is rather sensitive to the high concentration of nucleotides, therefore for kinetics in the presence of ADP and AMP-PNP radioactively labelled [γ-^{32}P]ATP was used and products of reaction were detected by TLC. In this case the maximal turnover of the reaction was kept below 10% of the initial concentration of ATP.

5.7.2 K^+ is absolutely needed for GroEL ATPase

The absence of KCl does not prevent binding of ATP or ADP [123, 143], but hydrolysis of ATP is fully inhibited. Maximal activity is reached at concentration of KCl 20 mM (Fig.35). K_M therefore is about 10 μM, this value fits well with the published results [130].

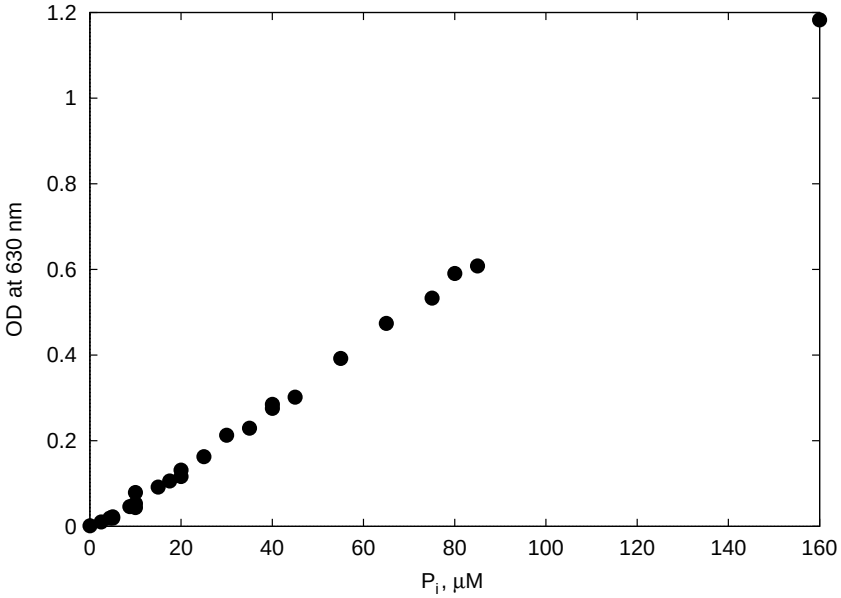

Figure 34: Calibration curve for the modified malachite green phosphate assay.

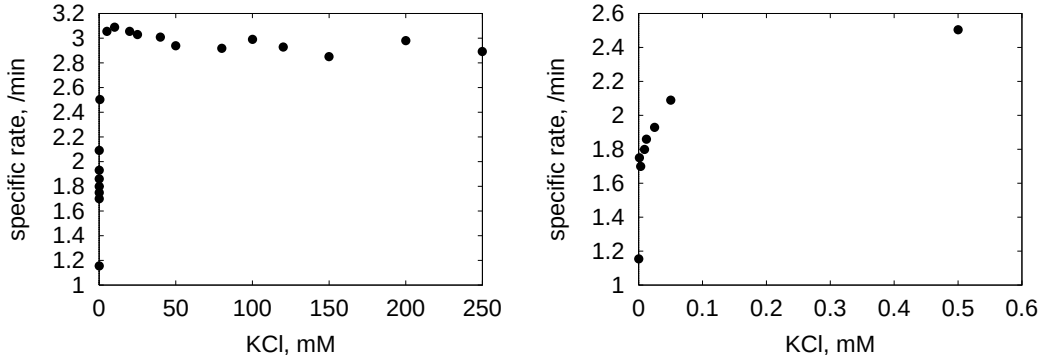

Figure 35: Dependence of the GroEL ATPase activity on the concentration of KCl. Concentration of GroEL monomers 0,9 μM, ATP 500 μM. The right panel is the magnification of the left one.

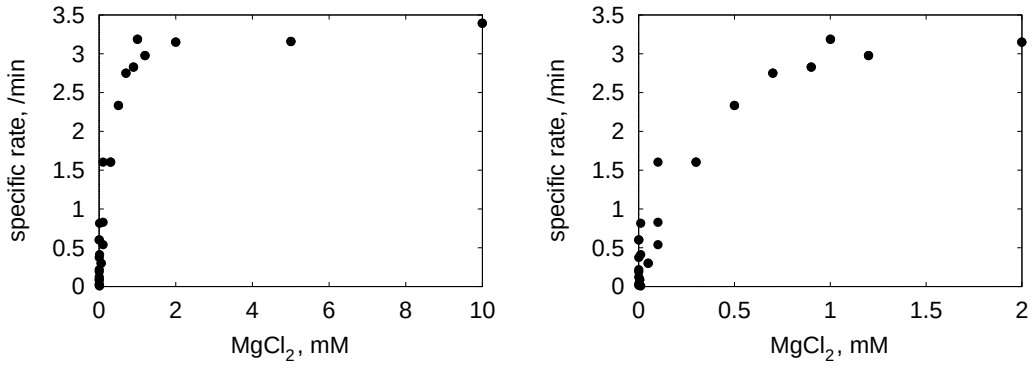

Figure 36: Dependence of GroEL ATPase activity on the concentration of $MgCl_2$. Concentration of GroEL 0,9 μM (monomers) and ATP 500 μM. The right panel is the magnification of the left one.

5.7.3 Dependence of ATPase activity on Mg^{2+}

Nucleotides can be bound only in a form of the complex with Mg^{2+}. In fact, almost all nucleotide binding and hydrolysing enzymes need Mg^{2+} to coordinate the substrate and to shield a negative charge of phosphate groups. The presence of this hexacoordinated ion in an active centre of hydrolysing enzymes assists the orientation of the phosphate moiety of a nucleotide for the cleavage to occur. As the crystal structure of *cis*-ADP GroEL-GroES complex revealed, Mg^{2+} ion is present directly in the nucleotide binding pocket of GroEL. Saturation of a steady state rate of hydrolysis occurs already at 2 mM $MgCl_2$, which gives an estimation of K_M about 200-300 μM (Fig.36).

5.7.4 Initial rate of hydrolysis depends on ATP

The complex allosteric behaviour of GroEL was discovered in experiments checking initial rate of hydrolysis depending on concentration of ATP [141]. The experimental curve shown in Fig.37 has a bisigmoidal shape reflecting two levels of the co-operativity. The maximal initial rate is achieved at 70 μM ATP, at this concentration one GroEL ring is saturated with ATP. Binding of the nucleotide within a ring proceeds with a positive co-operativity. In contrast, the second ring has a lowered affinity to the substrate. This effect is described as a negative co-operativity between two GroEL rings. At the concentration of a substrate exceeding 150 μM initial rate of reaction drops to half of the maximal rate level. The concentration of GroEL used in this test was 1 μM of monomers.

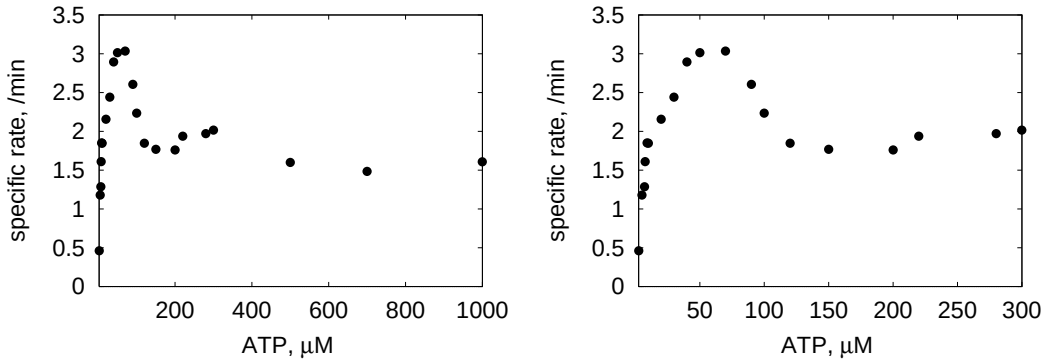

Figure 37: Initial rates of hydrolysis as a function of the concentration of ATP. Concentration of GroEL monomers was 1 μM. The right panel is the magnification of the left one.

5.7.5 Inhibition by GroES

GroES reduces the rate of ATP hydrolysis by GroEL to 50% of initial activity under steady state conditions (Fig.38). Effect is observed at equimolar concentration of GroES with respect to GroEL. One of the first explanations of this fact was so called "half-of-the-sites" activity of GroEL in the presence of GroES. That means, one ring of GroEL binds GroES in a tight complex and the second ring hydrolyses ATP with the same rate as without GroES [123, 124].

Later it has been demonstrated that the binding of ATP in the *trans*-ring of the *cis*-ADP complex of GroEL with GroES triggers dissociation of GroES, therefore *cis*-ADP complex is not stable in the presence of ATP. This dissociation is rather fast as compared to the rate of hydrolysis. In the presence of GroES the limiting step in the hydrolytic cycle reaction turns out to be not the cleavage of the phosphate bond itself, but a slow rearrangement of *cis*-ADP ring of GroEL after binding of ATP by *trans*-ring into an "activated" *cis*-ADP complex, readily dissociating afterwards [109].

5.7.6 Inhibition of hydrolysis by ADP

ADP inhibits the ATPase activity of GroEL completely, the typical experiment is presented in Fig.39. 50% effect is found at ADP concentration around 100 μM [70, 125]. This concentration corresponds to the apparent dissociation constant for binding of ADP by one ring of GroEL (Table 3). At the concentration above 5 mM, inhibition is practically complete.

The inhibition by ADP is a non-competitive process [73]. That means, that binding of ADP plays a regulatory role. ATP bound in the second ring of GroEL is not cleaved until ADP leaves the first ring. Therefore, if GroES is present in the

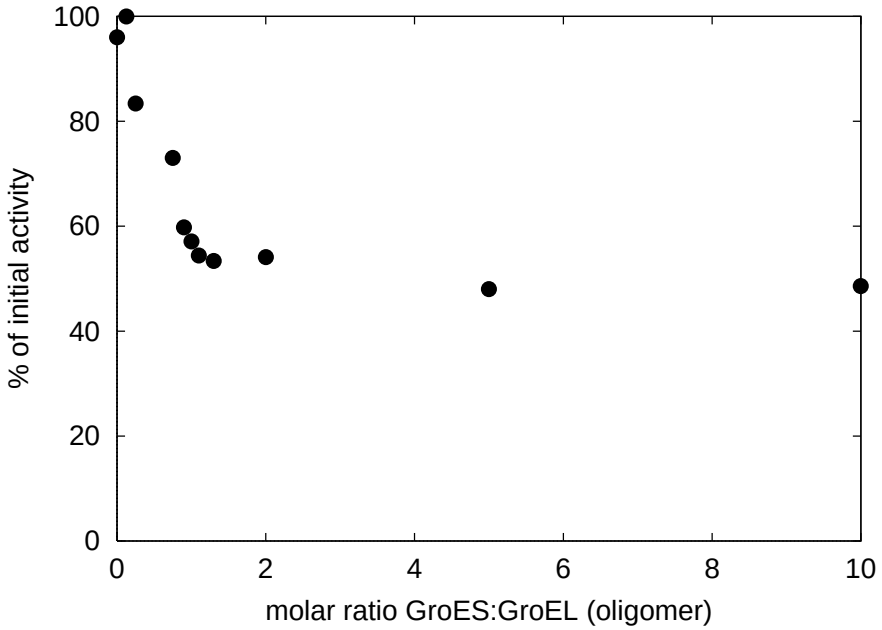

Figure 38: Inhibition of the ATPase activity of GroEL by co-chaperonin GroES. Concentration of GroEL monomers 1,4 μM, ATP 100 μM.

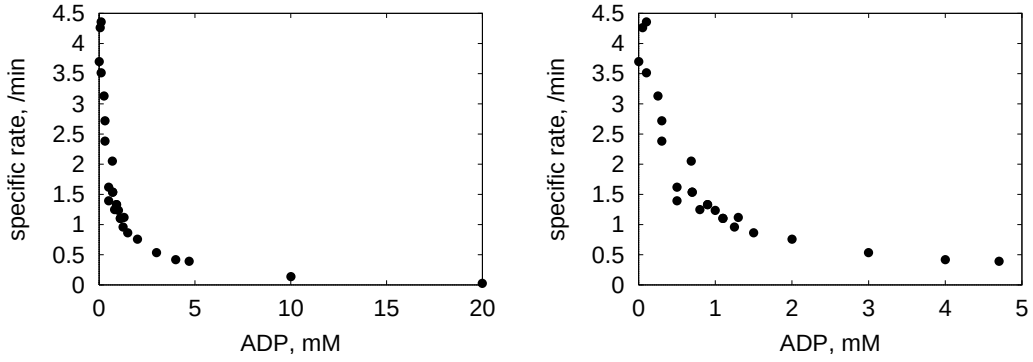

Figure 39: Inhibition of hydrolysis by ADP. Monomeric concentration of GroEL 23 μM, ATP 200 μM. The right panel is the magnification of the left one.

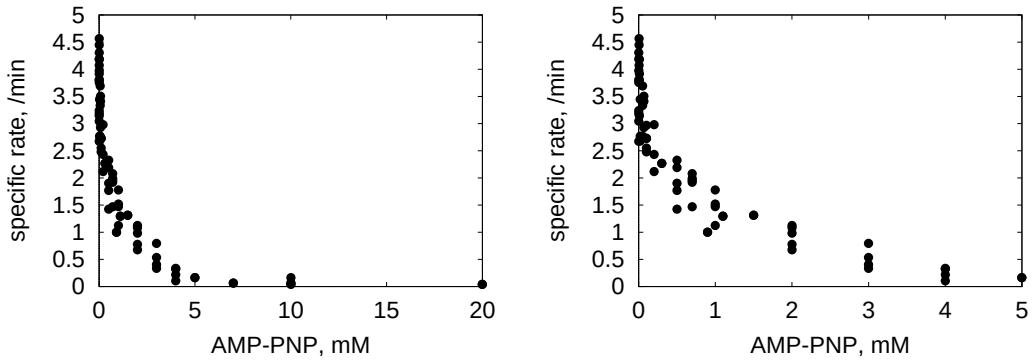

Figure 40: Inhibition of the ATP hydrolysis by AMP-PNP. Concentration of GroEL monomers 23 μM, ATP 200 μM. The right panel is the magnification of the left one.

reaction, the *cis*-ADP complex has to be dissociated after binding of ATP in the *trans*-ring to enable hydrolysis. This mechanism is the reason for the alternating activity of two GroEL rings within the reaction cycle.

5.7.7 Inhibition of hydrolysis by AMP-PNP

As a non-hydrolysable analogue of ATP AMP-PNP competes with ATP for the same binding site and inhibits the reaction. Results of titration of the ATPase activity of GroEL with AMP-PNP (Fig.40) are very similar to the already mentioned influence of ADP. 50% of inhibition effect is observed at the nucleotide concentration 200 μM. This finding is in line with the previous estimations of affinity of GroEL to this ATP analogue (Table 3, [68, 70]).

5.7.8 Influence of phosphate on the ATPase activity of GroEL

Inhibition effect of one of the products of ATPase reaction of GroEL, phosphate ion is presented in Fig.41. Dissociation of the products of hydrolysis is not the limiting step in the reaction cycle of GroEL [22]. Any visible influence on the ATPase activity starts from the concentrations of the phosphate above 40 mM. The saturation of the inhibition effect (about 1/3 of initial activity) is achieved at 200 mM and does not change significantly up to 400 mM. These data demonstrate why attempts to simulate an ATP bound state (or post-hydrolysis state) in the presence of ADP and concentrations of P_i in a range of 1-10 mM have failed [70, 123, 125]

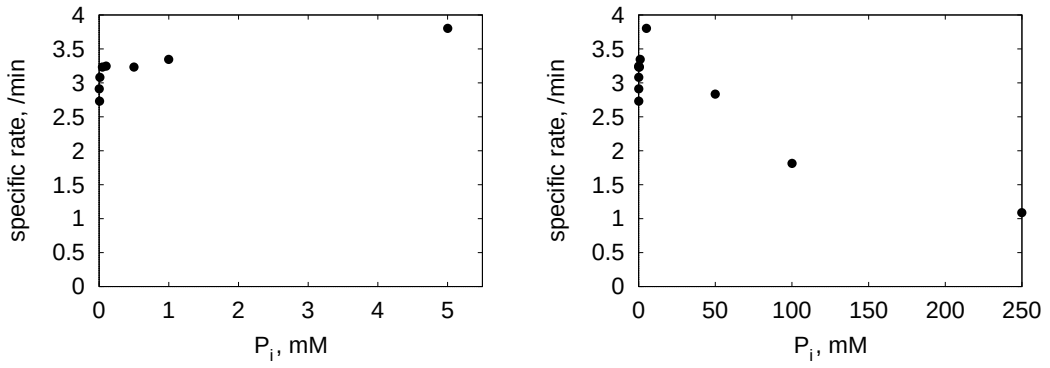

Figure 41: Inhibition of hydrolysis by phosphate. Concentrations: GroEL 23 μM, ATP 200 μM. The right panel is the magnification of the left one.

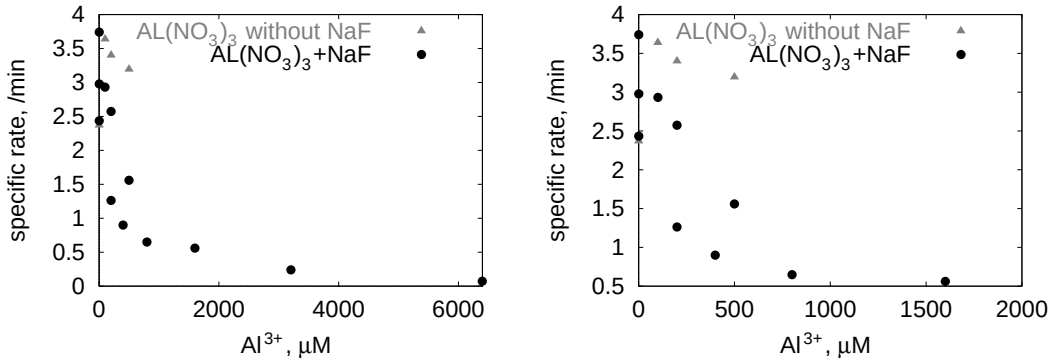

Figure 42: Inhibition of hydrolysis by aluminium fluoride complex. Concentration of GroEL 0,7 μM monomers, ATP 200 μM. The right panel is the magnification of the left one.

5.7.9 Inhibition of the ATPase activity of GroEL by AlF_x

The influence of the aluminium and beryllium fluorides on the steady state rate of the ATPase activity of GroEL (Fig.42) was a preliminary test for the crystallisation of GroEL in the presence of ADP complexed with fluoroaluminate.

NaF and $Al(NO_3)_3$ needed for the formation of aluminium fluoride complexes were present in the solution containing GroEL as well as in the solution of ATP which was used to start hydrolysis reaction. ADP in this case appears as a product of hydrolysis. As it was already mentioned fluoroaluminates are compounds which exist only in solution. The amount of fluoride-ions complexed with Al^{3+} depends on the concentration of the F^-. At 10 mM NaF the most populated complexes are negatively charged AlF_4^- and neutral AlF_3. Neither of the component alone (NaF and $Al(NO_3)_3$) influenced significantly the rate of the reaction. 50% of inhibition occurs at the concentration of $Al(NO_3)_3$ 500 μM. For the crystallisation was chosen the concentration 200 μM $Al(NO_3)_3$.

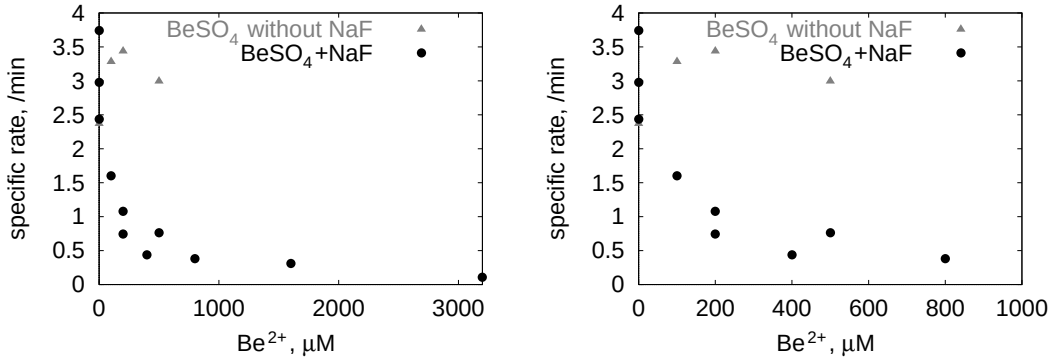

Figure 43: Inhibition of hydrolysis by beryllium fluoride complex. Concentration of GroEL 0,7 μM monomers, ATP 200 μM. The right panel is the magnification of the left one.

5.7.10 Inhibition of the ATPase activity of GroEL by BeF_x

This experiment was performed in the same way as the inhibition by AlF_x. Influence of BeF_x on a steady state rate of hydrolysis by GroEL is presented in Fig.43. The most populated species at given concentrations of salts is BeF_3^-. Comparison of Fig.42 with Fig.43 shows that the effect of beryllium fluoride is about two times more pronounced as compared with the aluminium salt. 50% activity remains at the 100 μM of $BeSO_4$ in the presence of 10 mM NaF.

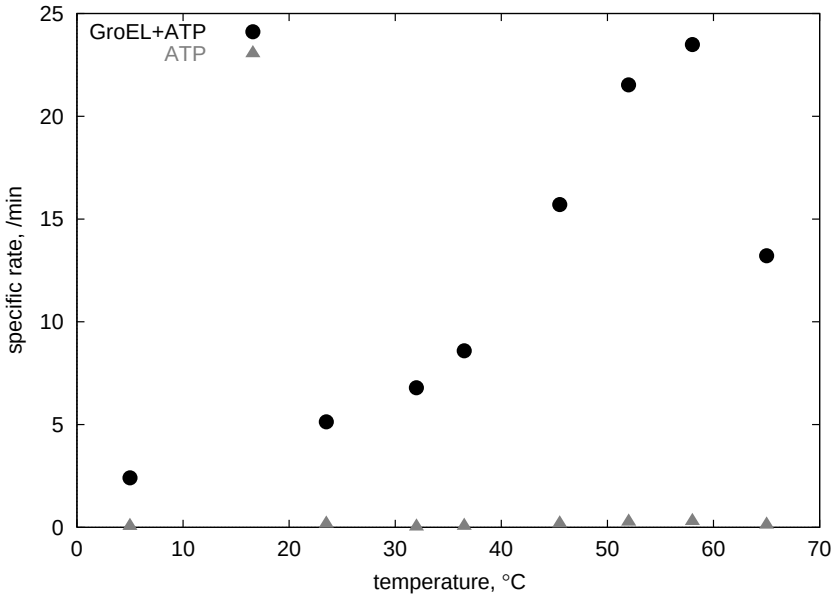

Figure 44: Temperature dependence of GroEL ATPase activity. GroEL was present in the concentration 0,7 μM of monomers, ATP 100 μM.

5.7.11 Temperature dependence

The temperature dependence of the steady state rate of hydrolysis (Fig.44) was checked in order to test the thermostability of the chaperonin. Reaction rate shows non-linear increase up to the temperature 57°C, then sharply declines probably due to thermal denaturation of the protein. Such a behaviour is in agreement with the published results [97]. Spontaneous hydrolysis of ATP in the absence of protein is negligible in comparison to the enzymatic reaction.

6 Discussion

Description of the reaction cycle of GroEL consists from the characterisation of distinct conformational states of GroEL having different affinities to nucleotides, GroES and substrate protein and from estimation of kinetic constants for the transition of the system from one state to the other. Small angle scattering was used here for both purposes.

Neutron small angle scattering was used to characterise the structural changes of one of the components of chaperonin system, namely GroES upon binding to GroEL in the presence of ADP and for the estimation of the affinity of GroEL to the second bound GroES in symmetric chaperonin complex.

Small angle x-ray scattering in combination with stopped flow device enables time resolved measurements of structural parameters during a single cycle of ATP hydrolysis by GroEL and GroEL-GroES complex.

6.1 Conformational states of the chaperonins studied by SANS

6.1.1 Matching point of pD-GroEL

Partial deuteration enabling a complete matching of one of the protein components of chaperonin system is a very important procedure in small angle neutron scattering study. Mass spectrometry was used to check the quality of chaperonin samples obtained from different *E.coli* strains (Fig.12). Although there is a broad distribution of partially deuterated species in the mass spectrum (see Fig.12), it was possible to make pD-GroEL practically invisible at 97% D_2O. These protein preparations were successfully used in SANS experiments.

The intensity of scattered by protein neutrons extrapolated to $q = 0$ depends on the molecular weight of the protein. Therefore intensities of the neutrons scattered by GroEL are two orders of magnitude higher than that of scattered by GroES. This problem of all small angle scattering methods one can overcome by the complete matching of the largest component of the reaction. This allowed to compare conformational state of GroES free in solution and bound to GroEL, otherwise contribution of GroES to the scattering of the GroEL-GroES complex is negligible. As seen in the Fig.13, being just two percent of D_2O content in buffer higher or lower than the matching point GroEL still has a considerable influence on the shape of $p(r)$ function of the complex. In the case of 95% of D_2O, GroEL has a negative contrast to a buffer, which is seen as a negative part of the distance distribution function. In 99% D_2O the contrast of pD-GroEL is positive. GroEL contribution to the pair distances in the complex is noticeable

at the distances above 90 Å. At 97% D_2O, which is exactly the matching point there is no visible GroEL contribution to the $p(r)$ and this function reflects only the structural features of GroES.

6.1.2 Dissociation constant for binding of the second GroES to GroEL

Symmetric complex was formed in the presence of unhydrolysable analogue of ATP AMP-PNP. Since it is well demonstrated that this nucleotide supports symmetric complex formation [32, 87], AMP-PNP was chosen for a titration experiment in order to stabilise this conformation, which is otherwise transient.

Symmetric complex is seen as two peaks in the distance distribution function. The second peak corresponds to the distance between the centres of mass of two GroES bound in symmetric complex. Due to the different affinities of both GroEL rings to GroES (described as a negative co-operativity between the rings), the symmetric complex is actually not quite symmetric. It is not possible to conclude anything about the shape of GroEL in this experiment, because it is well matched.

There is not much data available about the formation of the symmetric complex, although the weak affinity of the second GroES to GroEL even in the presence of ADP was estimated to be 555 μM (Table 4). This fact is in agreement with numerous studies, where in the presence of ADP such particles were never observed. The structural reasons for this are more or less clear from the structure of the GroEL-GroES complex with ADP. Outward movement of the equatorial domains in the *cis*-ring makes it impossible to keep interring contacts without compensating rearrangements of equatorial domains in the *trans*-ring [139, 137].

The fraction of symmetric particles was increased significantly when GroEL was allowed to bind a mixed population of adenine nucleotides [51], AMP-PNP and ADP in this case. It fits well in the reaction scheme described in [26, 73], where asymmetry of both rings is maintained throughout the cycle.

The formation of the symmetric complex can be described by the following scheme:

$$[\text{GroEL}]+[\text{GroES}] \underset{k_{-1}}{\overset{k_1}{\rightleftharpoons}} [\text{GroEL} * \text{GroES}]+[\text{GroES}] \underset{k_{-2}}{\overset{k_2}{\rightleftharpoons}} [\text{GroES} * \text{GroEL} * \text{GroES}],$$

$$K_{d2} = \frac{[GroEL * GroES][GroES]}{[GroES * GroEL * GroES]}$$

$$[GroES]_{total} = [GroES]_{free} + [GroEL * GroES] + 2[GroES * GroEL * GroES]$$

where $[GroES*GroEL*GroES]$ is proportional to the height of the second peak on the $p(r)$ of the symmetric complex.

$$[GroEL]_{total} = [GroEL * GroES] + [GroES * GroEL * GroES]$$

therefore,

$$[GroEL * GroES] = [GroEL]_{total} - [GroES * GroEL * GroES]$$
$$[GroES]_{free} = [GroES]_{total} - ([GroEL]_{total} - [GroES * GroEL * GroES]) -$$
$$-2[GroES * GroEL * GroES] =$$
$$= [GroES]_{total} - [GroEL]_{total} - [GroES * GroEL * GroES]$$

The main assumption in this model is:

$$k_1 \gg k_{-1}$$

$$K_{d1} = \frac{k_{-1}}{k_1} = 1 \div 5\ nM$$

In other words, all GroEL oligomers bind at least one molecule of GroES, there is no free GroEL at these conditions.

It is not possible to distinguish between free GroES and such bound to the asymmetric complex from $p(r)$ functions. But it is well known that this binding is a very tight one (Table 4). It is in the range of 1 nM: 0,6 nM [58], as measured by SPR in the presence of 2,5 mM AMP-PNP.

The K_d for the second GroES that results from this titration is approximately 0,5 μM.

6.1.3 GroES changes its conformation when bound to GroEL

Two sets of SANS experiments were carried out in order to compare the structure of chaperonin and co-chaperonin free in solution and bound to each other in the presence of ADP. Using a contrast variation method makes it possible to match one of the protein in the complex.

The first experiment was performed in the conditions of complete matching of GroES.

Comparison of distance distribution functions of unliganded GroEL and GroEL in complex with GroES (which is possible only in the presence of nucleotide) as

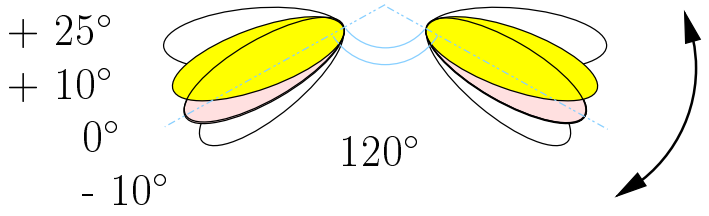

Figure 45: Schematic view of changing the angle between the core subunits of GroES used in the model calculations

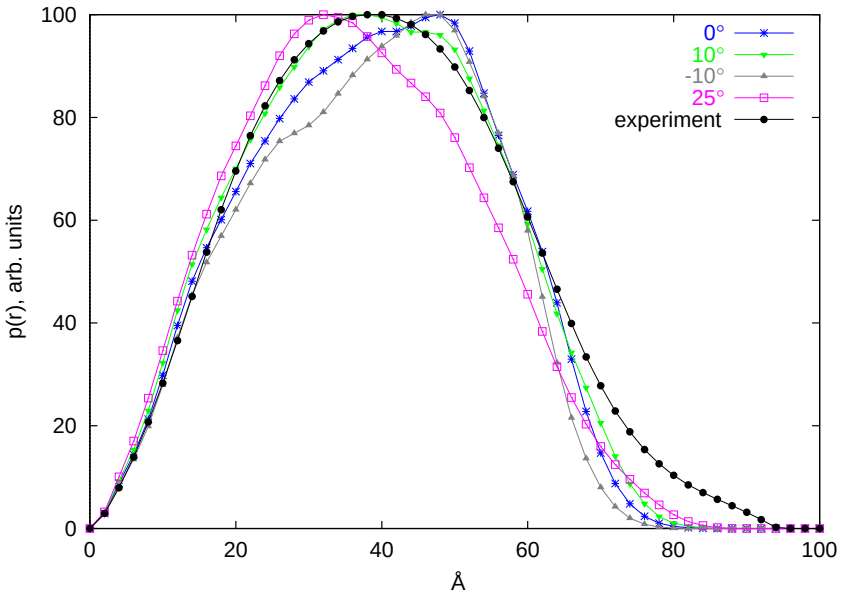

Figure 46: Distance distribution functions calculated from crystallographic model of GroES with systematically varied angle between core domains. Experimentally obtained $p(r)$ function for GroES in complex with GroEL is shown for comparison.

shown in Fig.16 does not reveal big changes between them. These differences although outside of experimental errors, but still too small to get any structural information. GroEL is too large and influence of domain rearrangement on the shape of $p(r)$ function is relatively small.

In the second experiment GroEL was fully matched and scattering curve of GroEL-GroES complex reflects only scattering of GroES oligomer.

The conformation of GroES in the *cis*-ADP complex as it is seen in SANS experiments is not the same as in the crystal structure of the asymmetric chaperonin complex [137]. Calculation of scattering curves from the crystallographic data and molecular modelling simulations were performed by Dr. M.Rößle and Dr. T.Hermann.

Crystal structure of free GroES was used for calculation of distance distribution function which can be compared with the experimental data. This comparison revealed that the $p(r)$ of free GroES in the crystal does not differ significantly from the $p(r)$ of free GroES calculated from the experimentally obtained scattering curve.

The structure of GroES in the *cis*-ADP complex [137] is similar to the crystal structure of free GroES [65] with the exception of mobile loops, which are fixed in the complex and disordered in the crystal of free GroES. The crystallographic data for the free GroES could not be applied directly as a model, because of the unresolved mobile loops (Glu16 to Ala33) of all but one subunits. Therefore the only resolved loop from one subunit was added to the rest of subunits in three different conformations, generated by the simulated annealing starting from the conformation of GroES in the crystal (these calculations were made by Dr. T.Hermann). Thus, $p(r)$ functions calculated from the x-ray data are in principle the same for GroES in the *cis*-ADP complex and free GroES and look similar to the conformation of the free GroES seen by SANS.

Comparing $p(r)$ obtained for three different conformations of mobile loops of GroES molecule showed that these changes do not alter the overall shape of the molecule as much, as it results from the SANS experiment.

The $p(r)$ for GroES in complex with GroEL obtained from neutron scattering solution data differs from the $p(r)$ calculated from atomic coordinates of the *cis*-ADP GroEL-GroES complex. As one can judge from the comparison of the distance distribution functions, GroES becomes more flat upon binding to GroEL. The shoulder in the $p(r)$ at the lower distances that is typical for hole structures vanished. In order to understand which intramolecular movements can cause those changes one can simulate domain movements in GroES, using crystallographic coordinates. These calculations were successfully performed by Dr. M.Rößle. Flatter structure was simulated by different angles of the opening of GroES dome (schematically these variations are shown in Fig.45 and $p(r)$

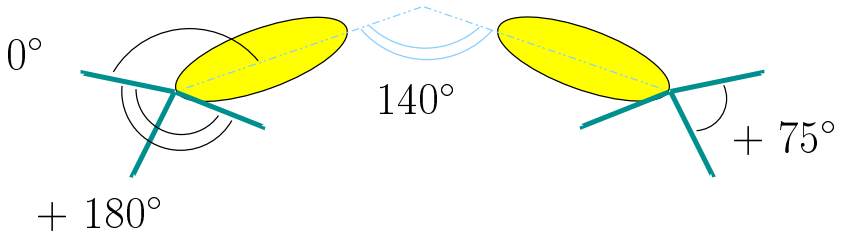

Figure 47: Schematic view of the the GroES with the fixed angle of the dome opening (+10°) with the varied angle between the core domain and the mobile loop.

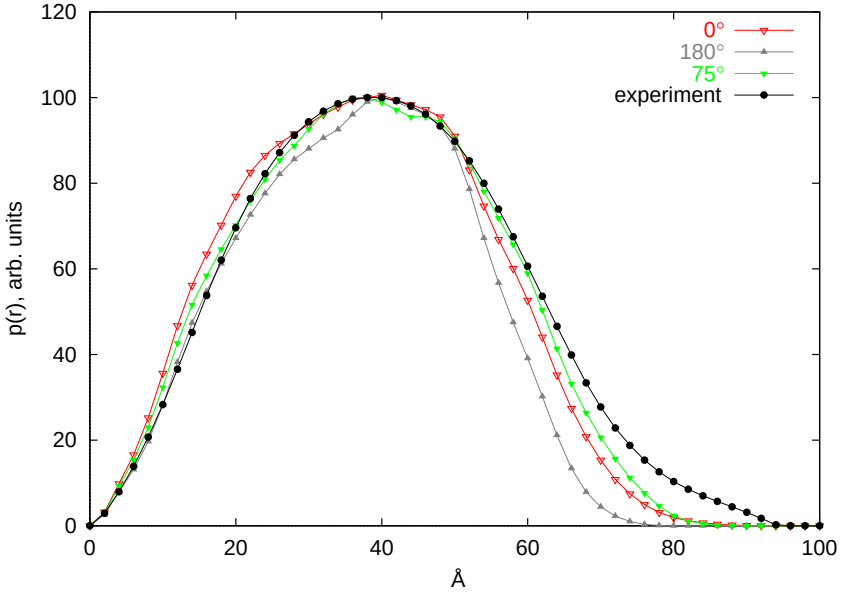

Figure 48: Distance distribution functions calculated with systematically varied angle between core domains of GroES subunits and flexible loops. Experimentally obtained $p(r)$ function for GroES in complex with GroEL is shown for comparison.

functions calculated from these models are compared in Fig.46). The model with +10° dome opening fits best the experimental data.

The second parameter varied was the angle of rotation of the mobile loop with respect to the core of the GroES subunit. The mobile loops of each monomer can be rotated outwards too. Comparison of calculated distance distribution functions for different angles showed that these changes bring about mostly to the distances around 50 Å. Schematically the tested structures are presented in Fig.47. The distance distribution functions calculated for three angles are shown in Fig.48.

The best fit for the experimental data was obtained from a model where GroES dom opens by 10° (+10) and mobile loops are fixed at the position 75° outwards

[121].

Some discrepancies between the structure of the protein in the crystal and in solution are not unusual. One reason could be that crystallographic buffers are far from physiological conditions, and conformation fixed in protein crystals is one of possible intermediate states existing at the equilibrium in solution. Thus, SANS even with its loss of information due to spatial and time averaging may be a very useful supplement for high resolution x-ray crystallography.

6.2 Perspectives of the crystallisation of different transition states of GroEL

6.2.1 Shifting of the one ring of GroEL along the interring plane

Crystallisation of GroEL with different analogues of ATP and ADP$*$P$_i$ transition states of hydrolysis results in the partially solved structure of GroEL co-crystallised with ADP and AlF$_x$. Fluoroaluminate exists in solution at given concentrations of aluminium and fluoride in two forms. There are AlF$_3$ and AlF$_4^-$. The crystals obtained with AlF$_x$ present both in drop and in reservoir have different cell parameters as compared to the known x-ray structures of GroEL (Table 8). This allows one to expect differences in the GroEL conformational state.

There are three GroEL tetradecamers in the unit cell. Two of them have an identical conformation closely resembling conformation of GroEL mutant obtained by Braig et al. [15, 16]. The third one differs significantly from the first two chaperonins. This molecule is the most interesting in this crystal. The rings of this oligomer are shifted about 6 Å along an interring plane as can be seen in Fig.49. This figure was obtained by superposition of the two molecules of GroEL in the crystal unit cell.

Preliminary interpretation of this finding is as follows. One can speculate about mechanism of hydrolysis. As demonstrated by numerous time resolved ATP binding experiments [22, 68, 73, 143] the binding of ATP is at least one order of magnitude faster than hydrolysis. Hydrolysis occurs in a concerted fashion in one ring at time when GroES is present [124]. In the absence of GroES as a regulator of GroEL activity the co-operativity in hydrolysis of ATP is less pronounced. If the reaction proceeds really in "all or nothing" fashion, time resolved kinetics would reveal a stepwise increase of the concentration of P$_i$, which is not observed.

ATPase assay used implies denaturation of proteins to stop the reaction. After denaturation the products of hydrolysis are no longer bound to GroEL. It was also demonstrated [22] that dissociation of products is not a limiting step in steady

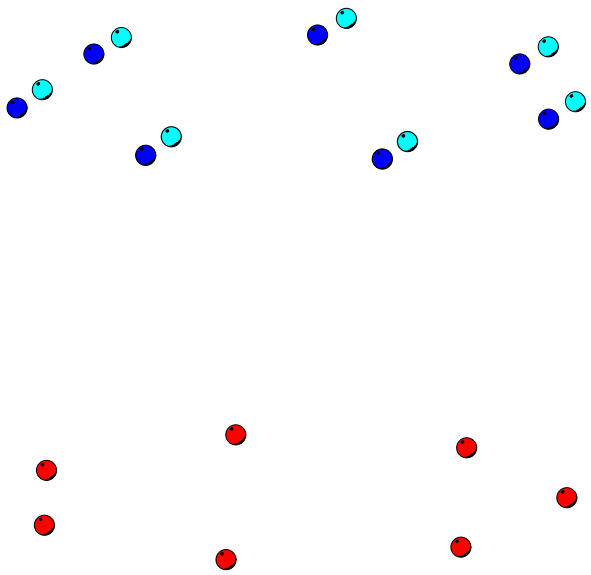

Figure 49: Positions of the centres of mass of GroEL subunits in the crystal grown with ADP$*$AlF$_x$. The lower rings are superimposed in order to emphasise the difference in a conformation of the upper ring between both GroEL molecules. Red points show the positions of centres of mass of the lower ring of GroEL; blue points: centres of mass of the upper ring if it were unshifted; cyan: positions of the shifted subunits in a third molecule of GroEL in the this crystal cell.

state hydrolysis in the case of GroEL without GroES.

It is also shown that a huge concentration of phosphate (about 0,5 M, Fig.41) should be used to suppress the dissociation of the products after reaction. Anyway, hydrolysis itself could be not, or better to say, not so much co-operative in comparison to the binding of nucleotides.

One can speculate that the GroEL with shifted ring is the GroEL performing a continuous hydrolysis of bound nucleotides. GroEL ring makes a turn around a shifted axis performing a round of hydrolysis when all subunits of the ring contain a substrate. So, that all subunits cleave of γ-phosphate one after the other. The binding or ATP must bring a ring into an ATP bound conformation. Nucleotide binding according to all published data happens in a concerted way, as a highly co-operative transition. Then hydrolysis, probably, proceeds in a sequential fashion releasing the products immediately after cleavage.

6.3 Time resolved conformational changes of chaperonin during hydrolytic cycle

Description of the reaction cycle includes characterisation of intermediate states of the reaction and also kinetics of transitions between them. SAXS allows to collect scattering curves of the protein sample with sufficient statistics using expositions as low as 50 msec. Taking into account dead time of the CCD detector the smallest possible time slices for kinetic measurements are 150 msec. Time resolution used here was 300 msec.

6.3.1 Conformation of GroEL after binding of ADP remains stable

The value of radius of gyration of GroEL stays at the same level through all the time course of the experiment shown in Fig.19. The absence of any visible time dependent changes allows to propose that the nucleotide binding is too fast to be detected within the time resolution used in these experiments.

6.3.2 Dynamics of the R_g of GroEL during single turnover of hydrolysis

Time resolved measurements of the ATPase activity of GroEL (page 55) and known steady state rate of reaction (Table 2) have demonstrated that the first turnover of the hydrolysis is finished in 6-8 sec after mixing of GroEL with ATP. In contrast to the linear behaviour of the ATPase activity, there is a biphasic behaviour of R_g during the single round of hydrolysis (Fig.50). During first 8 sec

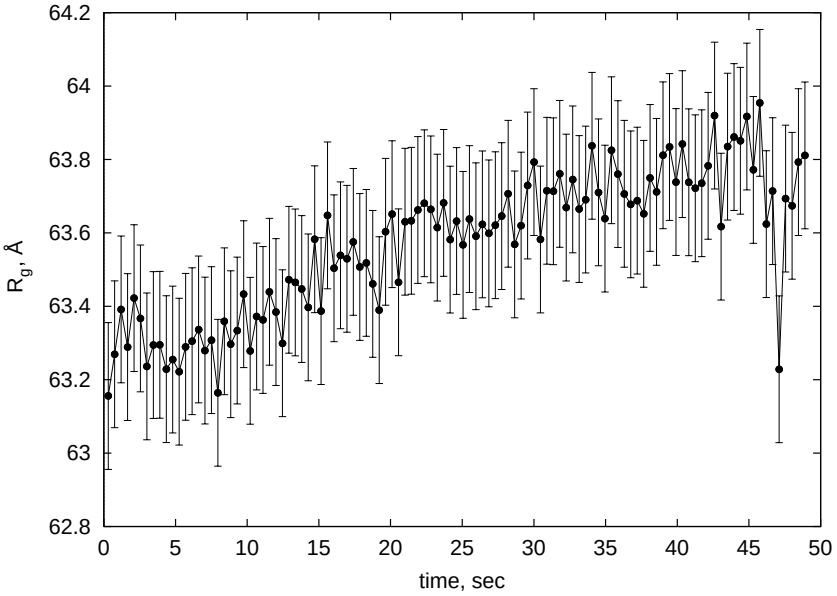

Figure 50: Time dependence of R_g of GroEL (88 μM of GroEL monomers) after mixing with 50 μM ATP.

radius of gyration remains stable at the level similar to the unliganded GroEL and GroEL after mixing with ADP (63,3 Å). After 8 sec R_g starts to raise reaching saturation in approximately 30 sec with R_g 63,8 Å.

First phase during which R_g does not change corresponds to the hydrolysis itself. Cleavage of the bond between γ- and β-phosphates of ATP starts immediately after the binding of substrate, as revealed by the time resolved ATPase activity assay. The hydrolysis starts immediately after binding of ATP which, in turn, occurs much faster than SAXS can register. One can speculate that the R_g value in the first phase (63,3 Å) reflects a hydrolysing state of GroEL. This state is practically a mixture of at least three GroEL species: GroEL(ATP), GroEL(ADP) and (at the very beginning) an empty GroEL. In this experiment binding of ATP is faster than the time resolution of the experimental device. It is not clear whether binding of one molecule of ATP already triggers a transition of the whole ring into the ATP bound conformation. GroEL free and GroEL containing ATP are not distinguishable. This phase could be interpreted as an ATP bound or "hydrolysing state" of GroEL having the same R_g as an unliganded GroEL.

The second phase could be explained by involving the slow relaxation of an active, "hydrolysing" state of GroEL to the "activated" ADP bound state after one round of reaction. When hydrolysis is completed, GroEL relaxes to another ADP bound conformation, which does not have the same R_g as an ADP bound GroEL immediately after hydrolysis. This second GroEL(ADP) state has a higher R_g

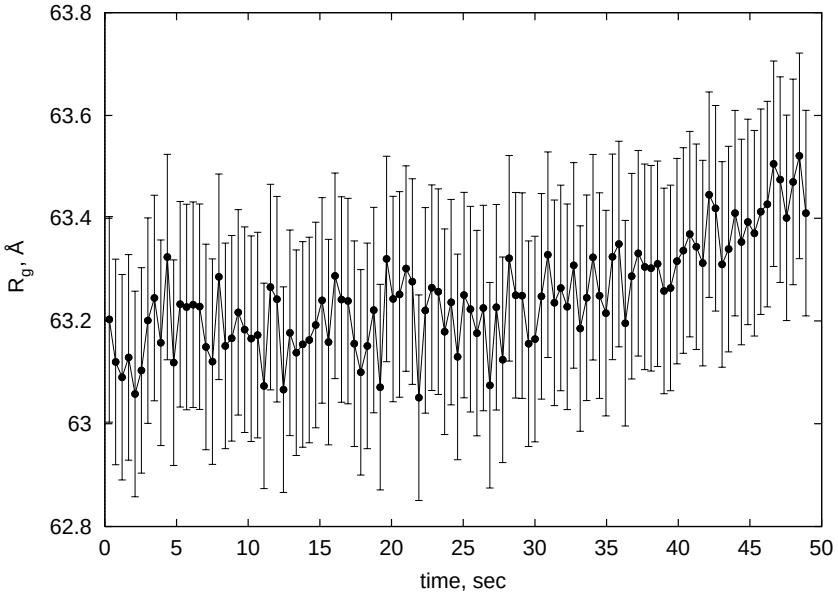

Figure 51: Time dependence of R_g of GroEL (88 μM monomers) after mixing with 500 μM ATP.

(63,8 Å). Rate of this transition is 0,04/sec. From such an interpretation two ADP bound conformations of GroEL could be outlined: "ground" (R_g 63,3 Å) observed in the control experiment and "activated" (R_g 63,8 Å). Dissociation of ADP in this case is also not observed. Or, better to say, in the observed timescale GroEL does not return to the unliganded state from the ADP bound state.

One can suppose that after some time this "activated" ADP bound conformation of GroEL have to return to the unliganded state after dissociation of nucleotide or adopt the ADP bound conformation similar to that obtained after mixing of GroEL with ADP ("ground" state). In order to answer this question one needs to measure this sample after a long time, for example, after one hour. If this suggestion is true, conformation with R_g 63,8 Å must return to the conformation having R_g 63,3 Å, thus finishing the cycle.

6.3.3 Conformations of GroEL during steady state hydrolysis

This experiment (Fig.51) is an attempt to simulate a steady state conditions, substrate is present in the concentration sufficient for ten rounds of reaction. R_g shows also a biphasic time dependence. As in the previous case radius of gyration remains constant during the first phase. However, the duration of a first phase increases significantly compared to the previous case. The main problem is that it is not a 10-fold increase, which could be expected, the duration of a first phase is increased only 3-4 times. A reasonable explanation would be a hydrolysis by

both rings of GroEL functioning independently on each other.

The concentration of ATP used in this experiment is enough to overcome a negative co-operativity between two rings (Fig.37). At 500 μM a second ring starts to bind a substrate. The concentration of substrate ATP decreases permanently due to hydrolysis. According to Fig.37, the maximal reaction rate is achieved at approximately 100 μM ATP. At this concentration only one ring of GroEL binds and cleaves ATP during one round of reaction. Therefore, it could be awaited that the rate of reaction increases upon depletion of substrate ATP. Additional complication to this picture is introduced by the ADP, whose concentration grows continuously during hydrolysis. ADP is a non-competitive inhibitor of the ATPase activity of GroEL with apparent inhibition constant around 1 mM according to the different estimations ([73], Table 3 and page 61). That means, that after 3-4 rounds of hydrolysis there is already enough ADP in the solution to influence observably the reaction rate. These two effects can compensate each other, yielding more or less constant rate. It is also true that out of SAXS data one can not obtain the rate of hydrolysis. The only parameter measured here is a conformational change of GroEL. As the time resolved ATPase assay shows, the rate of ATP hydrolysis remains constant during time course of the reaction.

The second phase is an increase in R_g as in the case of single turnover of reaction, but it does not reach a saturation in the given time scale. It could be explained as in the previous case by introduction of the second ADP bound conformation of GroEL ("activated" state).

6.3.4 Single turnover of hydrolysis in the presence of GroES, asymmetric complex formation

GroEL was rapidly mixed with solution containing equimolar amount of GroES and ATP. The sequence of events in this case could be described by a scheme shown in Fig.52. Fig.53 presents corresponding time course of radius of gyration.

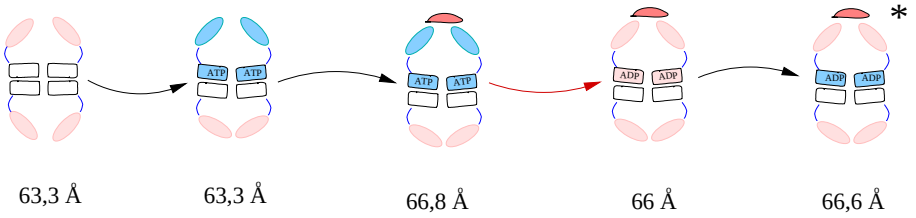

Figure 52: Schematic view of the reaction steps during the formation of the asymmetric GroEL-GroES complex after addition of ATP (single turnover). Hydrolysis is shown by a red arrow.

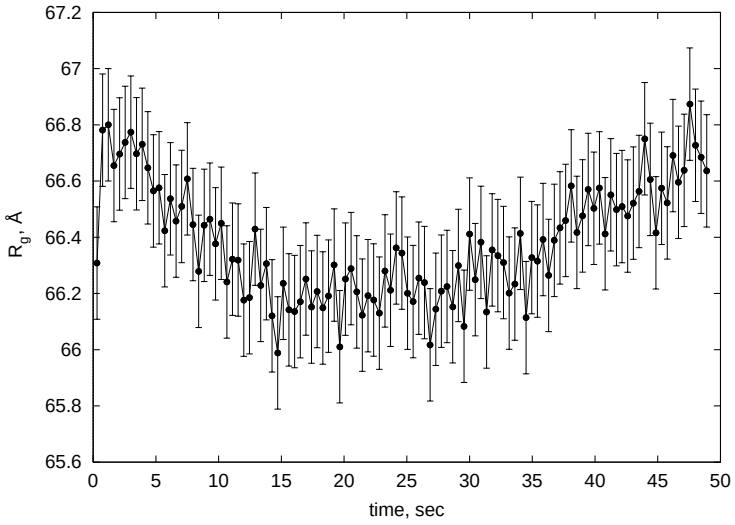

Figure 53: Time dependence of R_g during formation of GroEL-GroES complex in the presence of 50 μM ATP. Protein concentrations (monomers): GroEL 88 μM, GroES 44 μM.

First two states (binding of nucleotides by GroEL) are not resolved. This reaction is too fast to be seen within the time resolution used for these experiments. Nevertheless already from these data one can estimate a rate of GroES binding using an initial part of the curve. A rate constant has a value $1{,}14\times10^6$/M·sec (Table 4). After the binding of GroES R_g of the GroEL-GroES complex is significantly higher (3 Å) than R_g of GroEL. The following decay in R_g corresponds to the hydrolysis reaction itself and proceeds with the same rate constant. The hydrolytic step is completed in 27 sec and conformation of the complex at this time point resembles closely the *cis*-ADP GroEL-GroES complex with an R_g value of 66,1 Å. The following step which is a more slow relaxation of *cis*-ADP complex to the state with significantly higher R_g could be explained by the introduction of an additional conformation of the asymmetric GroEL-GroES. It is similar to the "activated" ADP bound state (designated by * in Fig.52) observed in the experiments with the fluorescently labelled GroEL of Rye et al. [70, 109].

Thus, the first phase is a sequential binding of ATP and GroES. It is accomplished in the first 5 sec. The next step is a hydrolysis, which is finished after 27 sec. The third phase is a relaxation of "hydrolysing" conformation of the complex. It seems that *cis*-ADP complex of GroEL with GroES appearing immediately after reaction and *cis*-ATP complex does not have the similar R_g, in contrast to the results obtained without GroES. In the absence of ATP, which triggers a dissociation of the *cis*-ring, *cis*-ADP complex of GroEL with GroES is stable, but undergoes a transition to another ADP bound conformation ("activated").

6.3.5 *cis*-ADP asymmetric complex during single round of hydrolysis

The experiment presented in Fig.55 differs from the previous one, which implies the formation of the *cis*-ATP complex between GroEL and GroES, in the initial state of the reaction components. In this case preformed *cis*-ADP GroEL-GroES complex was brought to react with ATP.

The reaction scheme suggested for this experiment is given in Fig.54. As shown in Fig.55 R_g shows a biphasic time dependence. First phase is an exponential increase in R_g from the starting level of 66,0-66,1 Å (*cis*-ADP) to the "hydrolysing" conformation having R_g 66,5 Å.

During the first phase R_g raises to the level similar to "hydrolysing" state (66,5 Å). There is no visible dissociation of GroES. Possible reason for this is that GroES exchange is too fast to be seen at the given time resolution. This step could be placed at the very beginning of the reaction, because it should happen before hydrolysis takes place.

Next phase is a decrease of R_g to the "ground" level of 66,1 Å with the apparent rate constant 0,13/sec. It corresponds to the steady state hydrolysis rate by GroEL (without inhibiting effect of GroES, which lowers the rate to 50%). Therefore, the second phase could be considered as a hydrolytic step of the reaction. This is in agreement with results obtained in time resolved ATPase measurements, showing that in the presence of GroES release of the phosphate after cleavage of ATP occurs with the same rate as in the absence of GroES.

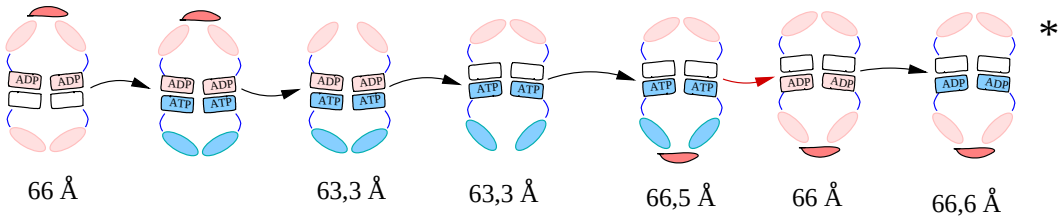

Figure 54: Schematic view of the reaction steps occurring when preformed *cis*-ADP GroEL-GroES complex is mixed with an equimolar amount of ATP.

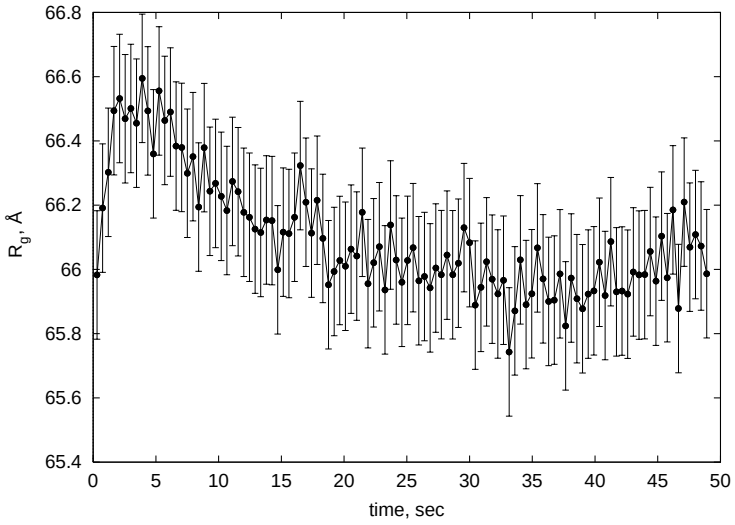

Figure 55: Time dependence of R_g of *cis*-ADP GroEL-GroES complex after mixing with equimolar amount of ATP (50 μM). Concentration of GroEL monomers 88 μM.

After 40 sec R_g shows some increase, but this phase is much less pronounced comparing with the experiment shown in Fig.53. Although the relaxation of the system to the "activated" ADP bound state is included in the scheme of the reaction in Fig.54, longer measurement would reveal whether this assumption is correct.

6.3.6 First round of the hydrolysis: structural changes and release of the phosphate

The main conclusions made from the results of the time resolved measurements of the ATPase activity of GroEL (page 55) and small angle x-ray scattering are summarised as follows:

1) First round of the hydrolysis proceeds with the same rate, no matter whether GroES is present or not. Inhibiting effect of the GroES becomes visible after approximately 10 seconds after the start of the reaction.

2) Binding of ATP is too fast to be detected by methods used.

3) Hydrolysis of ATP by the GroEL proceeds in a linear fashion, the subunits do not show any concerted action in the absence as well as in the presence of GroES. Otherwise one would expect a stepwise increase in the concentration of the phosphate. Despite of the hard attempts to detect any steps in the time course of the reaction, only a linear increase of the amount of P_i was observed.

6.4 Steady state ATPase activity of GroEL

Some measurements of the ATPase activity of GroEL were performed in order to test the quality of the protein preparation. The data obtained are in agreement with the published results.

The only measurement to be in contrast to the results obtained previously (described by Bochkareva et al. [90]) is the inhibition of the ATPase activity of GroEL by ADP. As it is reported ADP caused only 50% inhibition. Later this question was addressed by [73], where it was demonstrated that ADP inhibits ATP hydrolysis completely and inhibition is a non-competitive one. Apparent inhibition constant measured in this fluorescence assay is about 0,7 mM.

Inhibition of the ATPase activity in the presence of fluoroaluminates and fluoroberyllates was carried out as a control for crystallisation experiments for the first time.

7 Summary

The chaperonin system shows a rather high degree of conformational flexibility. During its reaction cycle (Fig.5) GroEL can adopt a lot of different conformations, which have different affinities to GroES, nucleotides and substrate protein. This raises the question whether the known x-ray structure of GroEL, GroES as well as the complex of both differs from the conformation of the protein in solution. Another aim of the present work was to study the transient states of the GroESL chaperonin system during its reaction cycle using x-ray and neutron small angle scattering as well as biochemical techniques.

Small angle x-ray and neutron scattering provide low resolution structural information obtained from molecules in solution. For this reason small angle scattering methods represent a very useful supplement to high resolution crystal structure analysis. One of the advantages of small angle neutron scattering is the possibility to make one of the reacting components invisible by contrast matching by means of D_2O and deuteration of the protein under study. This technique was used to analyse the solution structure of GroEL and GroES separately and in complex.

Differences between the solution and x-ray structure were identified by comparing the scattering curves or their Fourier transforms (distance distribution functions) with those calculated from crystallographic data. By changing domain orientation of the protein systematically, it was possible to find models which best fit the experimental data within the limits of accuracy of small angle neutron scattering data.

A comparison of small angle neutron scattering data with crystallographic model reveals that the conformation of GroEL and GroES free in solution is not significantly different from that in the crystal. GroES free has essentially the same conformation as GroES in the crystal. However, the conformation of GroES in solution changes significantly upon binding to GroEL. Moreover, these changes of the solution structure of GroES in the complex with GroEL are not found in the crystal structure of GroEL-GroES complex.

Solution data suggest that the GroES core domains forming the roof-like structure in complex with chaperonin become flatter and the mobile loops are turned down by 75° compared to the conformation of the mobile loops in the crystal structure of free GroES (Fig.45 and 47).

These data show that the structure of GroES bound to GroEL differs significantly in solution and in crystal. The significance of these different conformations in functional terms is not yet clear.

The most interesting intermediates in the reaction cycle of GroEL are the ATP-

bound states. These states are difficult to study, since ATP is hydrolysed permanently. Analysis of ATP-bound states must therefore include an analysis of kinetic parameters of transitions between these states.

Time-resolved small angle x-ray scattering is a new method applied to follow conformational changes of the chaperonin system during the first round of ATP hydrolysis. This technique takes advantage of the high flux synchrotron radiation, which allows measurement of scattering curves in the 300 msec range. An advantage of time resolved small angle x-ray scattering is that it provides direct structural information along with kinetic parameters. The structural information is restricted to information about changes of the radius of gyration (R_g), a structural parameter, which describes the overall shape of the molecule. Changes in R_g were used in order to follow conformational changes of the chaperonin system upon a single turnover of ATP hydrolysis.

Kinetic measurements appeared to be more sensitive than static measurements for determining small structural changes of GroESL. This is due to the fact that structural information (R_g) on different states at every stage could be obtained in one experiment.

The kinetics of R_g show rather interesting behaviour. In the absence of GroES there is a phase of about 8 sec, during which the radius of gyration remains constant (R_g=63,3 Å). This lag phase is followed by subsequent increase of R_g up to a value R_g=63,8 Å with a rate constant of k=0,04/sec.

In contrast to the structural parameter R_g which does not change within the initial phase, hydrolysis of ATP starts immediately after mixing of the reactants. This finding indicates that hydrolysis starts without change of GroEL conformation (detectable with small angle scattering). After 8 sec a rearrangement of GroEL monomers appears to occur, leading to the conformation with higher R_g (63,8 Å).

8 sec is the time interval required for one turnover of hydrolysis. It is therefore tempting to speculate that the rearrangement is triggered when hydrolysis is completed by all monomers in one ring.

One explanation for the increase of the radius of gyration could be that after hydrolysis the chaperonin enters a new transition state having an R_g=63,8 Å. Such a complex might be an "activated" GroEL(ADP), resembling the so-called "activated" T-state described earlier [70, 109]. The proposed "activated" GroEL(ADP)* conformation differs from the "ground" state by a higher R_g. The "ground" state is obtained simply by mixing of GroEL with ADP.

In the presence of GroES, the kinetic behaviour of the system is more complex. There is an initial increase of the radius of gyration by 3 Å, which is interpreted as binding of GroES to GroEL and formation of a GroEL(ATP)GroES complex.

During the first 5 sec after mixing of GroEL with GroES and ATP, R_g increases from the level corresponding to the unliganded GroEL (63,3 Å) to the value of GroEL-GroES complex with ATP (66,6 Å). Estimation of the rate of this reaction yields a value of k=1,14×10^6/M·sec.

The subsequent decrease of R_g within 10 sec from 66,6 Å to a value 66,2 Å probably reflects a conformational change of GroEL-GroES complex during hydrolysis. After the single round of hydrolysis is completed, the system relaxes slowly into a state with higher R_g= 66,8 Å, which might reflect an "activated" GroEL(ADP)GroES* complex as was suggested for GroEL without GroES.

If the assumption is correct that the kinetics show an"activated" ADP-bound state, the relaxation of the system into the ground state indicated by a decrease of the R_g has to be demonstrated, an experiment which requires an extension of the observation interval in the ATP-dependent kinetics. Another interesting modification of this experimental approach should include substrate protein in the ATPase cycle.

In conclusion: ATPase activity appears to be a non co-operative process, whereas the structural changes of GroEL subunits after hydrolysis show a concerted transition into an "activated" ADP- bound state.

Another intermediate of the chaperonin reaction cycle is the symmetric complex. This complex contains two GroES heptamers bound to opposite sites of GroEL. The symmetric complex can be stabilised by the non-hydrolysable ATP analogue, AMP-PNP. For this complex the dissociation constant for the second GroES molecule to the preformed GroEL-GroES complex was calculated for the first time from a titration curve of GroEL with GroES under contrast matching conditions for GroEL. Estimation of this parameter yielded a value K_d=0,5 μM. The centre-to-centre distance between the two GroES molecules in this complex was estimated to be 220 Å.

In the context of studies of the ATP-dependent GroEL conformations, small angle neutron scattering experiments were complemented by crystallographic studies. There are presently no high resolution data available for wild type GroEL complexed with ATP or ATP analogues. In order to simulate the transition states during hydrolysis, GroEL was co-crystallised with ADP and AlF_x. Complexes of ADP with aluminium and beryllium fluorides are widely used to simulate transition states of the ATPase reaction. The functionality of this analogue was supported by demonstrating its inhibitory effect on ATPase activity of GroEL.

The electron density map with a resolution up to 3,5 Å was obtained using molecular replacement. The unit cell contain three GroEL oligomers. Two of them show the same structure, while the third one shows a shift of the rings by 6 Å with respect to each other along the interring plane. A detailed analysis of this structure is in progress.

It is interesting to note that crystallisation conditions as well as the cell parameters found here differ from those previously published (Table 8).

First attempts were made to analyse the complex of chaperonin with substrate protein. Wild type GroEL was co-crystallised with the substrate protein citrate synthase, the folding mutant G276A. Preliminary structure analysis shows that GroEL does not differ from the known structure of mutant GroEL alone, which was used as a model for molecular replacement. No electron density was found inside of the GroEL cavity, which could be related to the substrate protein. This finding could be explained by assuming that the substrate bound to GroEL is disordered. However, one cannot exclude the possibility that citrate synthase is dissociated from GroEL during crystallisation. Low resolution neutron or x-ray diffraction studies might be necessary in order to localise the disordered substrate protein.

8 Materials and methods

Chemicals used in this work were of highest possible quality. They were purchased from Sigma, Roth, Serva, Fluka, Merck (Germany). Water for all buffers was purified in Millipore system.

8.1 Protein expression and purification

8.1.1 Expression of chaperonins

Wild type *E.coli* chaperonins GroESL were expressed in different *E.coli* strains (W3110, JM109, MRE600) bearing multicopy plasmid pOF39 [35, 36]. Cell culture was grown in rich medium LB or in minimal medium (for deuteration was used M63 as well as M9) [4]. Minimal media contained deuterated glucose or succinate (in the case of partially deuterated cells H-glucose was used) as a carbon source. The cell culture was grown until saturation.

Protein	*E.coli* strain	medium	yield mg/g of cells
pD-GroEL	JM109	M9	7
pD-GroES	JM109	M9	3
pD-GroEL	MRE600	M9	8,7
pD-GroES	MRE600	M9	3,9
D-GroEL	JM109	M9	20
H-GroEL	W3110	LB	6,5
H-GroES	W3110	LB	2,2

Table 9: Some yields of purification of GroE from different bacterial strains.

At that point the turbidity of the cell culture has reached about 3 OU at 600 nm. Partially and fully deuterated *E.coli* cells were grown by Dr. K.Vanatalu (Institute of Physics and Biophysics, Tallinn, Estonia). These cultures were grown in fermenter, giving a very high density cell culture. Wild type promoter in pOF39 does not need any induction. Cells were collected by centrifugation and frozen at -80°C.

8.1.2 Purification of GroEL

Protocols for wild type GroEL and SR1 GroEL mutant were adopted with some modification from procedures used in laboratory of Prof. Dr. F.-U.Hartl, kindly provided by Dr. F.Weber.

The frozen cells were thawed in lysis buffer (100 mM Tris-HCl pH 8,1, 1 mM DTT, 0,1 mM EDTA, 3 mg/ml lysozyme, 0,2 mg/ml PMSF) and disrupted in French Pressure Cell Press (American instrument company, USA). Cell debris were removed by centrifugation (30000×g, 1 hour at 4°C). Cleared lysate was loaded directly on DE52-Servacel (Serva) column. The column was equilibrated with 30 mM Tris-HCl, pH 7,8, 50 mM NaCl, 1 mM EDTA, 1 mM DTT. GroES and GroEL were eluted separately at approximately 240 mM and 320 mM of NaCl gradient (0-500 mM) respectively [57]. GroEL containing fractions were diluted 5-6-fold with 50 mM histidine-HCl buffer, pH 5,8-5,6 for two reasons: to decrease salt concentration till 50-100 mM of NaCl and to adjust pH for the next chromatography.

The second chromatographic step was performed on the same column, DE52-Servacel, equilibrated with 25 mM Histidine-HCl, pH 5,7, 1 mM DTT. GroEL was eluted with gradient of NaCl (0-500 mM) at 300-400 mM NaCl (GroES appears from the column at 200-300 mM NaCl). Pooled GroEL fractions were supplemented with 0,4 M $(NH_4)_2SO_4$ and loaded on Butyl Sepharose column (Pharmacia), equilibrated with 20 mM K-MOPS, pH 7,2, 1 mM DTT and 0,4 M $(NH_4)_2SO_4$. GroEL was eluted with the long gradient (0,4 M $(NH_4)_2SO_4$ - 0 M). Main part of contaminations was removed at the washing step (0,4 M $(NH_4)_2SO_4$). This step is of special importance when some GroES is still present. GroES normally does not bind to this column. GroEL was eluted also at the beginning of reverse gradient.

Rather diluted GroEL after Butyl Sepharose was concentrated (by ultrafiltration in stirring cell (Amicon) and PES membrane (Pall Filtron) with 10 kDa cut-off or by precipitation with 70% of saturation of $(NH_4)_2SO_4$ and applied on gel filtration Sephacryl S-300 column (Pharmacia), equilibrated with the storage buffer of choice (typically, 30 mM Tris-HCl, pH 7,8, 150 mM NaCl, 1 mM DTT, 0,1 mM EDTA, 0,02% NaN_3, 10% (w/v) glycerol). Pooled fractions of oligomeric GroEL were frozen in liquid nitrogen and stored at -80°C.

8.1.3 GroEL free from contaminations containing tryptophane

GroEL and GroES do not contain tryptophane. Therefore, fluorescence spectra of both proteins if they are pure enough must resemble a spectrum of tyrosine. In fact, GroEL after gel filtration was not free from tryptophane due to polypeptides

bound in it. These contaminations were effectively removed by treatment with the reactive red agarose (Sigma, type 120) [112]. The resin (about 10 ml of slurry) was added to approximately 100 ml of protein solution (0,1-0,5 mg/ml) in 20 mM K-MOPS, pH 7,2, 10 mM $Mg(Ac)_2$ and stirred overnight at 4°C. Resin was removed by centrifugation and filtration. The protein was concentrated with adjusting of buffer components to storage buffer. Resulting GroEL demonstrates pure tyrosine fluorescence spectrum, when measured as described by Blennow et al. [12].

8.1.4 Purification of GroES

According to the procedures described by Corrales et al. [27] fractions containing GroES after DEAE chromatography were incubated at 56°C 20-30 min. Precipitated material was removed by centrifugation (30000×g, 1 hour, at 4°C). After this treatment GroES was already about 90% pure. As a final purification step solution containing GroES was supplemented with 0,8 M $(NH_4)_2SO_4$ and loaded on Phenyl Sepharose column (Pharmacia) equilibrated with 20 mM K-MOPS pH 7,2, 0,8 M $(NH_4)_2SO_4$, 1 mM DTT, 0,02% NaN_3. GroES was eluted by reverse gradient of $(NH_4)_2SO_4$ (0,8 M - 0 M $(NH_4)_2SO_4$) as a broad peak. The GroEL binds very tightly to Phenyl Sepharose, it can be eluted only at the end of the gradient in the absence of salt. After concentrating (ultrafiltration or precipitation with $(NH_4)_2SO_4$ 70% of saturation) GroES was loaded of gel filtration (this step can be omitted) Sephacryl S-300 (Pharmacia) column and eluted with storage buffer of following composition: 30 mM Tris-HCl, pH 7,8, 150 mM NaCl, 10% (w/v) glycerol, 1 mM DTT, 0,1 mM EDTA, 0,02% NaN_3 and after concentrating stored at -80°C.

8.1.5 Purification of SR1 GroEL mutant

SR1 mutant of GroEL (R452E, E461A, S463A, V464A [100]) was purified from overproducing strain BL21 carrying the plasmid pET11a DE3 SR1-GroEL. The strain was kindly provided by Prof. Dr. F.-U.Hartl. The purification procedure used was the same as for GroEL. The last step in this protocol is gel filtration, but GroEL produced by host cell was not removed on Sephacryl S-300, which was used. The only treatment which removed GroEL from SR1 preparations was equilibrium centrifugation (26 hrs., 25 000 rpm, 4°C in the ultracentrifuge LE-80K, rotor SW28 (Beckman)) in glycerol gradient 10-35%. Gradient was made in 20 mM Tris-HCl, pH 7,8, 150 mM NaCl, 1 mM DTT.

8.1.6 Expression and purification of maltose binding protein mutant Y283D

Mutant MBP Y283D was obtained from overproducing *E.coli* strain carrying plasmid pHB 1204 Y283D, kindly provided by Prof. Dr. J.Buchner. Cells were grown in LB medium. When the culture reached a turbidity 0,8 OU at 600 nm, expression was induced by 1 mM IPTG. Expressed in this strain maltose binding protein is located in periplasma. It is recommended not to freeze the cells.

Cells were collected by centrifugation (5 000 rpm, 10 min, 4°C) and resuspended in 1/40 of culture volume in buffer A (50 mM NaCl, 20 mM MOPS, pH 7,5). After second centrifugation (12 000 rpm, 10 min, 4°C) cells were resuspended in the same volume (1/40) of buffer B (10 mM MOPS, 5 mM EDTA, 1 mg/ml polymyxin-sulfate for example, Sigma, #1405-20-5). Note, that polymyxin has to be added short before. Suspension was vortexed about 30 sec, then another portion of buffer B (1/80) was added, mixed thoroughly too and leaved to stay on ice for 20 min. After that cells were precipitated again by centrifugation (15 000 rpm, 20 min, 4°C) and resuspended in 1/80 of culture volume of buffer B following the similar treatment (vortexed, 10 min on ice) and precipitated again by centrifugation at 15 000 rpm, 4°C, 30 min. At this step lysates could be frozen for long storage and have to be checked for the presence of MBP. Buffer A supernatant should not contain MBP, it must be found in both lysates in buffer B. When needed, the polymyxin step can be repeated. It is recommended to keep the volume as low as possible.

Lysates in buffer B were directly applied on hydroxyapatite column (Bio-Rad, Bio-Gel, HT gel) equilibrated with 10 mM K-phosphate buffer, pH 7,0. Protein was eluted with gradient of K-phosphate 10-250 mM. Pooled fraction containing MBP were supplemented with $(NH_4)_2SO_4$ up to 1 M (by addition of the corresponding volume of 3-4 M $(NH_4)_2SO_4$ upon stirring). The next chromatographic step was Butyl Sepharose (Pharmacia), equilibrated with 1 M $(NH_4)_2SO_4$ in 20 mM K-MOPS, pH 7,0. Protein was eluted by reversed gradient of salt from 1 M to 0 M. Gel filtration on Superose 6 (Pharmacia) or Sephacryl S-300 in 20 mM K-MOPS, pH 7,0 to remove excess of salt is optional, because salt can be removed also during concentration.

Typical yield: 20 mg MBP from 14 g cells, harvested from 6 l of LB culture.

8.2 Preparation of the complex of GroEL with MBP Y283D

Substrate protein (MBP) is to be added in 4-fold excess to GroEL. Molar weight of MBP is 40 kDa, its active form is dimer. It binds to GroEL as a monomer. Stoichiometry of this complex is estimated in [118] and in SANS experiments.

An equal volume of 8 M urea in 20 mM Tris-HCl pH 7,8, 50 mM KCl, 10 mM $MgCl_2$ was added to highly concentrated MBP solution in the same buffer. Denaturation takes 2 hours at room temperature. Denatured MBP has to be diluted upon intensive mixing in buffer (20 mM Tris-HCl pH 7,5, 50 mM KCl, 5 mM $MgCl_2$) containing GroEL. It is good to keep dilution factor as big as possible (100-200), in order to reduce carry over effects of urea. For example, one can add about 1 ml of MBP in urea to 100 ml of GroEL solution directly in the ultrafiltration stirring cell and concentrate proteins afterwards. MBP remains bound to GroEL during gel filtration, but binding of two substrate molecules was never found after that.

8.3 Determination of protein concentration (Bradford assay)

Protein concentration was measured according manufacturer instruction (Bio-Rad). Calibration curve for chaperonins was based on quantitative amino acids analysis. Actually for GroES one can use a calibration with BSA as a standard. GroEL has a lower capacity to react with dye reagent, so the same concentration of GroEL shows a lower optical density in the assay than GroES or BSA by factor 0,83.

8.4 ATPase assay

8.4.1 Reaction conditions

ATPase activity of GroEL was measured typically in 20 mM Tris-HCl, pH 7,8, 50 mM KCl, 5-10 mM $MgCl_2$ and different amount of protein. Reaction was started by addition of different concentrations of ATP and fast mixing of the sample. Aliquots were taken at certain time points and reaction was quenched by dilution into the double volume of 0,375 M HCl or directly into the malachite green reagent. When TLC was applied for separation of the products of hydrolysis reaction was stopped by dilution into the eluent.

8.4.2 Malachite green assay in two variants

Determination of inorganic phosphate was performed according to Henkel et al. [61]. 200 μl of reaction mixture were rapidly mixed with 0,8 ml of malachite green reagent, freshly prepared from stock solutions (Table 10).

Protein was denatured in this resulting mixture, because it contains 1 M HCl. The main problem of this method is hydrolysis of the resting amount of ATP.

compound	concentration	remarks
polyvinyl ethanol in H_2O	5,75%	dissolves only in hot water
ammonium molybdate in 6 M HCl	5,72%	close to saturation
malachite green base	0,082%	has to be titrated with HCl

Table 10: Stock solutions used for malachite green assay.

In ATP concentration range used in the most experiments (200-2000 μM) this reaction proceeds linearly in the time interval 20-120 min. To account for this reaction, the absorbance was measured few times and extrapolated to the moment of mixing, which value gives a P_i content in the sample immediately after the enzymatic reaction stops. Dependence of the absorbance on concentration of phosphate was linear up to 1.6 OU. Concentration of phosphate which could be measured by this method is in the range 10-160 μM. Maximal protein concentration for this assay is 0,2 mg/ml in the enzymatic reaction mixture.

The highest protein concentration which can be used for this assay is 0,5 mg/ml. It is too low for single turnover experiments. For that purpose the assay was modified according Kodama et al. [77]. In this variant, reaction was quenched by dilution of 100 μl of reaction mixture into 200 μl of 0,375 M HCl on ice, where it can be left for an hour or two. Then 0,65 ml of modified malachite green solution was added and sample was left for 1 hour to develop colour. After that time the optical density of this solution is not stable any more. Optical density was measured at 630 nm, against sample containing only buffer instead of protein solution.

compound	concentration	HCl added	stock solution
triton X-100	0,05%	-	50% in H_2O
ammonium molybdate	0,2%	0,2 M	5,72% in 6 M HCl
malachite green base	0,003%	-	0,082%
HCl	0,7 M	0,5 M	11 M

Table 11: Composition of modified malachite green assay.

8.4.3 Thin layer chromatography ATPase assay

Reaction was started by addition of [α or γ-P^{32}]ATP (50-100 Ci/M ATP) to the reaction mixture containing GroEL and other additives. Thin layer chromatography was performed on PEI cellulose plates (Merck). 3 μl aliquots of reaction assay were added to 3 μl of 0,7 M LiCl, 1 M HCOOH to quench the reaction.

0,5-1 μl was applied to the plate and chromatography was performed in eluent containing 0,35 M LiCl and 0,5 M HCOOH. Chromatogram was visualised using Phosphoimager (Fudji, Japan). MacBas software (Fudji) was used for quantitation of chromatogram.

8.5 Electrophoretic methods

8.5.1 Non-denaturing PAGE

Electrophoresis in 4,5% polyacrylamide gel in non-denaturing conditions was performed as described earlier [80]. In order to get a better resolution 4% (v/v) of glycerol was added to the gel mixture. The gel buffer and running buffer were the same: 80 mM K-MOPS, pH 7,2. Because there is no interaction between GroEL and GroES in the absence of nucleotides, 2 mM $MgCl_2$ and 1 mM ADP or ATP were added to polymerising gel. Ten times smaller concentration of $MgCl_2$ and ADP were added also into the running buffer. Gels were run at the constant voltage 70 V and 20 mA for 4-6 hours at room temperature or at 4°C. Protein bands were visualised by staining with Coomassie Brilliant Blue R-250 in combination with Bismarck Braun R as described by Choi et al. [24]. 20% acetic acid was used for destaining of gels.

8.5.2 SDS-PAGE

In course of protein purification fractions were analysed by SDS-polyacrylamide gel electrophoresis in denaturing conditions. Gels were prepared and run according to the classical protocol of Laemmli [79]. Staining was performed in 20% acetic acid.

8.5.3 Agarose gels

Electrophoresis of GroEL-GroES complexes in 1-2% agarose was performed as described by Ding et al. [29]. Samples containing 5-10 μg of protein were supplemented with 1/5 of initial volume of loading buffer (50% glycerol, 0,02% Bromphenol Blue in 20 mM Tris-HCl pH 7,7) and horizontal gel was run under constant voltage 70 V until Bromphenol Blue reached the end of the gel. Running buffer was 40 mM Tris-OH, 20 mM acetic acid, pH 8,1, 1 mM $MgSO_4$. The gels were fixed and stained simultaneously in 25% iso-propanol and 7% acetic acid supplemented with 0,002% Coomassie for 1 hour. After drying gels were destained in 20% acetic acid.

8.6 SANS measurements

The SANS experiments were performed at the beam lines D22 and D11 at the Institute Laue-Langevin (Grenoble, France) and at Hahn-Meitner-Institute (Berlin). Measurements and data processing were carried out by Dr. M.Rößle, Dipl.Biol.J. Holzinger and Dr.R.Stegmann. Protein samples were measured in round flat quartz glass cuvettes (Hellma), 19 mm inner diameter, 1 mm path length. The cuvette holder was thermostated and a condensation of moisture from the air was prevented by a flux of dry air. The exposure time was set according to the protein concentration and the scattering contrast.

8.6.1 SANS data processing (principles)

The primary picture seen on detector looks like a set of concentric rings. The primary data were first averaged among all cells belonging to the same scattering angle. This procedure results in a one-dimensional scattering curve (for example, Fig.8).

The background scattering intensity and the scattering of the cuvette were subtracted from that curve. Absorption of neutrons by the sample itself is taken into account by dividing the sample intensity by its transmission. The transmission is the ratio between intensity of the coming flux of neutrons and that leaving the sample. Shortly, processing of SANS data is described by formula:

$$\frac{\frac{I_{\text{sample}}-I_{Cd}}{T_{\text{sample}}} - \frac{I_{ec}-I_{Cd}}{T_{ec}}}{\frac{I_{H_2O}-I_{Cd}}{T_{H_2O}} - \frac{I_{ec}-I_{Cd}}{T_{ec}}}$$

where I_{sample} and T_{sample} are the intensity of neutrons scattered by a sample and the corresponding transmission; I_{Cd} is the intensity observed with piece of cadmium or B_4C, which is non-transparent for the beam, this value gives a background scattering of surrounding instruments; I_{ec} is the scattering by an empty cuvette, T_{ec} is the transmission of an empty cuvette and I_{H_2O} and T_{H_2O} are the corresponding values for the buffer containing no D_2O used for subtraction of a background.

The scattering curve is the sum of scattering patterns of all possible orientations of the molecule. That means that all possible pairs of scatterers in the investigated molecule are reflected in the shape of the curve. Fourier transformation of a scattering curve results in a distance distribution function $p(r)$ [45], which reflects the probabilities of finding a given distance between all possible scattering centres in the molecule. From this distribution one can make conclusions about the overall shape and dimensions of a molecule as well as compare experimental

scattering curve and $p(r)$ with the functions calculated from a crystallographic model. These experiments can be performed only with rather large proteins, because $I(0)$ is proportional to the M_r^2. Therefore, only from a relatively large molecules could be obtained the data with a good statistics. Conformational changes should also be in the range of SANS resolution.

8.6.2 Sample preparation for SANS

Buffer used for SANS experiment contained 20 mM Tris-HCl, pH 7,8, 50 mM KCl, 10 mM $MgCl_2$. The pH level of D_2O containing buffer was calculated from the reading obtained with glass electrode according to the equation [110]:

$$pH = pD + 0,313\alpha + 0,0854\alpha^2$$

where α is a fraction of D_2O and pD is the value read from an electrode. For example, in case of buffers made on 99% D_2O pD 7,4 corresponds to pH 7,8.

GroEL concentration for reference measurements was kept 5 mg/ml. For titration series of GroEL with GroES constant concentration of GroEL 10 mg/ml was used in order to keep GroES concentration high enough to be measured reliably. For symmetric complex formation 30 mM AMP-PNP was present in solution, concentration of $MgCl_2$ in this case was also increased to 30 mM. Asymmetric complex was formed in 2 mM ADP or 5 mM AMP-PNP. All measurements were carried out at the room temperature.

8.6.3 GroES free and bound to GroEL

Free H-GroES as well as pD-GroES was measured in 99% D_2O in order to get a better sample contrast. At concentrations used (1-5 mg/ml) there was no visible interaction between GroES molecules in solution. Scattering curves of GroES in complex with GroEL were measured in buffer matching GroEL. In case of H-GroEL it was 40% D_2O, pD-GroEL was matched successfully in 99% or 97% D_2O. Nucleotides were added to the sample to enable binding. Control experiment revealed no visible interaction between GroES and GroEL in the absence of nucleotides.

8.6.4 Titration with GroES of the second binding site of GroEL

Titration was started from the point with the highest molar ratio GroES:GroEL equal to 5. Each following point was a dilution of previous one with solution,

having the same concentration of GroEL and nucleotide, but no GroES. Concentration of GroEL was kept constant 10 mg/ml. Measurements were performed in matching conditions for H-GroEL. H-GroEL is quite completely matched in buffer made on 40% of D_2O (20 mM TrisHCl, pH 7,8, 30 mM $MgCl_2$, 50 mM KCL, 30 mM AMP-PNP). Thus $p(r)$ function represents only interaction between two molecules of pD-GroES bound to H-GroEL and that significant fraction of pD-GroES which remains free. For estimation of dissociation constant the distance distribution functions were normalised to the total amount of GroES in the sample. The height of the peak at lower distances corresponds to the total amount of GroES. The height of the second peak reflects amount of GroES bound in the symmetric complex.

8.7 SAXS data collection and reduction

Two-dimensional picture read from detector has the same appearance as in SANS experiments. Exactly as for SANS the first step in data evaluation is radial averaging of scattering intensities for each scattering angle. After this procedure a two-dimensional detector picture is reduced to one-dimensional scattering curve, which looks quite similar to scattering curves obtained in SANS experiments. At this step a background scattering of water in the solution and surrounding devices was subtracted from the curve. Errors estimation was derived from errors of radial averaging of primary detector picture. For time resolved experiments error was calculated from parameters of the detector and averaging procedure and it was the same for the whole set of data (0,2 Å).

Scattering intensities were collected for 300 msec time slices during 50 sec, which was a typical timescale for kinetic studies. Every experiment was performed four times and the results shown are averaged data sets. R_g was calculated directly from the logarithmic plot of scattering curve extrapolated to $q = 0$.

R_g is sensitive to some structural changes in polypeptide and its changes with time is used for further analysis. There is an advantage of SAXS technique with respect to SANS methods: SAXS allows much more precise estimation of R_g. Such small differences of this parameter in SANS data are completely within error range.

8.8 Crystallisation conditions

Measurable crystals were obtained by sitting drop method. Two buffers were applied as reservoir: buffer A and B. Buffer A contained 100 mM Tris-HCL pH 8,3, 200 mM $MgCl_2$, 30% (v/v) MPD. Buffer B contained 100 mM Na-HEPES, pH 7,5, 20% PEG 4000, 200 mM $(NH_4)_2SO_4$. Concentration of protein in a drop

after mixing with an equal volume of reservoir buffer was in the range of 15-20 mg/ml. Crystals appeared at different time, in average after 1 week at 18°. Crystals grown in buffer B before freezing have to be soaked in cryobuffer, which was buffer B supplemented with 30% v/v of MPD or 30% v/v of glycerol. Both variants were successful.

9 References

References

[1] V.R.Agashe, F.-U.Hartl "Roles of molecular chaperones in cytoplasmic protein folding" Cell and Develop.Biol., 2000, v.11, p.15-25

[2] A.Aharoni, A.Horovitz "Inter-ring communication is disrupted in the GroEL mutant Arg13→Gly; Ala126→Val with known crystal structure" J.Mol.Biol., 1996, v.258, p.732-735

[3] C.B.Anfinsen "Principles that govern the folding of protein chains" Science, 1973, v.181, n.4096, p.223-230

[4] F.M.Ausubel et al.(Ed.) "Short protocols in molecular biology" 4th Ed., J.Wiley and Sons, Inc., 2000

[5] A.Azem, S.Diamant, M.Kessel, C.Weiss, P.Goloubinoff "The protein-folding activity of chaperonins correlates with the symmetric $GroEL_{14}(GroES_7)_2$ heterooligomer" Proc.Natl.Acad.Sci. USA, 1995, v.92, p.12021-12025

[6] A.Azem, M.Kessel, P.Goloubinoff "Characterization of a functional $GroEL_{14}(GroES_7)_2$ chaperonin hetero-oligomer" Science, 1994, v.265, p.653-656

[7] J.Behlke, O.Ristau, H.-J.Schönfeld "Nucleotide-dependent complex formation between the *Escherichia coli* chaperonins GroEL and GroES studied under equilibrium conditions" Biochemistry, 1997, v.36, p.5149-5156

[8] A.P.Ben-Zvi, J.Chatellier, A.R.Fersht, P.Goloubinoff "Minimal and optimal mechanisms for GroE-mediated protein folding" Proc.Natl.Acad.Sci. USA, 1998, v.95, p.15275-15280

[9] D.M.Berman, T.Kozasa, A.G.Gilman "The GTPase-activating protein RGS4 stabilizes the transition state for nucleotide hydrolysis" J.Biol.Chem., 1996, v.271, n.44, p.27209-27212

[10] J.Bigay, P.Deterre, C.Pfister, M.Chabre "Fluoroaluminates activate transducin-GDP by mimicing the gamma-phosphate of GTP in its binding site" FEBS lettr., 1985, v.191, p.181-185.

[11] J.Bigay, P.Deterre, C.Pfister, M.Chabre "Fluoride complexes of aluminium or beryllium act on G-proteins as reversibely bound analogues of the gamma phosphate of GTP" EMBO J., 1987, v.6, n.10, p.2907-2913

[12] A.Blennow, B.P.Surin, H.Ehring, N.F.McLennan, M.D.Spangfort "Isolation and biochemical characterization of highly purified *Escherichia coli* molecular chaperone Cpn60 (GroEL) by affinity chromatography and urea-induced monomerization" Biochimica et Biophysica Acta, 1995, v.1252, p.69-78

[13] E.S.Bochkareva, N.M.Lissin, G.C.Flynn, J.E.Rothman, A.S.Girshovich "Positive cooperativity in the functioning of chaperonin GroEL" J.Biol.Chem., 1992, v.267, n.10, p.6796-6800

[14] D.C.Boisvert, J.Wang, Z.Otwinowski, A.L.Horwich, P.B.Sigler "The 2.4 Å crystal structure of the bacterial chaperonin GroEL complexed with ATPγS" Nature Str.Biol., 1996, v.3, n.2, p.170-177

[15] K.Braig, Z.Otwinowski, R.Hegde, D.C.Boisvert, A.Joachimiak, A.L.Horwich, P.B.Sigler "The crystal structure of the bacterial chaperonin GroEL at 2.8 Å" Nature, 1994, v.371, p.578-586

[16] K.Braig, P.D.Adams, A.T.Brünger "Conformational variability in the refined structure of the chaperonin GroEL at 2.8 Å resolution" Nature Str.Biol., 1995, v.2, n.12, p.1083-1093

[17] K.Braig "Chaperonins" Curr.Opinion in Str.Biol., 1998, v.8, p.159-165

[18] C.Brossel, J.Orring "Studies on the consecutive formation of aluminium fluoride complexes" Svensk Kemisk Tidskrift, 1943, v.55, n.5, p.101-116

[19] R.Brunschier, M.Danner, R.Seckler "Interactions of phage P22 tail-spike protein with GroE molecular chaperones during refolding *in vitro*" J.Biol.Chem., 1993, v.268, n.4, p.2767-2772

[20] J.Buchner, M.Schmidt, M.Fuchs, R.Jaenicke, R.Rudolph, F.X.Schmid, T.Kiefhaber "GroE facilitates refolding of citrate synthase by suppressing aggregation" Biochemistry, 1991, v.30, p.1586-1591

[21] B.Bukau, A.L.Horwich "The Hsp70 and Hsp60 chaperone machines" Cell, 1998, v.92, p.351-366

[22] S.G.Burston, N.A.Ranson, A.R.Clarke "The origins and consequences of assymetry in the chaperonin reaction cycle" J.Mol.Biol., 1995, v.249, p.138-152

[23] G.N.Chandrasekhar, K.Tilley, C.Woolford, R.Hendrix, C.Georgopoulos "Purification and properties of the groES morphogenetic protein of *Escherichia coli*" J.Biol.Chem., 1986, v.261, n.26, p.12414-12419

[24] J.-K.Choi, S.-H. Yoon, H.-Y. Hong, D.-K. Choi, G.-S. Yoo "A modified Coomassie blue staining of proteins in polyacrylamide gels with Bismark brown R" Analytical Biochemistry, 1996, v.236, p.82-84

[25] J.L.Chuang, R.M.Wynn, J.-L.Song, D.T.Chuang "GroEL/GroES-dependent reconstitution of $\alpha_2\beta_2$ tetramers of human mitochondrial branched chain α-ketoacid decarboxylase" J.Biol.Chem., 1999, v.274, n.15, p.10395-10404

[26] M.J.Cliff, N.M.Kad, N.Hay, P.Lund, M.Webb, S.Burston, A.Clarke "A kinetic analysis of the nucleotide-induced allosteric transitions of GroEL" J.Mol.Biol., 1999, v.293, p.667-684

[27] F.J.Corrales, A.R.Fersht "Kinetic significance of $GroEL_{14}\cdot(GroES_7)_2$ complexes in molecular chaperone activity" Folding and Design, 1996, v.1, p.265-273

[28] F.J.Corrales, A.R.Fersht "Toward a mechanism for GroEL·GroES chaperone activity: an ATPase-gated and -pulsed folding and annealing cage" Proc.Natl.Acad.Sci. USA, 1996, v.93, p.4509-4512

[29] Y.Ding, R.L.Duda, R.W.Hendrix, J.M.Rosenberg "Complexes between chaperonin GroEL and the capsid protein of bacteriophage HK97" Biochemistry, 1995, v.34, p.14918-14931

[30] L.Ditzel, J.Lowe, D.Stock, K.O.Stetter, H.Huber, R.Huber, S.Steinbacher "Crystal structure of the thermosome, the archaeal chaperonin and homolog of CCT" Cell, 1998, v.93, p.125-138

[31] R.J.Ellis (Ed.) "The chaperonins" san Diego: Academic Press; 1996

[32] A.Engel, M.K.Hayer-Hartl, K.N.Goldie, G.Pfeifer, R.Hegerl, S.Müller, A.C.R. da Silva, W.Baumeister, F.U.Hartl "Functional significance of symmetrical versus asymmetrical GroEL-GroES chaperonin complexes" Science, 1995, v.269, p.832-836

[33] K.L.Ewalt, J.P.Hendrick, W.A.Houry, F.U.Hartl "In vivo observation of polypeptide flux through the bacterial chaperonin system" Cell, 1997, v.90, p.491-500

[34] G.W.Farr, K.Furtak, M.B.Rowland, N.A.Ranson, H.R.Saibil, T.Kirchhausen, A.L.Horwich "Multivalent binding of nonnative substrate proteins by the chaperonin GroEL" Cell, 2000, v.100, p.561-573

[35] O.Fayet, J.-M.Louarn, C.Georgopoulos "Suppression of the *Escherichia coli dnaA46* mutation by amplification of the *groES* and *groEL* genes" Mol.Gen.Genet., 1986, v.202, p.435-445

[36] O.Fayet, T.Ziegelhoffer, C.Georgopoulos "The *groES* and *groEL* heat shock gene product of *Escherichia coli* are essential for bacterial growth at all temperatures" J.Bacteriol., 1989, v.171, n.3, p.1379-1385

[37] W.A.Fenton, Y.Kashi, K.Furtak, A.L.Horwich "Residues in chaperonin GroEL required for polypeptide binding and release" Nature, 1994, v.371, p.614-619

[38] W.A.Fenton, A.L.Horwich "GroEL-mediated protein folding" Prot.Sc., 1997, v.6, p.743-760

[39] M.T.Fisher "On the assembly of dodecameric glutamine synthetase from stable chaperonin complexes" J.Biol.Chem., 1993, v.268, n.19, p.13777-13779

[40] A.J.Fisher, C.A.Smith, J.B.Thoden, R.Smith, K.Sutoh, H.M.Holden, I.Rayment "X-ray structure of the myosine motor domain of *Dictiostelium discoideum* complexed with MgADP$*$BeF$_x$ and MgADP$*$AlF$_x^-$" Biochemistry, 1995, v.34, p.8960-8972

[41] C.P.Georgopoulos, R.W.Hendrix, S.R.Casjens, A.D.Kaiser "Host participation in bacteriophage λ head assembly" J.Mol.Biol., 1973, v.76, p.45-60

[42] F. von Germar, A.Galan, O.Llorca, J.L.Carrascosa, J.M.Valpuesta, W.Mäntele, A.Muga "Conformational changes generated in GroEL during ATP hydrolysis as seen by time-resolved infrared spectroscopy" J.Biol.Chem., 1999, v.274, n.9, p.5508-5513

[43] P.Gervasoni, W.Staudenmann, P.James, A.Plückthun "Identification of the binding surface of β-lactamase for GroEL by limited proteolysis and MALDI-mass spectrometry" Biochemistry, 1998, v.37, p.11660-11669

[44] P.Gervasoni, P.Gehrig, A.Plückthun "Two conformational of β-lactamase bound to GroEL: a biophysical characterization" J.Mol.Biol., 1998, v.275, p.663-675

[45] O.Glatter "A new method for the evaluation of small angle scattering data" J.of Applied Crystallography, 1997, v.10, p.415-421

[46] M.S.Goldberg, J.Zhang, S.Sondek, C.R.Matthews, R.O.Fox, A.L.Horwich "Native-like structure of a protein-folding intermediate bound to the chaperonin GroEL" Proc.Natl.Acad.Sci. USA; 1997, v.94, p.1080-1085

[47] G.Goldstein "Equilibrium distribution of metal-fluoride complexes" Analytical Chemistry, 1964, v.36, n.1, p.243-244

[48] P.Goloubinoff, J.T.Christeller, A.A.Gatenby, G.H.Lorimer "Reconstitution of active dimeric ribulose bisphosphate carboxylase from an unfolded state depends on two chaperonin proteins and Mg-ATP" Nature, 1989, v.342, p.884-889

[49] P.Goloubinoff, S.Diamant, C.Weiss, A.Azem "GroES binfding regulates GroEL chaperonin activity under heat shock" FEBS lettr., 1997, v.407, p.215-219

[50] C.L.Gordon, S.K.Sather, S.Casjens, J.King "Selective *in vivo* rescue by GroEL/ES of thermolabile folding intermediate to phage P22 structural proteins" J.Biol.Chem., 1994, v.269, n.45, p.27941-27951

[51] B.M.Gorovits, J.Ybarra, J.W.Seale, P.M.Horowitz "Conditions for nucleotide-dependent GroES-GroEL interactions" J.Biol.Chem., 1997, v.272, n.43, p.26999-27004

[52] H.Grallert, K.Rutkat, J.Buchner "GroEL traps dimeric and monomeric unfolding intermediates of citrate synthase" J.Biol.Chem., 1998, v.273, n.50, p.33305-33310

[53] T.E.Gray, A.R.Fersht "Cooperativity in ATP hydrolysis by GroEL is increased by GroES" FEBS lettr., 1991, v.292, n.1,2, p.254-258

[54] I.Gutsche, L.-O.Essen, W.Baumeister "Group II chaperonins: new TRiC(s) and turns of a protein folding machine" J.Mol.Biol., 1999, v.293, p.295-312

[55] Gutsche I., J. Holzinger, M. Roessle, H. Heumann, W. Baumeister, R.P. May "Conformational rearrangements of an archaeal chaperonin upon ATPase cycling" Curr.Biol., 2000, v.10, p.405-408

[56] J.E.Hansen, A.Gafni "Thermal switching between enhanced and arrested reactivation of bacterial glucose-6-phosphate dehydrogenase assisted by GroEL the absence of ATP" J.Biol.Chem., 1993, v.268, n.29, 21632-21636

[57] J.R.Harris, A.Plückthun, B.Zahn "Transmission electron microscopy of GroEL, GroES, and the symmetrical GroEL/ES complex" J.Struct.Biol., 1994, v.112, p.216-230

[58] M.K.Hayer-Hartl, J.Martin, F.U.Hartl "Asymmetrical interaction of GroEL and GroES in the ATPase cycle of assisted protein folding" Science, 1995, v.269, p.836-841

[59] M.K.Hayer-Hartl, F.Weber, F.U.Hartl "Mechanism of chaperonin action: GroES binding and release can drive GroEL-mediated protein folding in the absence of ATP hydrolysis" EMBO J., 1996, v.15, n.22, p.6111-6121

[60] R.W.Hendrix "Purification and properties of groE, a host protein involved in bacteriophage assembly" J.Mol.Biol., 1979, v.129, p.375-392

[61] R.D.Henkel, J.L.VandeBerg, R.A.Walsh "A microassay for ATPase" Anal.Biochem., 1988, v.169, p.312-318

[62] T.Hohn, B.Hohn, A.Engel, M.Wurtz, P.R.Smith "Isolation and characterization of the host protein groE involved in bacteriophage lambda assembly" J.Mol.Biol., 1979, v.129, p.359-373

[63] W.A.Houry, D.Frishman, C.Eckerskorn, F.Lottspeich, F.U.Hartl "Identification of *in vivo* substrates of the chaperonin GroEL" Nature, 1999, v.402, p.147-154

[64] Y.-S.Huang, D.T.Chuang "Mechanisms for GroEL/GroES-mediated folding of a large 86-kDa fusion polypeptide *in vitro*" J.Biol.Chem., 1999, v.274, n.15, p.10405-10412

[65] J.F.Hunt, A.J.Weaver, S.J.Landry, L.Gierash, J.Deisenhofer "The crystal structure of the GroES co-chaperonin at 2.8 Å resolution" Nature, 379, 1996, p.37-45

[66] D.-J.Hwang, N.E.Tumer, T.M.A.Wilson "Chaperone protein GrpE and the GroEL/GroES complex promote the correct folding of tobacco mosaic virus coat protein for ribonucleocapsid assembly in vivo" Arch.Virol., 1998, v.143, p.2203-2214

[67] E.Inbar, A.Horovitz "GroES promotes the T to R transition of the GroEL ring distal to GroES in the GroEL-GroES complex" Biochemistry, 1997, V.36, p.12276-12281

[68] T.Inobe, T.Makio, E.Takasu-Ishikawa, T.P.Terada, K.Kuwajima "Nucleotide binding to the chaperonin GroEL: non-cooperative binding of ATP analogs and ADP, and cooperative effect of ATP" Biochimica et Biophysica Acta, 2001, v.1545, 160-173

[69] Y.Ishii, K.Murakami, H.I.-Ogawa, A.Kondo, Y.Kato "Production of MBP(maltose binding protein)-GroES fusion protein and utilization to stimulate GroEL-mediated protein refolding" J.Fermentation and Bioengineering, 1998, v.85, n.1, p.69-73

[70] G.S.Jackson, R.A.Staniforth, D.J.Halsall, T.Atkinson, J.J.Holbrook, A.R.Clarke, S.G.Burston "Binding and hydrolysis of nucleotides in the chaperonin catalytic cycle: implications for the mechanism of assisted protein folding" Biochemistry, 1993, v.32, p.2554-2563

[71] M.U.H.Javed, F.Michelangeli, P.A.Lund "GroEL protects the sarcoplasmic reticulum Ca^{2+} dependent ATPase from inactivation *in vitro*" Biochem. and Mol.Biol.int, 1999, v.47, n.4, p.631-638

[72] W.Jeong, N.-K.Shin, H.-C.Shin "Bacterial chaperones increase the production of soluble human TNF-alpha in Escherichia coli" Biotech.lettr., 1997, v.19, n.6, p.579-582

[73] N.M.Kad, N.A.Ranson, M.Cliff, A.R.Clarke "Asymmetry, commitment and inhibition in GroE ATPase cycle impose alternating functions upon the two GroEL rings" J.Mol.Biol., 1998, v.278, p.267-278

[74] K.Katsumata, A.Okazaki, G.P.Tsurupa, K.Kuwajima "Dominant forces in the recognition of a transient folding intermediate of α-lactalbumin by GroEL" J.Mol.Biol., 1996, v.264, p.643-649

[75] Y.Kawata, K.Hongo, K.Nosaka, Y.Furutsu, T.Mizobata, J.Nagai "The role of ATP hydrolysis in the function of the chaperonin GroEL: dynamic complex formation with GroES" FEBS lettr., 1995, v.369, p.283-286

[76] T.L.Kelson, T.Ohura, J.P.Kraus "Chaperonin-mediated assembly of wild-type and mutant subunits of human propionyl-CoA carboxylase expressed in *Escherichia coli*" Human Mol.Genet., 1996, v.5, n.3, p.331-337

[77] T.Kodama, K.Fukui, K.Kometani "The initial phosphate burst in ATP hydrolysis by myosin and subfragment-1 as studied a modified malachite green method for determination of inorganic phosphate" J.Biochem., 1986, v.99, p.1465-1472

[78] O.Kovalenko, O.Yifrach, A.Horovitz "Residue lysine-34 in GroES modulates allosteric transitions in GroEL" Biochemistry, 1994, v.33, p.14974-14978

[79] U.K.Laemmli "Cleavage of structural proteins during the assembly of the head of bacteriophage T4" Nature, 1970, v.227, p.680-685

[80] T.Langer, G.Pfeifer, J.Martin, W.Baumeister, F.-U.Hartl "Chaperonin-mediated protein folding: groES binds to one end of the GroEL cylinder, which accommodates the protein substrate within its central cavity" EMBO J., 1992, v.11, n.13, p.4757-4765

[81] H.Lederer, R.P.May, J.K.Kjems, W.Schaefer, H.L.Crespi, H.Heumann "Deuterium incorporation into *Escherichia coli* proteins. A neutron-scattering study of DNA-dependent RNA polymerase" Eur.J.Biochem., 1986, v.156, p.655-659

[82] A.L.Lehninger, D.L.Nelson, M.M.Cox "Principles of biochemistry" Worth Publishers, New-York, 1993

[83] O.Llorca, S.Marco, J.L.Carrascosa, J.M.Valpuesta "The formation of symmetrical GroEL-GroES complexes in the presence of ATP" FEBS lettr., 1994, v.345, p.181-186

[84] O.Llorca, J.L.Carrascosa, J.M.Valpuesta "Biochemical characterization of symmetric GroEL-GroES complexes" J.Biol.Chem., 1996, v.271, n.1, p.68-76

[85] O.Llorca, J.L.Carrascosa, J.M.Valpuesta "Symmetric GroEL-GroES complexes can contain substrate simultaneously in both GroEL rings" FEBS lettr., 1997, v.405, p.195-199

[86] O.Llorca, J.Perez-Perez, J.L.Carrascosa, A.Galan, A.Muga, J.M.Valpuesta "Effects of the inter-ring communication in GroEL structural and functional asymmetry" J.Biol.Chem., 1997, v.272, n.52, 32925-32932

[87] O.Llorca, S.Marco, J.L.Carrascosa, J.M.Valpuesta "Conformational changes in the GroEL oligomer during the functional cycle" J.Struct.Biol., 1997, v.118, p.31-42

[88] O.Llorca, A.Galan, J.L.Carrascosa, A.Muga, J.M.Valpuesta "GroEL under heat-shock. Switching from a folding to a storing function" J.Biol.Chem., 1998, v.273, n.49, p.32587-32594

[89] G.H.Lorimer "A quantitative assessment of the role of the chaperonin proteins in protein folding in vivo" FASEB J., 1996, v.10, p.5-9

[90] G.H.Lorimer, M.J.Todd "GroE structure galore" Nature Str.Biol., 1996, v.3, n.2, p.116-121

[91] Z.-I.Luo, Z.-C.Hua "Increased solubility of glutathione S-transferase-P16 (GST-P16) fusion protein by co-expression of chaperones GroES and GroEL in Escherichia coli" Bioch.and Mol.Biol.int., 1998, v.46, n.3, p.471-477

[92] S.Machida, Y.Yu, S.P.Singh, J.-D.Kim, K.Hayashi, Y.Kawata "Overproduction of β-glucosidase in active form by an *Escherichia coli* system co-expressing the chaperonin GroEL/ES" FEMS Microbiol.lettr., 1998, v.159, p.41-46

[93] G.Maier, E.Manakova, H.Heumann "Effect of *Escherichia coli* chaperonin GroELS on heterologously expressed human immunodeficiency virus type 1 reverse transcriptase in vivo and in vitro" Applied Biochemistry and Biotechnology, 2000, v.87, p.103-115

[94] T.Makio, M.Arai, K.Kuwajima "Chaperonin-affected refolding of α-lactalbumin: effects of nucleotides and the co-chaperonin GroES" J.Mol.Biol., 1999, v.293, p.125-137

[95] J.Martin, T.Langer, R.Boteva, A.Schramel, A.L.Horwich, F.-U.Hartl "Chaperonin-mediated protein folding at the surface of groEL through a 'molten globule'-like intermediate" Nature, 1991, v.352, p.36-42

[96] J.R.Mattingly Jr., A.Iriarte, M.Martinez-Carrion "Homologous proteins with different affinities for GroEL. The refolding of the aspartate aminotransferase isozymes at varying temperatures" J.Biol.Chem., 1995, v.270, n.3, p.1138-1148

[97] J.A.Mendoza, T.Warren, P.Dulin "The ATPase activity of chaperonin GroEL is highly stimulated at elevated temperature" Biochem.Biophys.Res.Comm., 1996, v.229, p.271-274

[98] F.C.Neidhardt, R.A.VanBogelen, V.Vaughn "The genetics and regulation of heat-shock proteins" Ann.Rev.Genet., 1984, v.18, p.295-329

[99] S.E.Nieba-Axmann, M.Ottiger, K.Wüthrich, A.Plückthun "Multiple cycles of global unfolding of GroEL-bound cyclophilin A evidenced by NMR" J.Mol.Biol., 1997, v.271, p.803-818

[100] K.L.Nielsen, N.J.Cowan "A single ring is sufficient for productive chaperonin-mediated folding in vivo" Mol.Cell, 1998, v.2, p.93-99

[101] D.A.Parsell, S.Lindquist "The function of heat-shock proteins in stress tolerance: degradation and reactivation of damaged proteins" Ann.Rev.Genet., 1993, v.27, p.437-496

[102] N.A.Ranson, N.J.Dunster, S.G.Burston, A.R.Clarke "Chaperonins can catalyse the reversal of early aggregation steps when a protein misfolds" J.Mol.Biol., 1995, v.250, p.581-586

[103] A.Raw, D.E.Coleman, A.G.Gilman, S.R.Sprang "Structural and biochemical characterization of the GTPγS-, GDP$*$P$_i$-, and GDP-bound forms of of a GTPase-deficient Gly42$\rightarrow$Val mutant of G$_{i\alpha 1}$" Biochemistry, 1997, v.36, p.15660-15669

[104] K.Rittinger, P.A.Walker, J.F.Eccleston, S.J.Smerdon, S.J.Gamblin "Structure at 1,65 Å of RhoA and its GTPase activating protein in complex with a transition-state analogue" Nature, 1997, v.389, p.758-762

[105] M.Rössle, E.Manakova, J.Holzinger, K.Vanatalu, R.P.May, H.Heumann "Time-resolved small-angle neutron scattering of proteins in solution" Physica B, 2000, v.276, p.532-533

[106] M.Roessle, E.Manakova, I.Lauer, T.Nawroth, J.Holzinger, T.Narayanan, S.Bernstoff, H.Amenitsch, H.Heumann "Time-resolved small angle scattering: kinetic and structural data from proteins in solution" J. of Appl.Cryst., 2000, v.33, p.548-551

[107] A.M.Roseman, S.Chen, H.White, K.Braig, H.R.Saibil "The chaperonin ATPase cycle: mechanism of allosteric switching and movements of substrate-binding domains in GroEL" Cell, 1996, v.87, n.2, p.241-251

[108] H.S.Rye, S.G.Burston, W.A.Fenton, J.M.Beechem, Z.Xu, P.B.Sigler, A.L.Horwich "Distinct actions of *cis* and *trans* ATP within the double ring of the chaperonin GroEL" Nature, 1997, v.388, p.792-798

[109] H.S.Rye, A.M.Roseman, S.Chen, K.Furtak, W.A.Fenton, H.R.Saibil, A.L.Horwich "GroEL-GroES cycling: ATP and nonnative polypeptide direct alternation of folding-active rings" Cell, 1999, v.97, p.325-338

[110] S.Sawata, M.Komiyama, K.Taira "Kinetic evidence based on isotope effects for the nonexistence of a proton-transfer process in reactions catalyzed by a hammerhead ribozyme: implication to the double-metal-ion mechanism of catalysis" J.Am.Chem.Soc., 1995, v.117. p.2357-2358

[111] M.Schmidt, K.Rutkat, R.Rachel, G.Pfeifer, R.Jaenicke, P.Viitanen, G.Lorimer, J.Buchner "Symmetric complexes of GroE chaperonins as part of the functional cycle" Science, 1994, v.265, p.656-659

[112] C.Schneider (Ed.) "Chaperonin protocols" Methods in Molecular Biology, v.140, 2000 Humana Press, Totowa, New Yersey

[113] M.Shtilerman, G.H.Lorimer, S.W.Englander "Chaperonin function: folding by forced unfolding" Science, 1999, v.284, p.822-825

[114] P.B.Sigler, Z.Xu, H.S.Rye, S.G.Burston, W.A.Fenton, A.L.Horwich "Structure and function in GroEL-mediated protein folding" Annu.Rev.Biochem., 1998, v.67, p.581-608

[115] K.E.Smith, M.T.Fisher "Interactions between the GroE chaperonins and rhodanese" J.Biol.Chem., 1995, v.270, n.37, p.21517-21523

[116] K.E.Smith, P.A.Voziyan, M.T.Fisher "Partitioning of rhodanese onto GroEL. Chaperonin binds a reversibly oxidized form derived from the native protein" J.Biol.Chem., 1998, v.273, n.44, p.28677-28681

[117] J.Sondek, D.G.Lambright, J.P.Noel, H.E.Hamm, P.B.Sigler "GTPase mechanism of Gproteins from the 1,7-Å crystal structure of transducin α*GDP*AlF_4^-" Nature, 1994, v.372, p.276-279

[118] H.Sparrer, H.Lilie, J.Buchner "Dynamics of the GroEL-protein complex: effects of nucleotides and folding mutants" J.Mol.Biol., 1996, v.258, p.74-87

[119] H.Sparrer, K.Rutkat, J.Buchner "Catalysis of protein folding by symmetric chaperone complexes" Proc.Natl.Acad.Sci. USA, 1997, v.94, p.1096-1100

[120] R.A.Staniforth, S.G.Burston, T.Atkinson, A.R.Clarke "Affinity of chaperonin-60 for a protein substrate and its modulation by nucleotides and chaperonin-10" Biochem.J., 1994, v.300, p.651-658

[121] R.Stegmann, E.Manakova, M.Rößle, H.Heumann, S.E.Nieba-Axmann, A.Plückthun, T.Hermann, R.P.May, A.Wiedenmann "Structural changes of the *Escherichia coli* GroEL-GroES chaperonins upon complex formation in solution: a neutron small angle scattering study" J.Struct.Biol., 1998, v.121, p.30-40

[122] P.Thiyagarayan, S.J.Henderson, A.Joachimiak "Solution structures of GroEL and its complex with rhodanese from small-angle neutron scattering" Structure, 1996, v.15, n.4, p.79-88

[123] M.J.Todd, P.V.Viitanen, G.H.Lorimer "Hydrolysis of adenosine-5'-triphosphate by *Escherichia coli* GroEL: effects of GroES and potassium ion" Biochemistry, 1993, v.32, p.8560-8567

[124] M.J.Todd, P.V.Viitanen, G.H.Lorimer "Dynamics of the chaperonin ATPase cycle: implications for facilitated protein folding" Science, 1994, v.265, p.659-666

[125] M.J.Todd, G.H.Lorimer "Stability of the asymmetric *Escherichia coli* chaperonin complex. Guanidine chloride causes rapid dissociation" J.Biol.Chem., 1995, v.270, n.10, p.5388-5394

[126] M.J.Todd, G.H.Lorimer, D.Thirumalai "Chaperonin-facilitated protein folding: optimization of rate and yield by an iterative annealing mechanism" Proc.Natl.Acad.Sci. USA, 1996, v.93, p.4030-4035

[127] Z.Török, L.Vigh, P.Goloubinoff "Fluorescence detection of symmetric $GroEL_{14}(GroES_7)_2$ heterooligomers involved in protein release during the chaperonin cycle" J.Biol.Chem., 1996, v.271, n.27, p.16180-16186

[128] G.P.Tsurupa, T.Ikura, T.Makio, K.Kuwajima "Refolding kinetics of staphylococcal nuclease and its mutants in the presence of the chaperonin GroEL" J.Mol.Biol., 1998, v.277, p.733-745

[129] S.M. van der Vies, A.A.Gatenby, C.Georgopoulos "Bacteriophage T4 encodes a co-chaperonin that can substitute for *Escherichia coli* GroES in protein folding" Nature, 1994, v.368, p.654-656

[130] P.V.Viitanen, T.H.Lubben, J.Reed, P.Goloubinoff, D.P.O'Keefe, G.H.Lorimer "Chaperonin-facilitated refolding of ribulosebisphosphate carboxylase and ATP hydrolysis by chaperonin-60 (GroEL) are K^+ dependent" Biochemistry, 1990, v.29, p.5665-5671

[131] P.V.Viitanen, A.A.Gatenby, G.H.Lorimer "Purified chaperonin 60 (groEL) interacts with the nonnative states of a multitude of *Escherichia coli* proteins" Prot.Sc., 1992, v.1, p.363-369

[132] P.A.Voziyan, B.C.Tieman, C.-M.Low, M.T.Fisher "Changing the nature of the initial chaperonin capture complex influence the substrate folding efficiency" J.Biol.Chem., 1998, v.273, n.39, p.25073-25078

[133] J.D.Wang, J.S.Weissman "Thinking outside the box: new insights into the mechanism of GroEL-mediated protein folding" Nature Str.Biol., 1999, v.6, n.7, p.597-600

[134] A.Weijland, A.Parmeggiani "Toward a model for the interaction between elongation factor Tu and the ribosome" Science, 1993, v.259, p.1311-1314

[135] J.S.Weissman, H.S.Rye, W.A.Fenton, J.M.Beechem, A.L.Horwich "Characterization of an active intermediate of a GroEL-GroES-mediated protein folding reaction" Cell, 1996, v.84, p.481-490

[136] R.M.Wynn, J.-L.Song, D.T.Chuang "GroEL/GroES promote dissociation/reassociation cycles of a heterodimeric intermediate during $\alpha_2\beta_2$ protein assembly" J.Biol.Chem., 2000, v.275, n.4, p.2786-2794

[137] Z.Xu, A.L.Horwich, P.B.Sigler "The crystal structure of the asymmetric GroEL-GroES-$(ADP)_7$ chaperonin complex" Nature, 1997, v.388, p.741-750

[138] Y.-W. Xu, S.Morera, J.Janin, J.Cherfils "AlF_3 mimics the transition state of protein phosphorylation in the crystal structure phosphate kinase and MgADP" Proc.Natl.Acad.Sci. USA, 1997, v.94, p.3579-3583

[139] Z.Xu, P.Sigler "GroEL/GroES: structure and function of a two-stroke folding machine" J.Struct.Biol., 1998, v.124, p.129-141

[140] O.Yifrach, A.Horovitz "Two lines of allosteric communication in the oligomeric chaperonin GroEL are revealed by a single mutation Arg196→Ala." J.Mol.Biol., 1994, v.243, p.397-401

[141] O.Yifrach, A.Horovitz "Nested co-operativity in the ATPase activity of the oligomeric chaperonin GroEL" Biochemistry, 1995, v.34, n.16, p.5303-5308

[142] O.Yifrach, A.Horovitz "Allosteric control by ATP of non-folded protein binding to GroEL" J.Mol.Biol., 1996, v.255, p.356-361

[143] O.Yifrach, A.Horovitz "Transient kinetic analysis of adenosine 5'-triphosphate binding-induced conformational change in the allosteric chaperonin GroEL" Biochemistry, 1998, v.37, p.7083-7088

[144] O.Yifrach, A.Horovitz "Mapping the transition state of the allosteric pathway of GroEL by protein engineering" J.Am.Chem.Soc., 1998, v.120, p.13262-13263

[145] R.Zahn, P.Lindner, S.E.Axmann, A.Plückthun "Effect of single point mutations in citrate synthase on binding to GroEL" FEBS lettr., 1996, v.380, p.152-156

[146] R.Zahn, A.Plückthun "Thermodynamic partitioning model for hydrophobic binding of polypeptides by GroEL. II. GroEL recognizes thermally unfolded mature β-lactamase" J.Mol.Biol., 1994, v.242, p.165-174

[147] R.Zahn, S.Perrett, A.R.Fersht "Conformational states bound by the molecular chaperones GroEL and SecB: a hidden unfolding (annealing) activity" J.Mol.Biol., 1996, v.261, p.43-61

[148] A.Ziemienowicz, D.Skowyra, J.Zeilstra-Ryalls, O.Fayet, C.Georgopoulos, M.Zylicz "Both the *Escherichia coli* chaperone systems, GroEL/GroES and DnaK/DnaJ/GrpE, can reactivate heat-treated RNA polymerase" J.Biol.Chem., 1993, v.268, n.34, p.25425-25431

[149] S.B.Zimmerman, S.O.Trach "Estimation of macromolecule concentrations and excluded volume effects for the cytoplasm of Escherichia coli" J.Mol.Biol., 1991, v.222, p.599-620

10 Abbreviations

ADP adenosine 5'-diphosphate

ATP adenosine 5'-triphosphate

AMP-PNP 5'-adenylylimidodiphosphate

ATPγS adenosine 5'-o-(3-thiotriphosphate)

BSA bovine serum albumin

CCD charged coupled device

DHFR dihydrofolate reductase

DTT dithiothreitol

EDTA ethylenediaminetetraacetic acid

EM electron microscopy

MBP maltose binding protein

MOPS 3-[N-morpholino]propanesulfonic acid

P_i phosphate ion

PAGE polyacrylamide gel electrophoresis

RuBisCo ribulose bisphosphate carboxylase large subunit

SANS small angle neutron scattering

SAXS small angle x-ray scattering

TEMED N,N,N',N'- tetramethylethylenediamine

TLC thin layer chromatography

Tris tris[hydroxymethyl]aminomethane